TARGETED DRUG DELIVERY AND ENHANCED INTRACELLULAR RELEASE USING FUNCTIONALIZED LIPOSOMES

A DISSERTATION

SUBMITTED TO THE FACULTY OF THE GRADUATE SCHOOL

OF THE UNIVERSITY OF MINNESOTA

BY

ASHISH GARG

IN PARTIAL FULFILLMENT OF THE REQUIREMENTS

FOR THE DEGREE OF

DOCTOR OF PHILOSOPHY

PROFESSOR EFROSINI KOKKOLI

DECEMBER 2009

Acknowledgements

It is my pleasure to thank those who made this thesis possible. First of all I would like to thank my advisor Professor Efrosini Kokkoli for her guidance and enormous support throughout this project. She introduced and gave me the opportunity to work in the field of targeted drug delivery. I would also like to thank Professor Michael Tsapatsis for his constant encouragement and support he has made available in a number of ways. I owe my deepest gratitude to Professor Ronald Siegel for his valuable feedback and helping me in understanding this work from the perspective of a pharmaceutical scientist.

I am deeply indebted to all Kokkoli group members especially Anastasia Mardilovich, Brett Waybrant, Maroof Adil, Alison Tisdale, and Emilie Rexeisen. This thesis would not have been possible without the hard work of several undergraduate students I mentored during the course of my thesis – Eman Haidari, Jeremy Lois, Erika Gemzer, Colin Anderson, and Shalene Sankhagowit.

I express my profound appreciation to my fiancé Pooja Garg for being patient and understanding during the hard times of this study, along with the rest of her family for their support and making me feel welcomed in their home.

Finally and most importantly, I would like to thank my parents and family for their undying love and encouragement. I would not have gotten this far without the sacrifices of my parents who raised me to get good education and supported me in all my pursuits. They currently reside in India and wish they would be here with me to celebrate this success.

Dedication

Dedicated to my parents…

Abstract

The ability to target cancer cells using an appropriate drug delivery system can significantly reduce the associated side effects from cancer therapies and can help in improving the overall quality of life, post cancer survival. Integrin $\alpha_5\beta_1$ is expressed on several types of cancer cells, including colon cancer and plays an important role in tumor growth and metastasis. Thus, the ability to target the integrin $\alpha_5\beta_1$ using an appropriate drug delivery nano-vector can significantly help in inhibiting tumor growth and reducing tumor metastasis.

The work in this thesis focuses on designing and optimizing, functionalized stealth liposomes (liposomes covered with polyethylene glycol (PEG)) that specifically target the integrin $\alpha_5\beta_1$. The PEG provides a steric barrier allowing the liposomes to circulate in the blood for longer duration and the functionalizing moiety, PR_b peptide specifically recognizes and binds to integrin $\alpha_5\beta_1$ expressing cells. The work demonstrates that by optimizing the amount of PEG and PR_b on the liposomal interface, nano-vectors can be engineered that bind to CT26.WT colon cancer cells in a specific manner and internalize through $\alpha_5\beta_1$-mediated endocytosis. To further improve the efficacy of the system, PR_b functionalized pH-sensitive stealth liposomes that exhibit triggered release under mild acidic conditions present in endocytotic vesicles were designed. The study showed that PR_b functionalized pH-sensitive stealth liposomes, undergo destabilization under mildly acidic conditions and incorporation of the PR_b peptide does not significantly affect the pH-sensitivity of the liposomes. PR_b functionalized pH-sensitive stealth liposomes bind to CT26.WT colon carcinoma cells that express integrin $\alpha_5\beta_1$, undergo cellular

internalization, and release their load intracellularly in a short period of time as compared to other formulations. PR_b-targeted pH-sensitive stealth liposomes encapsulating 5-fluorouracil (5-FU) show significantly higher cytotoxicity than the PR_b-targeted inert stealth liposomes and the non-targeted stealth liposomes (both pH-sensitive and inert). The studies demonstrated that optimized PR_b functionalized pH sensitive liposomes have the potential to deliver a payload, such as chemotherapeutic agents, directly to colon cancer cells in an efficient and specific manner.

Table of Contents

List of Tables

List of Figures

1. Targeted drug delivery

Frequently the use of novel therapeutics in medicine is opposed by the lack of efficiency in delivery of these therapeutic agents to the target organs. After a therapeutical agent is administered to the body it undergoes even bio-distribution throughout the body. In order to reach the therapeutical site of action these agents have to cross several biological barriers in the body like organs, tissues, cells etc, where these agents could be adsorbed, metabolized or excreted out of the body [1]. Therefore, to increase the effectiveness of drug it is usually administered in large quantities. In case of the potent drugs, these results in deleterious effects on the healthy organs of body commonly referred to as *side effects*.

Targeted drug delivery can address the above problems. Paul Ehrlich first introduced the concept of targeted drug delivery nearly a century ago as “magic bullets” which guide a drug directly to its target organ and prevents it from affecting the healthy parts of the body. During the last three decades there has been intense effort directed towards the development of *drug delivery systems* (DDS) for treatment of diseases. In a broader sense, DDS can be defined as a strategy to efficiently transport the drug to its therapeutical site of action by the appropriate choice of carrier, route, and target. The selection of all three critically determines the efficacy of the DDS.

1.1. Advantages of drug delivery systems

The use of a carrier system for delivering drugs to the body provides several opportunities for achieving the goal of drug targeting. Some potential advantages of DDS are [1, 2]:

a. Maintenance of constant drug levels in the therapeutical range.
b. Reduction of drug toxicity and fewer side effects when targeted to specific tissues or organs.
c. Facilitation of administration - increases patient compliance.
d. Protection of biologically active drug molecules like peptides and proteins from degradation during transport.
e. Smaller amounts of drug and decrease in the number of dosages.

1.2. Classification of drug delivery systems

Drug delivery systems have been classified based on either their physical form [1, 3, 4] or their functional properties [5, 6]. In the former classification, DDS are broadly divided into *particle type*, *soluble*, and *cellular carriers*. Particle type DDS include liposomes, microspheres, and nanoparticles. Examples of soluble DDS are plasma proteins, peptides, polysaccharides and monoclonal antibodies. The cellular DDS comprise of whole cells and viruses.

The functional classification categorizes the DDS into *first*, *second*, and *third generation* [5, 6]. The first generation includes systems which do not have the capability of carrying the drug to their target site and are therefore implanted as close as possible to the target. Microspheres, microcapsules, and other similar systems qualify in this category. The second generation comprises of systems that are both capable of carrying (when administered through a general route) and releasing the drug at the target site of action. These include particulate and soluble carriers less than 1μm in diameter like passively targeted liposomes, nanocapsules, nanospheres and more advanced DDS like temperature or pH sensitive liposomes, and magnetic nanospheres that release their

contents upon receiving a specific signal. The third generation is further ahead of their predecessors in terms of their ability for specific recognition of the target. Targeted liposomes, polymeric nanoparticles, and other second generation DDS modified with ligands like peptides or antibodies fall under this category.

1.3. Methods of drug targeting

As of today several methods of drug delivery are available and employed in experimental and clinical settings [7, 8]:

a. *Direct application of drugs*: As the name suggests, the drug is directly applied on to the affected organ or tissue.

b. *Passive targeting*: This method exploits the increase in permeability of vascular endothelium in regions of inflammation and tumors. Drug carriers within the size range of 10-500 nm can extravasate and accumulate in the interstitial space in the regions of enhanced permeability (enhanced permeation and retention effect) *e.g.*, tumors. Since the maximum size of the carrier that can extravasate at a particular site varies on case basis, the size of the drug carrier can be used to control the efficacy of the drug.

c. *Physical targeting*: This type of targeting could be achieved by both endogenous and exogenous methods. The former method exploits the difference in the physical environment (such as temperature/pH) in the affected area compared to the healthy regions *e.g.*, temperature sensitive liposomes, pH sensitive liposomes. Where in the exogenous approach, application of an external signal forces the drug carrier to release its contents at the target site. For example, use of a

magnetic field to localize the drug delivery carriers possessing ferromagnetic properties.

d. *Active targeting*: This is a more advanced approach in which the drug delivery carrier has specific affinity for the target. The drug molecule could either be coupled to the targeting moiety or could be encapsulated in a carrier, which in turn is coupled to the targeting vector. Examples of targeting moieties are antibodies and their fragments [9], lectins, proteins, peptides [10], lipoproteins [11], hormones, charged molecules, polysaccharides, and oligonucleotides [12].

1.4. Targeted drug delivery

The use of a targeted drug delivery system is an effective method of reducing toxicity of anti-cancer therapeutics. Figure 1.1 shows a general concept of target drug delivery. The first examples of targeted drug delivery system were described in literature nearly three decades ago [13, 14]. There has been a strong focus towards their development since then, and depends on four primary parameters described below:

a. *Target site*: For successful targeting it is important that the target receptor or antigen should have high density on target cells and should be overexpressed on the diseased tissue and minimally expressed on the healthy tissue.

b. *Targeting ligand*: Choice of the targeting ligand is a crucial parameter in determining the ability of the DDS to identify the target molecule of interest. The ligand should bind with affinity and specificity.

c. *Carrier*: There are several choices for drug carriers as discussed earlier. Liposomes are a great choice for a drug carrier and will be discussed in detail in chapter 3.

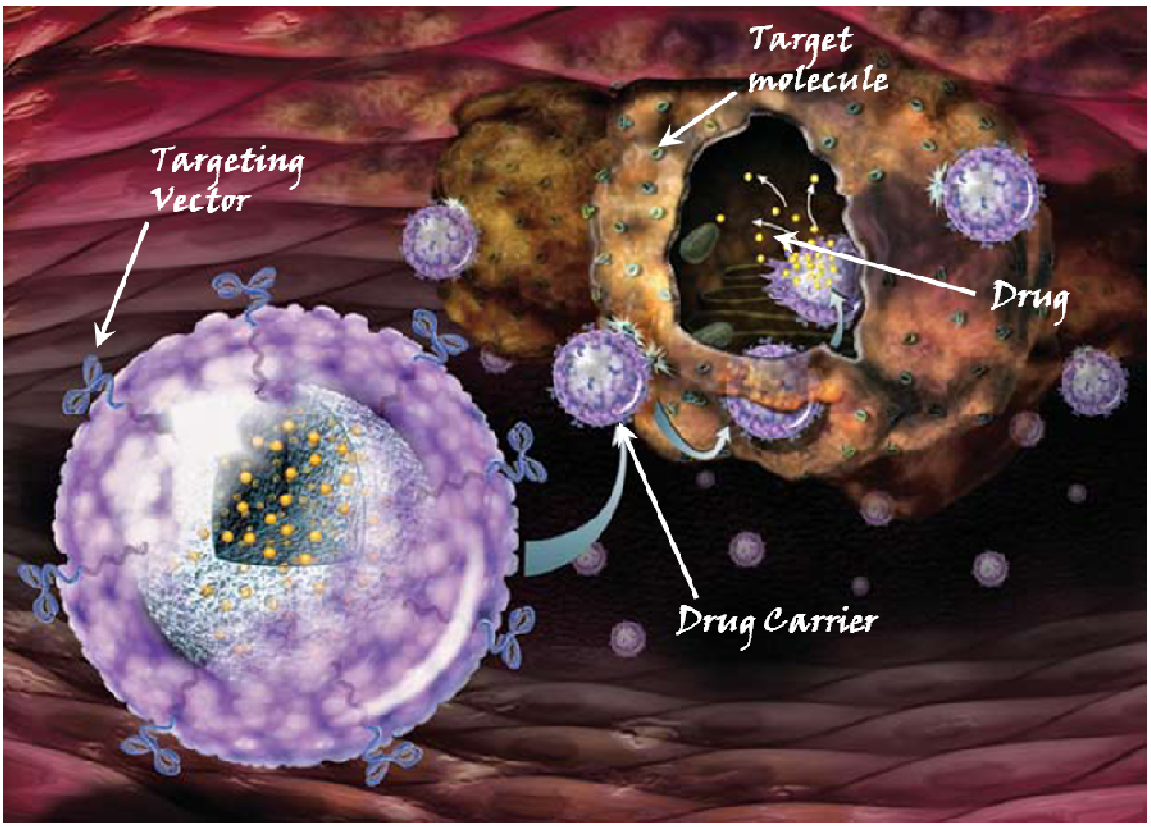

Figure 1.1 A successful targeted drug delivery system consist of four main components (a) a target molecule - uniquely expressed (or overexpressed) on diseased tissue; (b) a targeting vector that binds to target molecule of interest with high affinity and more importantly specificity; c) a carrier - stable in systemic circulation and releases its load when it reaches it therapeutic site of action; d) the drug which should be optimal and offer an advantage when delivered through a DDS. Reprinted with permission from Nicolle Rager Fuller. Copyright (2008), Sayo-Art.

d. *Drug*: The appropriate choice of drug is another important parameter as this eventually governs the efficacy of the targeted delivery system. The method of drug delivery should be optimal and confer an advantage over traditional methods of drug delivery.

In spite of the promise that targeted drug delivery holds for the future there are still several challenges for the researchers [15]. The first and foremost concern for a targeted drug delivery system is to recognize the target organ and subsequently deliver the drug to it. Usually it is difficult to identify target molecules that are upregulated in the region of interest and minimally expressed in healthy tissues. The second challenge is the

undesired extravasation of drugs/carriers in the healthy tissues/organs (*e.g.*, liver, spleen etc.) that may occur and can be deleterious when delivering a highly potent drug. After the carrier reaches its target site it should be able to penetrate into specific cells or tissue. Even if the drug is able to recognize and reach the target and does not accumulate in other tissues, release of drugs from the carrier poses another problem. Last but not least, control of residence time at the receptor site may be another issue which could ultimately also affect the drug efficacy.

2. Target site selection and choice of targeting ligand

Development of an effective targeted drug delivery system is dependent on selection of four primary factors - target site, targeting ligand, drug carrier and drug, as described in chapter 1. This chapter will focus on selection of the target site and the targeting ligand. Chapters 3 and 4 will discuss liposomes as drug carriers, and chapters 5, 6, and 7 will focus towards their development for achieving the goal of drug targeting.

2.1. Target site selection

For successful targeting it is necessary that the receptor or target molecule of interest should be expressed on the diseased tissue at high levels so that the drug will accumulate at pharmacological relevant levels. In addition, the target should be easily accessible from the systemic circulation and be distinct qualitatively (or at least quantitatively) from those expressed in healthy tissue. Ideally it will be desirable to have a target whose expression is upregulated because downregulation will ultimately lead to emergence of resistance and subsequently the failure of the DDS.

Several different targets have been investigated for site-specific delivery [16]. These include histones; receptors which are over expressed in tumor cells (e.g. folate receptor) [10]; cell adhesion molecules (CAM) – neural (N-CAM), platelet endothelial receptor (PECAM-1), vascular (VCAM-1) and intracellular (ICAM-1 and 2); cadherins (N-, and E- cadherins); integrins ($\alpha_5\beta_1$ or $\alpha_v\beta_3$); selectins (E- and P- selectins); and very recently, chemokines are also being explored for site-specific delivery [17]. The main focus of this thesis is targeting the integrin $\alpha_5\beta_1$ and some work has been done towards targeting fractalkine, a chemokine molecule.

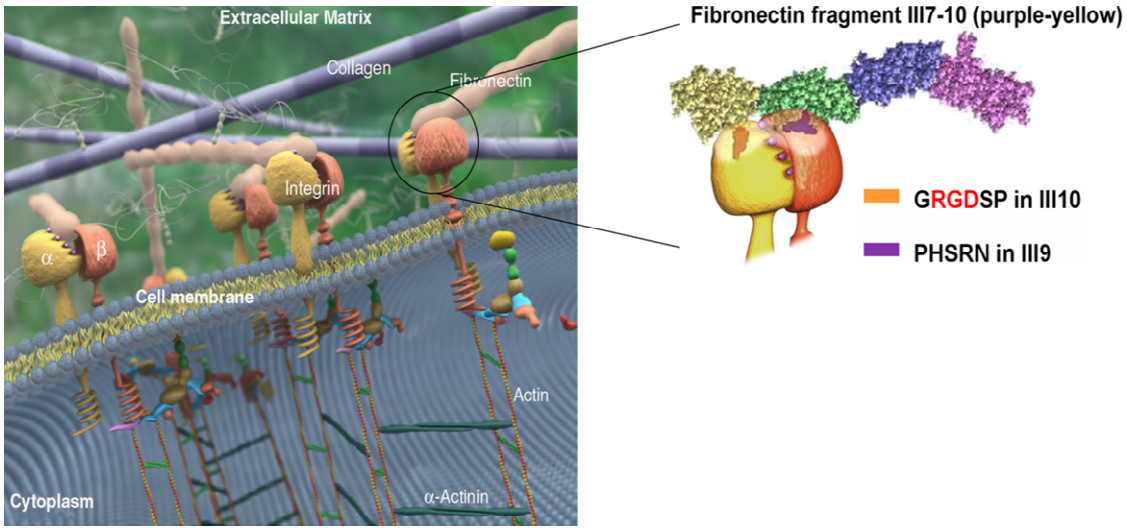

Figure 2.1 Integrins are composed of two subunits (α and β), and they hold a cell in place by binding to ECM proteins, like fibronectin, and at the other end connect to the structural framework of the cell. Integrins recognize specific adhesion domains on the ECM proteins. Reprinted from [18], Copyright (2002) with permission from Elsevier.

2.1.1. Integrins

Integrins have heterodimeric structure composed of α and β subunits non-covalently associated with each other. Integrins are present on most of the cell types and are key players in cell-cell adhesion and adhesion of cells to the extracellular matrix (ECM). Figure 2.1 shows the structure of integrin $\alpha_5\beta_1$ and its binding to fibronectin. Integrin $\alpha_5\beta_1$ binds to ECM protein, fibronectin by recognizing the specific sites on the protein [18] as will be discussed in this chapter.

Proliferating endothelial cells express several integrin molecules, like $\alpha_5\beta_1$, $\alpha_v\beta_3$, and $\alpha_4\beta_1$ [19-21], which are not expressed on quiescent endothelial cells in normal tissue or blood vessels. In particular, integrin $\alpha_5\beta_1$ is minimally expressed in normal vasculature but is significantly up-regulated in tumor vasculature [20] and on tumor cells such as prostate, breast, colon and rectal cancer [20, 22-27].

Previous studies suggest that peptide and antibody antagonists of the integrin $\alpha_5\beta_1$ are potent inhibitors of tumor growth, tumor induced angiogenesis, and tumor metastasis [20, 22, 23, 28-33]. Additionally, ligands that bind to the integrin $\alpha_5\beta_1$ with high affinity are capable of mediating cellular internalization [34-39]. Therefore, integrin $\alpha_5\beta_1$ is a strong candidate for targeting colon, breast and prostate cancer [10].

2.1.1. Fractalkine

Fractalkine (neurotactin for mice, CX_3CL1) is a recently identified molecule and the only member of the CX_3C family of chemokines which posses several unique properties when compared to other chemokines [40]. Fractalkine is upregulated on vascular endothelium during inflammation or infection and exists both as a membrane-anchored protein and as a soluble protein, and can serve as an adhesion molecule in addition to its chemotactic properties [41].

Figure 2.2 represents a schematic of the extracellular domain of fractalkine. The membrane anchored form of fractalkine can recruit and arrest a subset of leukocytes (monocytes, natural killer (NK) and T cells) from the systemic circulation in a selectin and integrin independent manner [42-47]. It has been demonstrated that fractalkine binds to its receptor strongly with a K_d ~ 30-740 pM [41, 44, 48-51]. The reason for the variation in K_d values is because of the different assay methods and experimental conditions used by the various investigators [50]. This unique feature of fractalkine allows recruitment and arrest of a subset of leukocytes (monocytes, natural killer (NK), and T cells) from the systemic circulation in a selectin and integrin independent manner [42-47].

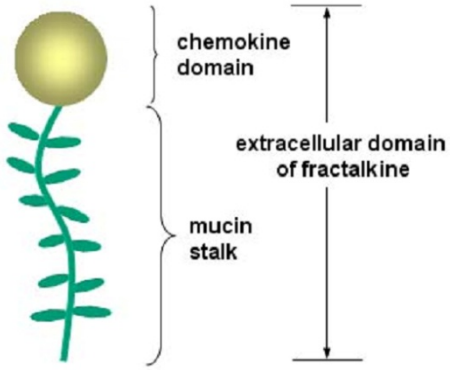

Figure 2.2 Schematic structure of the extracellular domain of fractalkine. Reprinted from [17], Copyright (2005) with permission from Elsevier.

The role of fractalkine has been established in several inflammatory diseases like, rheumatoid arthritis, atherosclerosis, allograft rejection, AIDS, and very recently cancer [52-59]. These observations strongly suggest that fractalkine could be an important target for targeted drug delivery to auto-inflammatory diseases and cancer.

2.2. Choice of targeting ligand

Once a target molecule (expressed on diseased tissue) has been identified, the selection of an effective targeting ligand is crucial for the success of a targeted drug delivery system. There are several types of targeting ligands e.g. peptides, proteins, antibodies, and aptamers [60]. The most important factor in the selection of the targeting ligand is that it should bind to the receptor of interest with high affinity and more importantly, specificity. Specificity is important as it governs the overall effectiveness of targeted drug delivery system in reducing toxic side effects.

Different types of ligands have their own advantages and disadvantages. Antibody based ligands have higher affinity and specificity but the biggest disadvantages include a possible immunogenic response from the use of rodent antibodies, and in addition the antibodies are expensive and time consuming to produce. Although the problems with

immunogenic response are currently being addressed by development of chimeric antibodies, antibody fragments, and humanized antibodies [61], their low stability presents another hurdle. On the other-hand ligands such as peptides are inexpensive, readily available and are more stable. They do not cause an immunogenic response but usually have lower affinity and sometimes poor specificity. The lower affinity of peptide based ligands can be improved by increasing the concentration of the targeting ligands on the drug carrier, as it has been shown that when multiple ligands on a single carrier bind to multiple receptors present on the target site, the resulting affinity can be significantly greater than that for a single ligand to a single receptor interaction [62]. To improve the specificity of the ligand targeted drug delivery system, a dual-ligand targeting approach has also been explored recently [63]. This approach reduces the non-specific ligand binding to off-target cells by using a sub-optimal concentration of a targeting ligand and exploiting the coincident over-expression of multiple receptors on the target site to achieve high affinity and specificity.

2.2.1. PR_b - targeting ligand for integrin $\alpha_5\beta_1$

Researchers have primarily employed RGD peptide based ligands for targeting integrin $\alpha_5\beta_1$ [35, 37, 38, 64-66]. RGD mimics the cell adhesion domain on fibronectin, the native ligand for integrin $\alpha_5\beta_1$. However their therapeutic use has been limited, as RGD does not accurately mimic the fibronectin binding domain for integrin $\alpha_5\beta_1$, and thus lacks the synergistic effect provided by the PHSRN site [67, 68]. RGD is also recognized by several other integrins such as $\alpha_5\beta_1$, $\alpha_8\beta_1$, $\alpha_v\beta_3$, $\alpha_v\beta_6$, $\alpha_v\beta_8$, and $\alpha_{IIb}\beta_3$ and therefore lacks specificity.

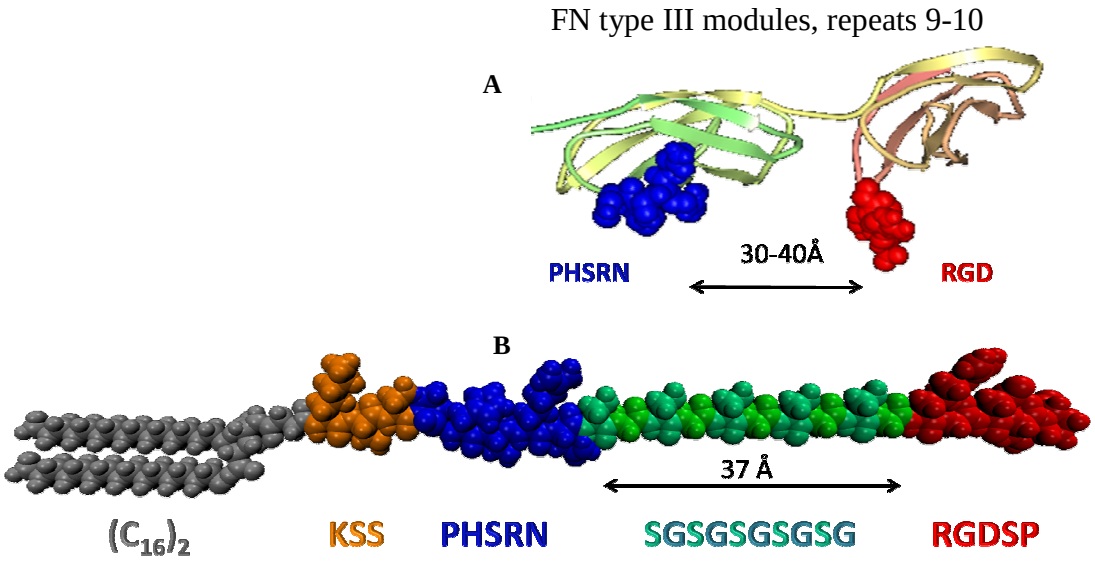

Figure 2.3 Design of fibronectin mimetic peptide PR_b. A) Fibronectin's primary binding ligand for the integrin $\alpha_5\beta_1$, RGD (natively found in the tenth type III module, FNIII10), and the synergy site PHSRN (in fibronectin type III repeat 9, FNIII9). The domains are separated by a distance of 30-40 Å [69]. B) PR_b-peptide amphiphile. On the PR_b peptide RGD and PHSRN domains are separated by a theoretical distance of 37 Å, to mimic the binding domain of fibronectin.

Figure 2.3A shows the cell binding domain on fibronectin, the primary binding site for the integrin $\alpha_5\beta_1$, RGD (natively found in the tenth type III module, FNIII10), and the synergy site PHSRN (in fibronectin type III repeat 9, FNIII9). The domains are present on the same face of the native protein and separated by a distance of 30-40 Å [69].. Efforts in the past to construct a single peptide sequence incorporating both RGD and PHSRN domains have shown limited success [70-74]. The peptide sequences have been constructed by connecting the two domains via: no linker [70], linker consisting of glycine (G) amino acids (G_3-G_{13}) [71-73] or a bivalent PEG hybrid linker [74]. The results from adhesion experiments for short durations of time (*i.e.*, before cells start secreting their own ECM proteins), demonstrate that all the peptides perform poorly when compared to fibronectin. One of the studies further showed that ECM production is lowest on the samples functionalized with RGDG_{13}PHSRN compared to the samples functionalized with a scrambled peptide sequence RDGG_{13}HPRNS or RGD [73]. This

stresses the need for designing a peptide sequence which closely mimics the binding domain of fibronectin.

We have previously developed a novel peptide sequence (referred as PR_b) that is a fibronectin mimetic peptide and specifically binds to $\alpha_5\beta_1$ [75]. The PR_b peptide (Figure 2.3B) consists of four building blocks: a spacer (KSS), PHSRN (the synergy site for $\alpha_5\beta_1$), linker $(SG)_5$, and RGDSP (the primary recognition site for $\alpha_5\beta_1$) and is conjugated to C_{16} dialkyl tails to form a peptide-amphiphile (PR_b peptide-amphiphile) [76]. The distance between the PHSRN and RGD domains on native fibronectin is approximately 30-40 Å [69] and the ratio of hydrophilic to hydrophobic residues between the two domains is close to one [77]. The PR_b linker has been designed to mimic these two important criteria; the length of the $(SG)_5$ linker is approximately 37 Å (10 amino acids × 3.7 Å per amino acid residue [77, 78]), and the ratio of the hydrophilic serine (S) residues to hydrophobic glycine (G) residues is equal to one. The role of the KSS spacer is to extend the bioactive region further away from the interface as the accessibility of the peptide can significantly affect its binding affinity for the target receptor [17, 77, 79].

The performance of the PR_b peptide-amphiphile was evaluated in terms of cell adhesion, spreading, cytoskeletal organization, and extracellular fibronectin production. Figure 2.4 shows that Langmuir-Blodgett films of the PR_b peptide-amphiphile outperformed all other peptide sequences that were tested as well as fibronectin in terms of HUVEC adhesion [75]. The specificity of the PR_b peptide was established by blocking the endothelial cells with anti-$\alpha_5\beta_1$ antibodies which showed 78% reduction in cell adhesion, Figure 2.5 [75].

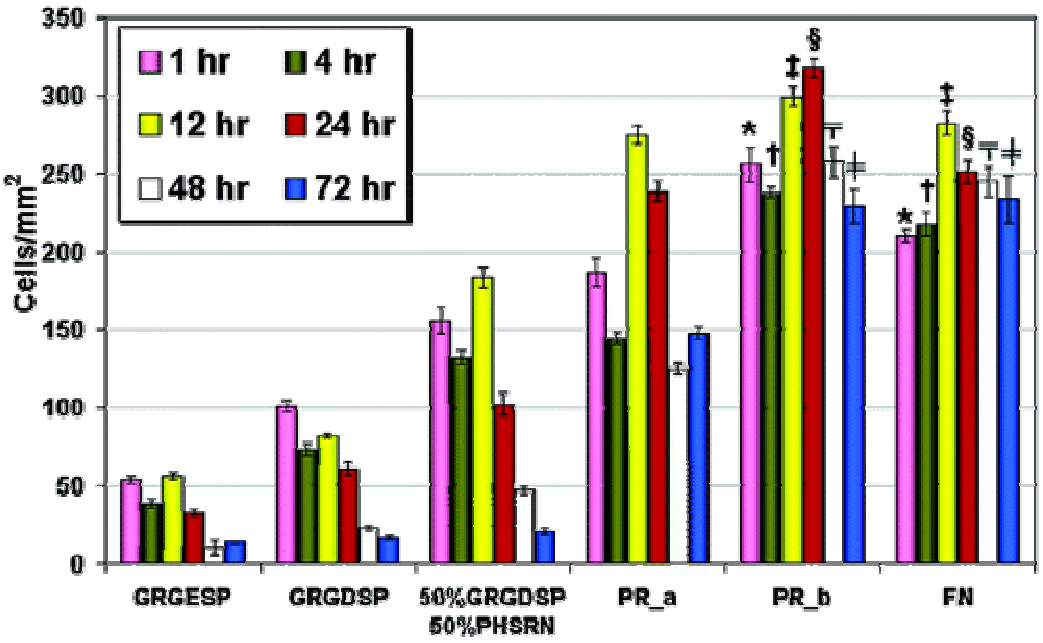

Figure 2.4 Effect of time and surface composition on HUVEC adhesion. Cell adhesion was evaluated on LB membranes of the following peptide−amphiphiles: GRGDSP, 50% GRGDSP−50% PHSRN, PR_a, and PR_b. The GRGESP peptide−amphiphile was used as a negative control, and the FN substrates were used as a positive control. HUVECs were incubated on these substrates for 1−72 hrs at 37 °C, 5% CO_2, in the absence of FBS. The initial cell density was 497 cells/mm^2. The PR_b peptide−amphiphile outperforms all other peptide surfaces and, compared to the positive control FN, gives higher adhesion for 1−24 hrs (z-test analysis for *,†,‡, and §: $p < 0.007$) and similar adhesion for 48−72 hrs (z-test analysis for ∓and ⊫: $p < 0.1$, signifying no statistical difference). Each histogram represents the mean ± SD. For all substrates, $n = 2$ (two independent experiments performed on different days). Reprinted with permission from [75]. Copyright (2006) American Chemical Society.

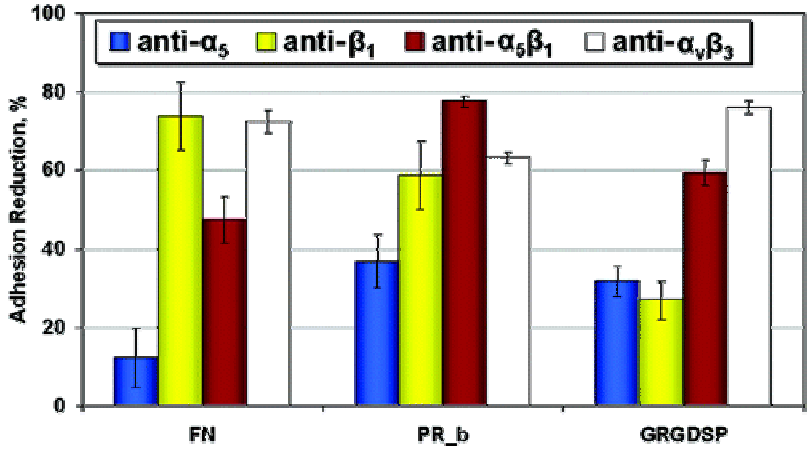

Figure 2.5 Integrin specificity. Inhibition assay using anti-integrin blocking antibodies against α_5 (P1D6), β_1 (P5D2), $\alpha_5\beta_1$ (JBS5), and $\alpha_v\beta_3$ (LM609) to determine the integrin engagement profile for HUVEC adhesion on FN, PR_b, and GRGDSP substrates after 1 hrs of incubation at 37 °C and 5% CO_2, in the absence of FBS. Results are reported as the percentage of reduction in cell adhesion by blocking antibodies compared to the control (nonblocked cells). Reprinted with permission from [75]. Copyright (2006) American Chemical Society.

The data presented strongly suggests that PR_b peptide shows high affinity to integrin $\alpha_5\beta_1$, comparable to the native protein fibronectin. In addition, PR_b is also very specific and does not bind to other integrins like RGD. Therefore, PR_b peptide when incorporated into liposomes should be capable of targeting integrin $\alpha_5\beta_1$ expressing cells with affinity and specificity, and results are discussed in detail in chapter 5 and 6.

2.2.2. NTFR-fractalkine targeting ligand

The N-terminus of the chemokine receptors critically determines their binding affinity and specificity to their respective chemokines [80-93]. The use of chimeric receptors, where the N-terminus of one receptor is replaced by that of another, has demonstrated a strong involvement of the N-terminus in several cases [80-83, 86, 88, 92]. Additionally, it has also been suggested that the N-terminus may alone be sufficient for binding and specificity [87]. Peptide sequences derived from the N-terminus of the chemokine receptors and tested using NMR titration studies, demonstrate that N-terminal derived peptides from chemokine receptors do bind to their respective chemokines, though with lower affinity when compared to their actual receptor [93-98].

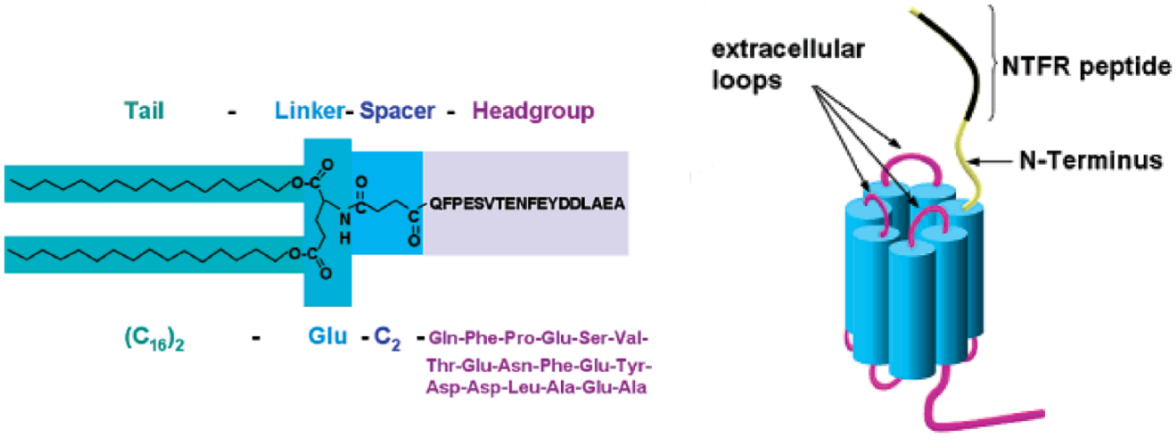

Figure 2.6 The design of the NTFR peptide-amphiphile based on the residues 3-20 of N-terminus of the fractalkine receptor. Reprinted from [17], Copyright (2005) with permission from Elsevier.

Work from the Kokkoli lab has shown that a peptide sequence (QFPESVTENFEYDDLAEA) corresponding to residues 3-20 of the N-terminus of the fractalkine receptor (NTFR) binds specifically to the fractalkine molecule [17]. Figure 2.6 shows the design of the NTFR peptide-amphiphile which is based on the N-terminus of the fractalkine receptor. In this work bio-artificial membranes (resembling a liposome surface in two dimensions) comprising of NTFR peptide-amphiphiles (NTFR peptide-amphiphile) and DPPC (1,2-Dipalmitoyl-sn-Glycero-3-Phosphocholine) phospholipids were constructed using the Langmuir-Blodgett (LB) technique. The binding of NTFR to fractalkine was determined using an atomic force microscope (AFM). In order to establish the specificity of interaction, the adhesion receptor integrin $\alpha_5\beta_1$ and its ligand peptide sequence GRGDSP were used as controls.

Figure 2.7 shows adhesion measurements between NTFR peptide-amphiphile:DPPC surfaces and AFM tips functionalized with $\alpha_5\beta_1$ integrins or fractalkine [17]. The adhesion measurements between fractalkine (immobilized on the AFM tip) and NTFR peptide amphiphile:DPPC mixed monolayers clearly demonstrates the binding of NTFR to fractalkine. The maximum adhesion was obtained for mixed surfaces with NTFR peptide-amphiphile:DPPC in the molar ratio 3:1, as compared to pure NTFR peptide-amphiphile surfaces, because the presence of shorter DPPC molecules allow more room for the NTFR peptide to bend and present the bioactive sequence for binding to fractalkine molecule (DPPC membranes showed minimal adhesion to fractalkine molecule [17]). Adhesion force measurement between the $\alpha_5\beta_1$ (immobilized on the AFM tip) and NTFR surfaces gave minimal adhesion as compared to fractalkine and NTFR (Figure 2.7 and Figure 2.8).

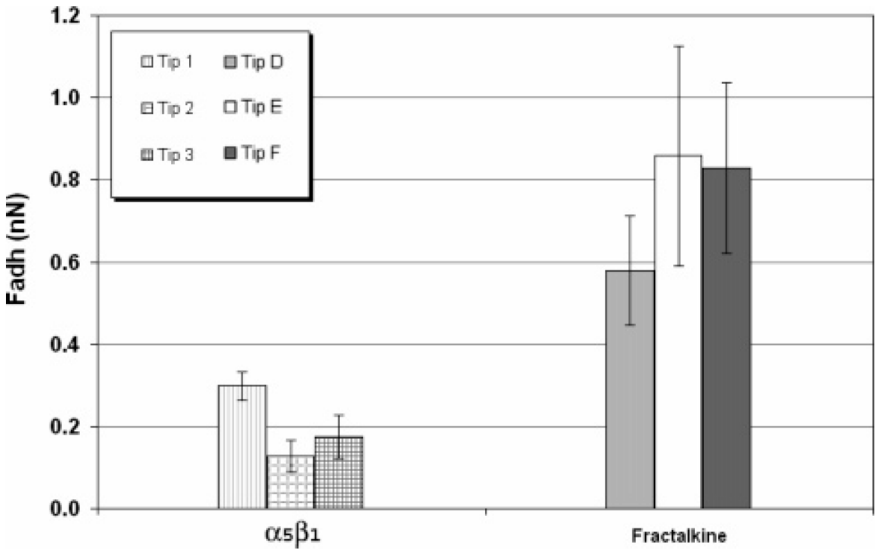

Figure 2.7 Adhesion measurements between 3:1 NTFR peptide-amphiphile:DPPC surfaces and AFM tips functionalized with $\alpha_5\beta_1$ integrins or fractalkine. The measurements with the $\alpha_5\beta_1$ integrins were performed in 1 mM $MnCl_2$ solution at pH 6.5-7, as Mn^{2+} ions have been shown to activate isolated integrins[99]. Measurements with fractalkine tips were collected in DI water at pH 6.5-7. Each column represents the average from 30-50 measurements on each surface. The error bars show standard deviations and reflect the fact that the number of pairs that interact may vary from one measurement to another. Reprinted from [17], Copyright (2005) with permission from Elsevier.

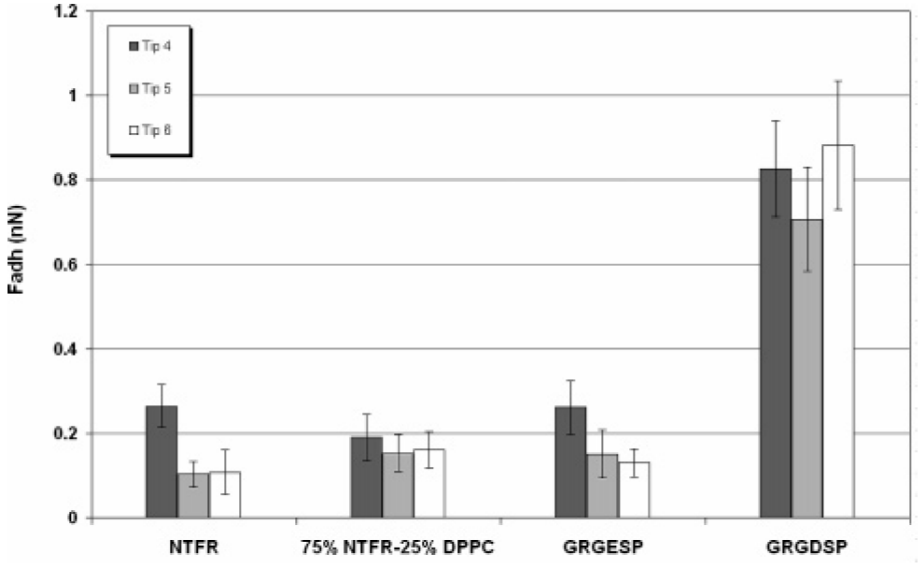

Figure 2.8 Adhesion measurements between AFM tips functionalized with $\alpha_5\beta_1$ integrins and different surfaces in 1 mM $MnCl_2$ solution at pH 6.5-7. Each column corresponds to an average of 30-40 force measurements on each surface. The error bars represent standard deviations and reflect the fact that the number of pairs that interact every time the two surfaces are brought into contact can vary from one measurement to another. Reprinted from [17], Copyright (2005) with permission from Elsevier.

The NTFR-$\alpha_5\beta_1$ interaction was of comparable value or smaller than the $\alpha_5\beta_1$-GRGESP interaction and much smaller than the $\alpha_5\beta_1$-GRGDSP adhesion as shown in Figure 2.8. GRGDSP is the specific ligand for $\alpha_5\beta_1$ and GRGESP is an inactive peptide that served as a negative control. The data presented demonstrates that the NTFR binds preferentially to fractalkine with an affinity that is comparable to the $\alpha_5\beta_1$-GRGDSP specific interaction, when comparing AFM adhesion forces. This suggests that the NTFR peptide when incorporated into liposomal membrane could promote binding of NTFR-liposomes to fractalkine expressing cell lines, and the results of these experiments are discussed in chapter 7.

3. Liposomes – as drug delivery systems

Liposomes were discovered four decades ago by Bangham et al. [100] as closed vesicles formed by the self-assembly of phospholipids in water. The ability of these vesicles to encapsulate solute molecules was quickly identified and formed the basis for use of liposomes as drug carriers in the early 70's [101, 102]. Subsequently, significant effort was made in this research area with liposomes ultimately finding their use as drug delivery systems. Table 3.1 lists liposomal drugs approved for clinical application or currently undergoing clinical evaluation [103].

Liposomes are phospholipid bilayer vesicles 0.025~5.0 μm in diameter which form spontaneously when certain lipids are hydrated in aqueous media. Figure 3.1 shows a schematic structure of liposomes. When dispersed in water the amphiphilic nature of the lipids, the hydrophilic headgroup and lipophilic tails, leads to their self-assembly forming closed bilayer vesicles. Bilayer vesicles are one of the several structures formed by lipids and depends upon the relative size of the headgroup and tail. Typically double chained lipids with large headgroup areas and fluid chains with truncated cone shape, form flexible bilayer vesicles [104].

Phospholipids are the building block of the cell membrane. Figure 3.2 shows the general structure of a phospholipid molecule [105]. A phospholipid consists of a glycerol backbone with a hydroxyl group at position 1 and 2 replaced by the fatty acid chains and position 3 is esterified to a phosphoric acid. One of the oxygen of the phosphoric acid is further esterified to organic molecules like glycerol, choline, serine, ethanolamine, inositol etc., forming the polar headgroup. The fatty acid chains constitute the lipophilic tail. The tails can be both symmetric and asymmetric and can contain saturated as well as

unsaturated carbon-carbon bonds. Phospholipids can be obtained from both synthetic and natural sources. Synthetic phospholipids are usually preferred over natural sources because of the possibility of viral contamination that can arise from the natural source. Saturated lipids (or with one unsaturated C-C bond in each chain) with 12 to 18 carbon-long chains are commonly used for making liposomes. DPPC (1,2-Dipalmitoyl-sn-Glycero-3-Phosphocholine) and DSPC (1,2-Distearoyl-sn-Glycero-3-Phosphocholine) are the usual choices for forming liposomes and are most commonly found phospholipids in the cell membranes.

Cholesterol is a steroid found in biological membranes and modulates the membrane fluidity, elasticity, and permeability. When incorporated in the membrane, it fills in the gaps between the lipid molecules due to their imperfect packing. Cholesterol is used in liposomes for improving the bilayer characteristics as it decreases the membrane fluidity and permeability to the solute molecules, thus making liposomes more stable under physiological conditions [105].

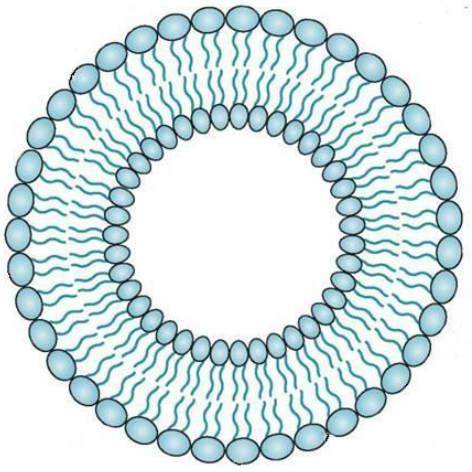

Figure 3.1 Liposomes are composed of phospholipid bilayer vesicles. Adapted by permission from Macmillan Publishers Ltd: Nature Reviews [103], Copyright (2005).

Table 3.1 Liposomal drugs approved for clinical application or undergoing clinical evaluation. Reprinted by permission from Macmillan Publishers Ltd: Nature Reviews [103], Copyright (2005).

Active drug	Product name‡	Indications
Daunorubicin	DaunoXome	Kaposi's sarcoma
Doxurubicin	Mycet	Combinational therapy of recurrent breast cancer
Doxorubicin in PEG-liposomes	Doxil/Caelyx	Refractory Kaposi's sarcoma; ovarian cancer; recurrent breast cancer
Amphotericin B	AmBisome	Fungal infections
Cytarabine	DepoCyt	Lymphomatous meningitis
Vincristine	Onco TCS	Non-Hodgkin's lymphoma
Lurtotecan	NX211	Ovarian cancer
Nystatin	Nyotran	Topical antifungal agent
All-*trans* retinoic acid	Altragen	Acute promyelocytic leukaemia; non-Hodgkin's lymphoma; renal-cell carcinoma; Kaposi's sarcoma
Platinum compounds	Platar	Solid tumours
Annamycin		Doxorubicin-resistant tumours
E1A gene		Various tumours
DNA plasmid encoding HLA-B7 and α2 microglobulin	Allovectin-7	Metastatic melanoma
Liposomes for various drugs and diagnostic agents (lipoMASC)		Broad applications

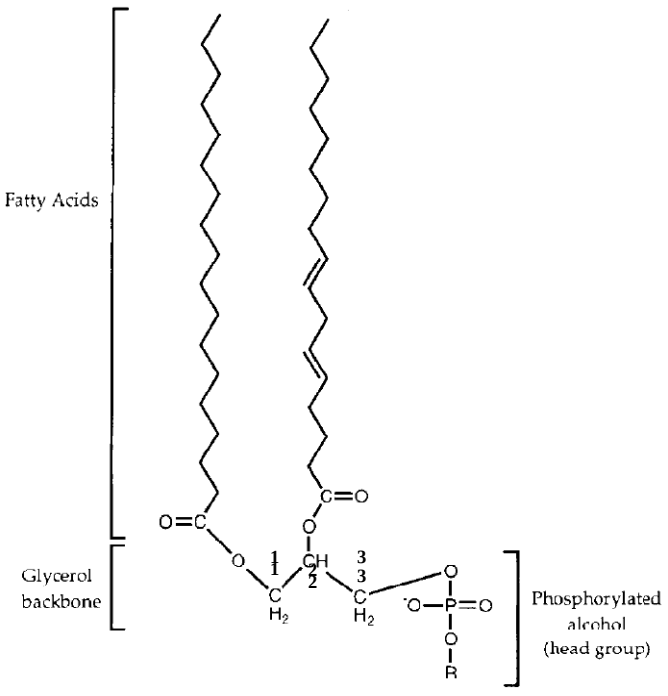

Figure 3.2 Structural formula of phosphatidic acid. Reprinted from [105], Copyright (1995), with permission from Elsevier.

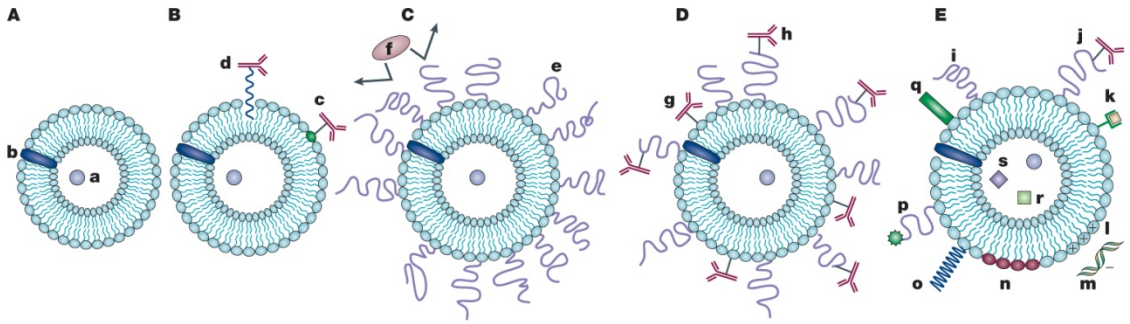

Figure 3.3 Evolution pattern of liposomes. Reprinted by permission from Macmillan Publishers Ltd: Nature Reviews [103], Copyright (2005).
A. Early traditional liposomes (or conventional liposomes) entrapping a water-soluble drug **(a)** into the aqueous core, and a water-insoluble drug **(b)** incorporated into the liposomal membrane. **B**. Targeted liposomes with antibody **(c)** covalently coupled to the reactive phospholipids in the membrane, or hydrophobically anchored **(d)** into the bilayer after preliminary modification with a hydrophobic moiety. **C**. Long-circulating liposome decorated with a hydrophilic polymer **(e)** usually PEG and protects the liposome surface from interacting with the opsonizing proteins **(f)**. **D**. Long-circulating targeted liposomes, decorated both with a protective polymer and an antibody, which can be attached either to the liposome surface **(g)** or to the distal end of the grafted polymeric chain **(h)**. **E**. New-generation liposomes, the surface of which can be modified (separately or simultaneously) by several moieties or can incorporate variety of molecules, each having different functions. These modifications include: attaching a hydrophilic polymer **(i)**; or a polymer and a targeting ligand, such as antibody **(j)**; attaching/incorporating a diagnostic label **(k)**; use of positively charged lipids **(l)** allows liposomes to complex with DNA **(m)**; including the stimuli-sensitive lipids **(n)** or the stimuli-sensitive polymers **(o)**; attaching cell-penetrating peptide **(p)** allowing for intracellular delivery or the incorporation of viral components **(q)**. In addition to a drug, liposomes can also be loaded with magnetic particles **(r)** allowing for magnetic targeting and/or with colloidal gold or silver particles **(s)** for electron microscopy.

3.1. Types of liposomes

Figure 3.3 shows a schematic evolution pattern of liposomes used in drug delivery [103]. Based on their composition there are several types of liposomes [106]:

a. *Conventional Liposomes*: The simplest liposomes just composed of neutral and/or negatively charged lipids and cholesterol as membrane stabilizer. They usually undergo coated-pit endocytosis and are rapidly taken up by the macrophages of the reticulo-endothelial system (RES), thus have short-circulation lifetimes and are useful for targeting RES.

b. *Long-circulating liposomes*: Short circulation lifetimes of conventional liposomes can be improved by incorporating PEG conjugated lipids, monosialoganglioside

(GM1) or hydrogenated phosphatidyl inositol (HP1) (5-10 mol%). The presence of hydrophilic molecules provides a steric barrier for adsorption of proteins and subsequently decreases their uptake by RES. Due to the hydrophilic coating these liposomes can circulate up to 100 times longer in blood as compared to conventional liposomes [107]. Circulation lifetimes of up to 48 hrs have been reported in humans for sterically stabilized liposomes.

c. *pH-sensitive liposomes*: These are usually made up of phospholipids such as dioleyl phospahtidylethanaolamine (DOPE) with cholesteryl hemisuccinate (CHEMS) or oleic acid (OA). They undergo endocytosis by the coated-pit mechanism, and destabilize at low pH thus delivering their contents intracellularly. They are useful for targeting region of inflammations where pH is slightly acidic.

d. *Temperature-sensitive liposomes*: These liposomes are made from phospholipids that undergo gel to liquid phase transition slightly above the normal body temperature. They can be useful in targeting the sites of inflammation where temperatures are slightly above 37°C or also could be forced to release their content at a specific location by local hyperthermia.

e. *Cationic Liposomes*: As the name suggests these liposomes have small positive charge on their surface and are suitable for intracellular gene delivery (since DNA is negatively charged). They are made of cationic lipids like POPC (palmitoyloleoyl phosphatidylcholine) and also possibly fuse with cell membranes and deliver their load intracellularly.

f. *Targeted liposomes*: This is the most advanced category of liposomes having the ability of specific recognizing their target *e.g.,* receptor-ligand identification. Usually they are either conventional liposomes or long-circulating liposomes with a targeting moiety attached to the surface of liposomes which could be either an antibody, peptide or aptamer. These liposomes can either undergo receptor-mediated endocytosis or release their contents extracellularly near the target.

Liposomes have been frequently characterized as “actively” or “passively” targeted depending upon the presence or absence of site directing ligands on their surface [16]. All the above liposomes fall under the category of passive targeting except targeted liposomes which have the active targeting capabilities.

3.2. Fate of liposomes

There are several factors which control the interaction of liposomes with cells and body, and the physicochemical composition of liposome formulations itself can affect the *in-vivo* behavior of liposomes. Therefore, a complete understanding of all the physicochemical aspects of liposomes is essential to realize their goal as DDS.

3.2.1. Interaction of liposomes with cells

Interaction of liposomes with cells can be grouped into several categories as follows [108]:

a. *Non-specific uptake*: This is primarily phagocytosis of liposomes by the macrophages of RES through the process of opsonization. The constitutive uptake of liposomes through the process of pinocytosis also falls under this category.

b. *Receptor-mediated endocytosis*: Liposomes coated with ligands specific for cell surface receptors are be taken up by the process of receptor-mediated endocytosis.

The choice of ligand is critical in determining whether the liposomes is internalized or remain bound on the surface.

c. *Fusion*: Liposomes incorporating fusogenic lipids or viral fusogens can enter cells by fusing directly with the plasma membrane and delivering their load intracellularly.

d. *Lysosomes*: After their uptake through endocytosis, liposomes are readily broken down in lysosomes. For drugs that are not stable under the extreme conditions present in lysosomes, pH-sensitive liposomes are used which are able to release their content earlier in the endocytotic pathways before reaching lysosomes.

3.2.2. Interactions with the whole body

Liposomes can be administered through a variety of routes into the body including intravenous, intramuscular, intraperitoneal and oral [109]. Usually intravenous is more practical and preferred route of administration. The interactions of liposomes *in-vivo* can be classified as [108]:

a. *Intravenous administration*: The RES through the process of opsonization rapidly takes up liposomes entering through blood streams. Coating of liposomes with PEG reduces opsonization and identification of liposomes by macrophages and thus increasing the circulation lifetimes.

b. *Natural tissue distribution*: The natural tissue distribution of liposomes is primarily determined by the size of liposomes as long as they are able to avoid RES. Small liposomes are able to pass through the fenestrae of the liver while the larger liposomes get lodged into the microvasculature (*e.g.* lungs). Intermediately sized liposomes usually show longer circulation lifetimes. The permeability of

vasculature can also effect the distribution of liposomes and this concept is exploited in passive targeting of tumors in chemotherapy.

c. *Targeting*: Liposomes labeled with targeting moieties are able to localize into tissues bearing their receptor provided the tissue is accessible through the systemic circulation.

d. *Lymphatic drainage*: Liposomes administered peripherally can enter the lymph tissue via the lymphatics. Here the liposomes bearing antigens can enter antigen-possessing cells and can evoke a strong immune response.

e. *Cutaneous administration*: Liposome formulations can be also be applied topically and can deliver their load to the dermis or transdermally.

f. *Oral delivery*: Oral delivery of liposomes can help in the uptake of drugs that get broken down by the digestive enzymes. After delivery, liposomes themselves get broken down by the digestive enzymes and gut surfactants, and the entrapped material gets dispersed in lipid micelles and eventually enters the systemic circulation.

3.2.3. Parameters affecting their behavior *in-vivo*

The physicochemical properties of the liposome formulations can be altered in order to optimize their drug content, stability, biodistribution and delivery. The parameters which modulate their behavior *in-vivo* are bilayer fluidity, surface charge, hydration and size distribution [110]:

a. *Bilayer fluidity*: Liposomes with higher fluidity are readily taken up by RES as compared to liposomes with lower fluidity [111]. Therefore usually lipids with phase transition temperature above 37°C are used for liposome formulations.

b. *Surface charge*: Both the charge density and its nature affect the interaction of liposomes with cells. Negatively charged liposomes are predominantly taken up by coated pit endocytosis [110]. Neutral liposomes do not interact with cells and drugs enter the cell after liposomes release their contents extracellularly [112]. While cationic liposomes undergo membrane fusion with the plasma membrane or endosome without undergoing degradation in lysosomes [113, 114].

c. *Surface hydration*: Presence of hydrophilic moieties like PEG, on the surface of liposomes prevents adsorption of plasma proteins on surface of liposomes and their subsequent uptake by macrophages [115, 116].

d. *Size distribution*: Liposomes smaller than 100nm in diameter are opsonized more slowly as compared to large liposomes (>100nm in diameter) [117]. Also the extravasation of liposomes to various tissues also depends on the size of liposomes.

3.3. Advantages of liposomes as drug delivery systems

In addition to the advantages of DDS, there are several advantages of liposomes which makes them superior as drug carriers in comparison to other DDS like microspheres, microcapsules, nanospheres, nanocapsules, dendrimers, etc. [118]. The foremost advantage is their biodegradability and biocompatibility because of their resemblance to cell membranes. Several polymeric systems are non-degradable and therefore sometimes present biocompatibility issues. Secondly, liposomes can carry large payloads of drug without the need of any special coupling techniques. Although polymeric systems carrying drug in their core also do not require these additional capabilities, but their carrying capacities are limited. Liposomes have another advantage

of being capable of carrying both hydrophilic and lipophilic drugs. This is a great added feature when compared to several other DDS, which are capable of carrying only one of the species. The flexibility of size and composition, aids in tailoring the liposome as dictated by the needs of the drug and its target. However, in contrast to the polymeric carriers which are relatively stable, liposomes face stability issues and have shorter shelf life and circulation lifetimes. Therefore liposomes require special modifications like coating the liposome surface with hydrophilic polymer like PEG [116] to increase their circulation lifetime and other special handling techniques like lyophilization for improving their stability and shelf life.

3.4. Long circulating liposomes

Conventional liposomes are rapidly taken up by the macrophages of reticulo endothelial system and thus have short circulation lifetimes. Long circulating liposomes have special surface properties to evade this rapid uptake and can circulate upto 100 times longer in blood as compared to conventional liposomes [107]. The first generation consisted of liposomes incorporating ganglioside GM1 or hydrogenated phosphatidylinositol in their phospholipid bilayer [111, 119]. These liposomes were called ‘stealth liposomes®’. However, GM1 comes from an animal source and thus is expensive and poses potential risk of viral contamination [120]. The next generation consisted of liposomes containing lipids conjugated with polyethylene glycol (PEG) like distearoyl phosphatidylethanolamine-polyethylene glycol (DSPE-PEG). The hydrophilic polymer on the surface of the liposomes prevents opsonization, increasing their circulation life times. This class of liposomes was called ‘sterically stabilized liposomes’. These liposomes are preferred over their predecessors in therapeutic application both

because of low cost and increased safety. Several PEG based liposomes formulations have already received FDA approval and are currently being used in clinical practice (Table 3.1).

Sterically stabilized liposomes have great potential as therapeutical carriers and have been used in two major types of applications and a third is currently under intense research [15, 120]. These classify as:

a. *Carriers for sustained release*: Drugs having short half-life in the body can be encapsulated in liposomes. This will prevent them from degradation and will favorably alter the pharmacokinetics and biodistribution of the drug.

b. *Passive targeting to diseased tissue*: Sterically stabilized liposomes have long circulating lifetimes and extravasate into tissue regions of the body having 'leaky vasculature' (blood vessels having increased permeability). For example, in angiogenesis (formation of new blood vessels) or in tumors, blood vessels have increased permeability as compared to normal vasculature and small liposomes accumulate in these regions.

c. *Actively targeted sterically stabilized liposomes*: This is the latest generation of liposomes and is currently under intense research. These liposomes have both the steric properties and ability to identify their target specifically. The site-specific targeting could be achieved by attaching a "homing device" to the liposomes surface such as monoclonal antibody or a receptor-specific ligand. These devices can either be directly attached on the surface or liposome along with PEG molecules or can be attached at the distal end of the polymer chain. Ideally it will be desirable to design targeted liposomes capable of delivering drug solely to the

diseased tissue. However in reality a significant portion of dose may never be able to locate its target and will undergo biodistribution and clearance mechanisms similar to those for passively targeted liposomes. In designing targeted liposomes, the choice of the target site and the method of ligand targeting are the most critical parameters which ultimately will dictate their effectiveness as DDS and were discussed in chapter 2 [16].

4. Liposomes – preparation and characterization

4.1. Preparation of liposomes

Liposomes invented in 1960's have gone through an intense research, due to the interest arising from their inherent resemblance to cell membranes. Liposomes are formed when thin lipid films are deposited onto a glass substrate and hydrated in water. Upon hydration above their glass transition temperature, lipid films become fluidic and swell to form stacks of liquid crystalline bilayers. When agitated these hydrated lipid sheets detach to form large closed structures called multilamellar vesicles (MLVs). The formation of closed structures prevents water from interacting with the hydrocarbon core of the bilayer. Once formed these vesicle are reduced in size by sonication or extrusion. Figure 4.1 represents a schematic diagram for formation of liposomes.

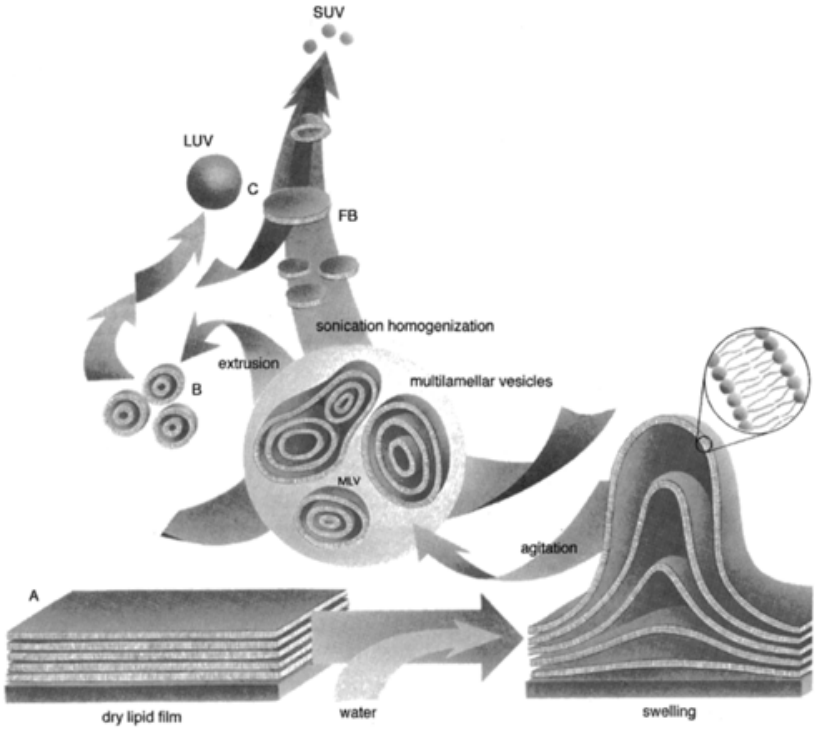

Figure 4.1 Schematic representation of liposome formation. Reprinted from [121], Copyright 1997 with permission from CRC Press.

As of today, several methods are available for preparing liposomes, giving rise to vesicles of different size, distribution, and encapsulation efficiencies. The choice of the method is dictated by the needs of the investigator based on the above-mentioned parameters. Broadly, these can be divided under three categories:

4.1.1. Mechanical methods

a. *Film Method*: This is the simplest method for preparing liposomes, originally developed by Bangham et al. [100], but has limited applicability due to low encapsulation efficiency. This technique involves deposition of a thin film of lipids on a glass wall by shaking at temperatures above the T_g (glass transition temperature) and removing the solvent at reduced pressure in a rotary evaporator. The dried lipid film is then hydrated with a buffer containing a water-soluble marker. As the lipid gets hydrated they start to form closed vesicles entrapping only small amounts of the solute. This technique yields a heterogeneous sized population of MLVs over 1 μm in diameter and homogenization techniques are further employed to achieve a unimodal distribution.

b. *Ultrasonication:* This technique involves ultrasonicating an aqueous mixture of phospholipids in a bath or probe sonicators. This technique usually results in small unilamellar vesicles (SUVs) down to 25 nm in diameter.

4.1.2. Methods based on organic solvent removal

a. *Ether vaporization method*: In this method a mixture of phospholipids is dissolved in an organic solvent (diethyl ether, ethanol, etc.) and injected slowly into a warm aqueous media. This technique yields unilamellar vesicles with high

encapsulation efficiencies (ten times of the sonicated and handshaken vesicles) which are osmotically active and have well defined size distribution [122].

b. *Reverse-phase evaporation (REV) method*: The mixture of phospholipids is added to a round bottom flask and the solvent is removed in a rotary evaporator under reduced pressure. The system is purged with an inert gas to prevent oxidation of lipids. Lipids are re-dissolved in an organic phase (usually diethyl ether and isopropyl ether) and the aqueous phase is added, while keeping the system continuously under an inert gas. The two-phase system is sonicated until it becomes a clear one-phase dispersion. Organic solvent is removed again over a rotary evaporator until a gel is formed. Non-encapsulated material is removed using a gel filtration column. The resulting large unilamellar vesicles have high encapsulation efficiencies [123].

4.1.3. Methods based on resizing of preformed vesicles

a. *Freeze-thaw extrusion method*: MLVs obtained from the film method are subjected to repeated freeze–thaw cycles (freeze in a dry ice/acetone bath or liquid nitrogen, thaw in water above T_g and vortex). The dispersion is extruded several times through a stack of polycarbonate membrane of definite pore size and the resulting liposomes are called large unilamellar vesicles by extrusion technique (LUVET) [124, 125]. The LUVETs typically have very high internal solute concentrations as compared to the external solute concentrations.

b. *Dehydration-rehydration method*: This method involves a process dehydration followed by rehydration in order to entrap solute molecules inside the liposomes. SUVs suspended in buffer are mixed with the solute and freeze dried. The freeze-

dried vesicles are then rehydrated in limited amount of water. The vesicles become more concentrated during dehydration and flatten and fuse to form multilamellar planes where the solute is sandwiched, resulting in formation of larger vesicles. Although being a simple technique performed under mild conditions, the major limitation is the heterogeneity in the size population of the liposomes obtained upon rehydration [126].

c. *Detergent removal method*: In this method the lipids are first solubilized in an aqueous solution of detergent containing the solute or the protein to be encapsulated. The detergent is later on removed by dialysis (detergent concentration should be above critical micelle concentration so that it is easily removed by dialysis). This results in formation of liposomes within a narrow size range of 80 to 200 nm. This method is particularly suitable for reconstitution of membrane proteins in liposomes [127].

Amongst the above-mentioned techniques, LUVET is the most widely used for laboratory preparation of liposomes. In addition to being an easier technique, the other advantages include high encapsulation efficiency, homogenous size distribution and reproducibility.

Liposomes were prepared using the LUVET method in this work. Lipids were dissolved in chloroform in desired stochiometric ratios. Peptide-amphiphiles are not soluble in chloroform and therefore they were dissolved in water and mixed with the lipid-chloroform mixture. Few drops of methanol were added until solution became clear. Solvents were removed by evaporating under a gentle stream of argon at 65°C. Lipid film was re-dissolved in chloroform and dried again under a gentle stream of argon at 65°C.

Sometimes it was necessary to add couple of drops of methanol in the re-dissolving stage to form a homogenous mixture of lipids with the peptide-amphiphile. In that case, the re-dissolving and re-drying steps were repeated until the mixture dissolved in pure chloroform. This was followed by drying the film under vacuum overnight. The lipid film was hydrated in an appropriate buffer at 65°C at a concentration of 10 mM total lipids and osmolarity of 300 mOsm. Hydrated lipids were freeze-thawed five times, then extruded for 21 cycles through two stacks of 100 nm polycarbonate membranes using a hand-held extruder.

Liposomes were purified over a Sepharose CL-4B column to remove unencapsulated fluorescent dye or drug, which did not get incorporated in the liposomes. Figure 4.2 shows a typical chromatogram obtained over a fast performance liquid chromatography (FPLC) machine AKTA-FPLC from GE Biosciences. The first peak at the void volume is liposomal peak which is collected over a fraction collector and the second peak at column volume is the peak for unencapsulated fluorescent dye or drug. Liposome were stored at 4-8°C and used within two weeks of preparation.

4.2. Synthesis and characterization of peptide amphiphile

Peptide-amphiphiles, as the name suggests are molecules that have both hydrophilic and lipophilic properties. The first structures of bilayer forming peptide-amphiphiles were suggested by Kunitake et al. [128], where a peptide headgroup (hydrophilic component) is connected to dialkyl carbon tail using a connector and spacer (lipophilic component). Figure 4.3 shows the structure of the peptide-amphiphile synthesized in the Kokkoli lab and used to functionalize liposomes with peptide moieties.

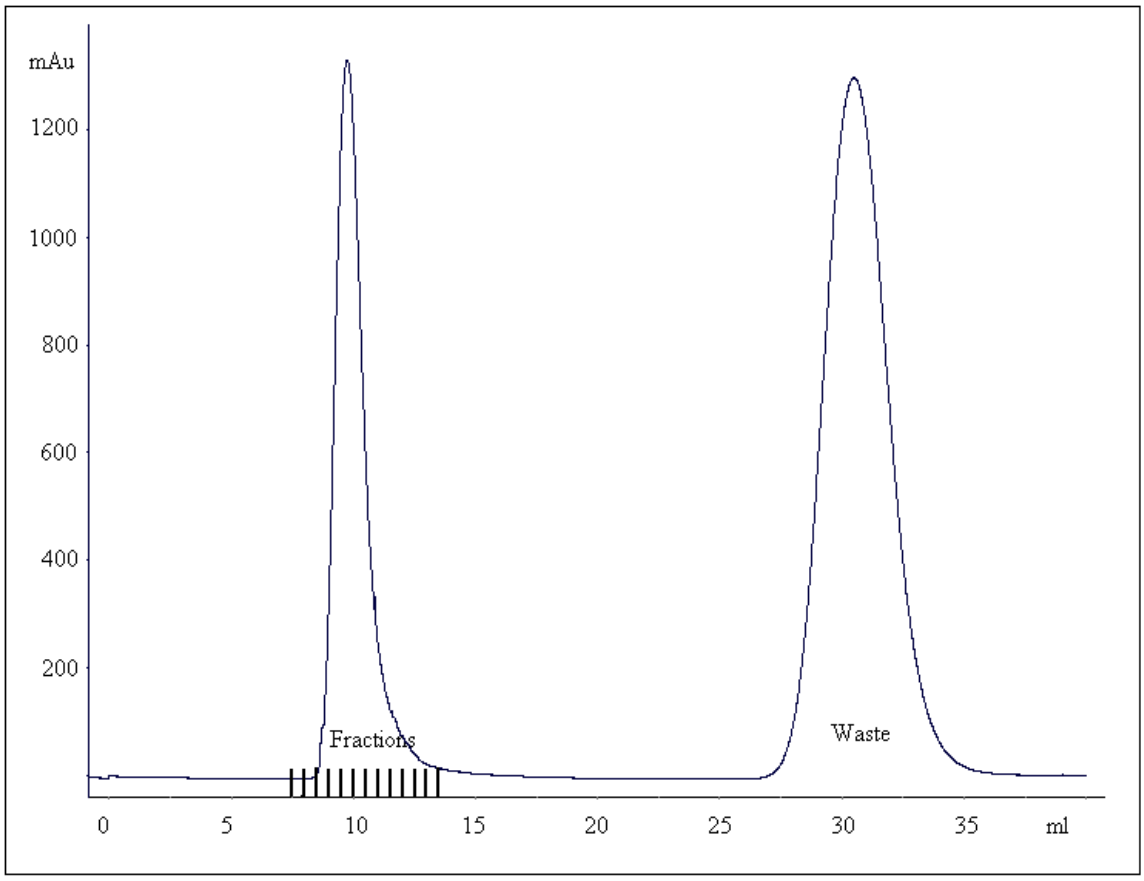

Figure 4.2 Typical liposome purification chromatogram obtained over a FPLC machine. First peak is the liposomal peak which is collected on a fraction collector. Second peak corresponds to unencapsulated dye or drug and is sent to waste.

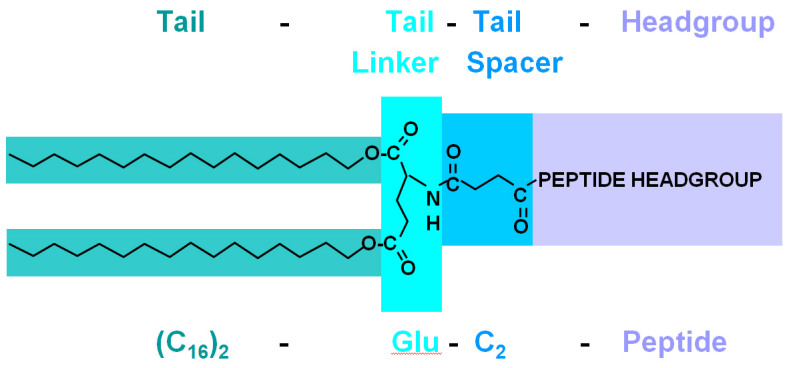

Figure 4.3 Structure of Peptide amphiphile. Peptide-amphiphiles consist of hydrophilic headgroup and lipophilic tails. These molecules can self assemble in bilayers when mixed with other bilayer forming lipids to form functionalized liposomes.

The structure consists of a peptide headgroup (hydrophilic component) connected to a lipophilic component. The lipophilic component (tail-liker-spacer) of the peptide amphiphile consists of two alkyl tails (usually 16 carbon tails) linked together with a glutamic acid and connected with a two carbon spacer. The peptide amphiphiles were synthesized in a two step process as described by Anastasia Mardilovich [76] with slight modifications. The tails were synthesized in solution phase and peptide-amphiphiles were synthesized by coupling peptides to the tails using a solid-phase peptide synthesis.

4.2.1. Synthesis of lipophilic component

Synthesis of the lipophilic component is a two step process as shown in Figure 4.4 and described below. The protocol was obtained from the previous work of Dr. Kokkoli, adapted from Asakuma et al. [129].

In the first step, the two alkyl tails were linked to the glutamic acid with ester bond formation by a condensation reaction in toluene, in the presence of p-toluene sulfonic acid monohydrate (pTos). The L-glutamate (glutamic acid) not only allows the two tails to be linked together but also provides the correct spatial arrangement to the tails, so that the amphiphilic molecules have right molecular architecture for bilayer formation. In the next step, the tail-linker component was further linked to a two carbon spacer, which is added in order to extend the bioactive sequence away from the interface. This was carried out using an acylation reaction of tail-linker with succinic anhydride in equimolar mixture of tetrahydrofuran/chloroform and in the presence of n,n-diisopropylethylamine (DIEA). The product (tail-linker-spacer) was recovered from the solution phase by repeated crystallization in cold ethyl acetate (-20°C) and was dried and the structure was verified with nuclear magnetic resonance (NMR).

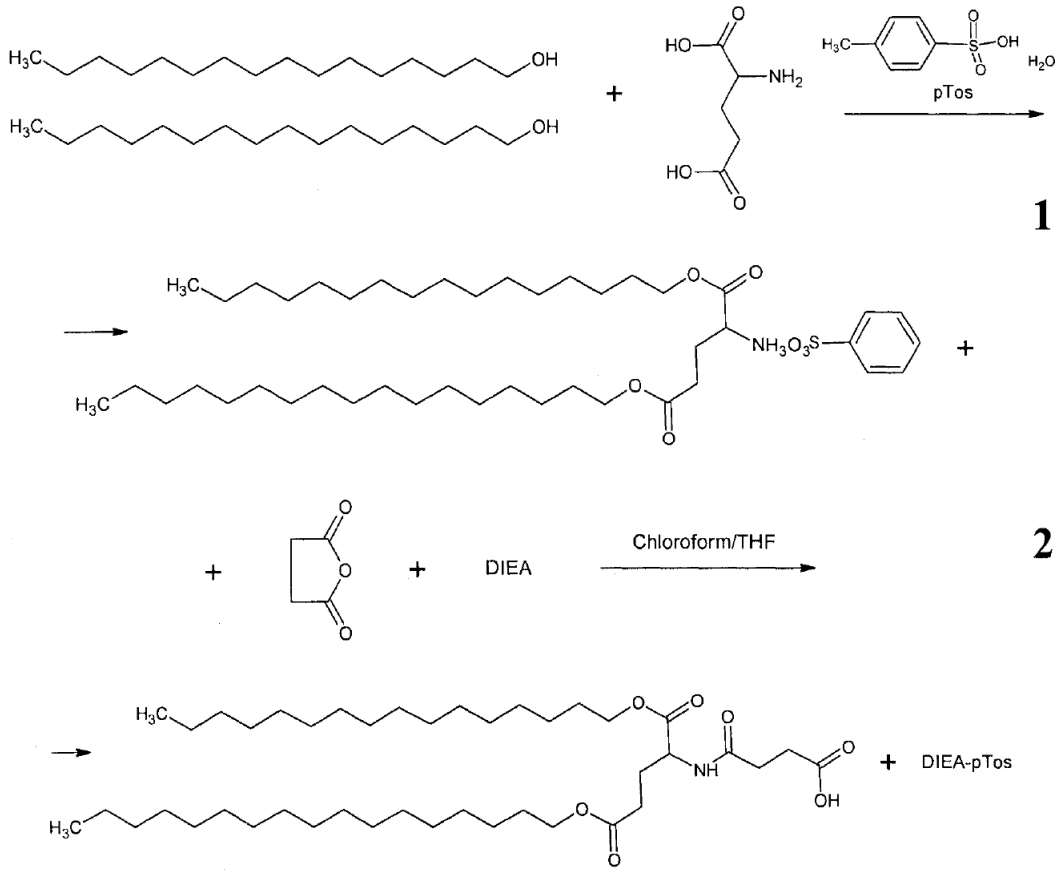

Figure 4.4 Schematic reaction diagram of tail-liner (1) and tail-linker-spacer (2) synthesis procedure. Reprinted from [76], Copyright (2006) with permission from Mardilovich.

4.2.2. Synthesis of peptide-amphiphiles

Peptide-amphiphiles were synthesized by conjugation of the N-terminus amine of the peptide headgroup to the carboxylic group present on the lipophilic component using a solid phase peptide-amphiphile synthesis. The synthesis protocol obtained from the previous work of Dr. Kokkoli and adapted from Berndt et al. [130], served as a starting point. During the course of work, several improvements and modifications developed in the Kokkoli lab, were incorporated in the protocol. Peptides were obtained from the Oligonucleotide and Peptide Synthesis Facility at the University of Minnesota. Peptides were ordered linked to the resin beads (PAL resin) on the C-terminus with a free amine

on the N-terminus. The peptides were obtained in the protected form, with Fmoc protection on the amine end and all the side chain groups protected.

Figure 4.5 shows a schematic protocol for the synthesis of peptide-amphiphile. Before the start of synthesis it was ensured that beads were fully swollen. This was carried out by transferring the beads to a reaction vessel and shaking them in dichloromethane (DCM) for a minimum of 30 min. After the beads were fully swollen up, the base-labile Fmoc group protecting the N-α-amine was selectively removed by shaking the beads with 20% piperidine in dimethylformamide (DMF) for 20 min (Step 1). The beads were thoroughly rinsed 2-3 times with DMF to remove excess piperidine and the presence of free amine was verified by the formation of blue color on the beads with the Kaiser test [131]. This was followed by the coupling step. The coupling mixture was prepared by dissolving the tails (lipophilic component) in 50:50 mixture of DMF/DCM with the peptide coupling reagent HBTU (o-benzotriazole-n,n,n’,n’-tetramethyl-uronium-hexafluoro-phosphate) and DIEA (n,n-diisopropylethylamine). The coupling mixture was then added to the peptide-resin beads in a four to six fold molar excess with respect to the molar amounts of peptide and was allowed to react with the free amine group on the peptide for 2-3 hrs (Step 2). The reaction was stopped by removing the solvent and rinsing the beads several times with DMF. The beads were rinsed finally with DCM to remove residual DMF and were dried in vacuum overnight. The completion of coupling reaction was verified by the presence of clear beads with the Kaiser test. The coupled product (*i.e.*, peptide amphiphile) was deprotected and cleaved off the solid support by shaking for 2-3 hrs in a round bottom flask with the cleaving reagent B (triisopropylsilane-phenol-water-trifluoroacetic acid, 2.5:5:5:87.5) as shown in Step 3.

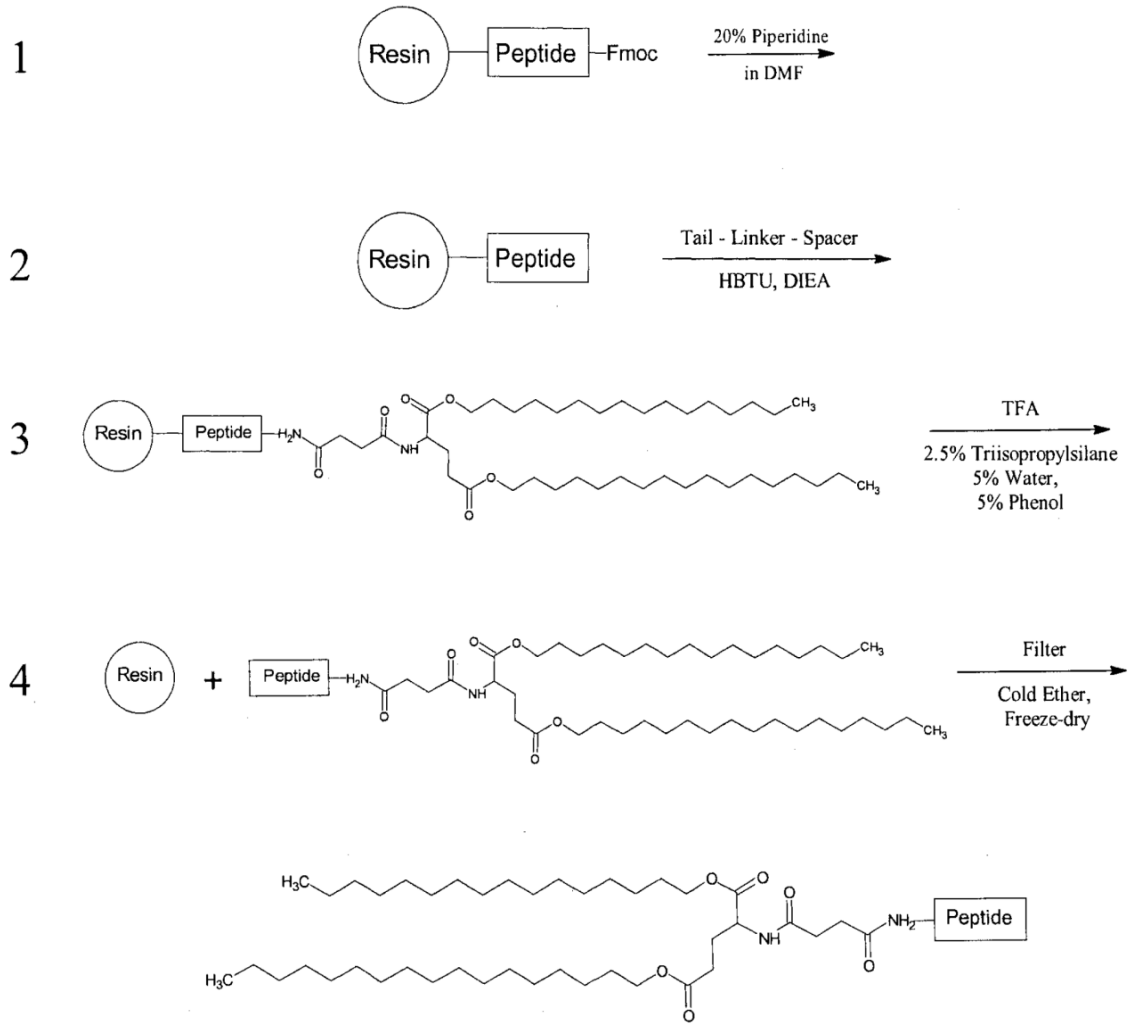

Figure 4.5 Solid phase peptide-amphiphile synthesis procedure. Reprinted from [76], Copyright (2006) with permission from Mardilovich.

The peptide-amphiphile was recovered from the solution by removing the beads with a buchner funnel and precipitating the peptide-amphiphile in cold diethyl ether (-20°C) (Step 4). The vessel was stored overnight at -20°C to ensure the precipitation process was complete (this step increases the yield). Precipitate was recovered by centrifuging the mixture at 5000 rpm for 10 min and 4°C. The supernatant was removed and the pellet was re-dissolved in minimal amount of DMF and precipitated again with cold diethyl

ether (-20°C). The above step of centrifuging and re-dissolving was repeated several times (usually 4-5 times) until a white pellet was obtained. This ensures maximum removal of the residual coupling and cleaving reagents. The pellet was finally dissolved in MilliQ water and freeze dried over a lyophilizer.

4.2.3. Purification and characterization of peptide-amphiphiles

Peptide-amphiphiles obtained from the post-synthesis purification with ether were still in crude form and they contained impurities like un-reacted lipophilic component, peptide, and other chemicals used during synthesis. Therefore it was necessary to purify the crude peptide-amphiphiles before incorporating them in the lipid bilayers. Peptide-amphiphiles were purified on a semi-prep RP HPLC (reverse phase high performance liquid chromatography) from Agilent 1100 (Agilent Technologies Inc., Palo Alto, CA) using a Macrosep C_4 column from Shimadzu Scientific Instruments (Columbia, MD). Crude peptide-amphiphiles were obtained from the lyophilizer in powder form and were dissolved in 50% ACN (acetonitrile) and 50% water containing 0.1% TFA (trifluoroacetic acid) at an approximate concentration of 1 mg/ml. To improve the solubility of crude peptide-amphiphiles, sometimes it was necessary to lyophilize the crude peptide-amphiphiles several times by dissolving them in pure water, re-freezing, and re-lyophilizing. All solvents used were of HPLC grade and the mobile phase consisted of ACN and water with 0.1% TFA.

Separation was done at 30°C using a gradient method and the gradient profile is shown in Table 4.1. Fractions were collected at every 0.5 min and the fractions corresponding to different peaks were analyzed with a mass spectrometer, ESI (electrospray ionization) or MALDI (matrix-assisted laser desorption/ionization), for

presence of peptide-amphiphile. The vials corresponding to the peptide-amphiphile were collected together and the organic solvent from the purified product was evaporated under gentle stream of argon (or air) and lyophilized.

MALDI is a soft-ionization mass spectrometry technique used for analysis of biomolecules (also polymers and other large organic molecules) which are prone to dissociation or fragmentation when ionized using conventional techniques. A matrix is used to assist vaporization and ionization of biomolecules, and in addition, the matrix protects the biomolecules against disintegration from the direct laser beam. 2,5-dihydroxy benzoic acid (DHB) was used as matrix for analysis of molecular weight. Samples were prepared by making a saturated solution of DHB in tetrahydrofuran (THF) and applying 0.5 μl of the solution on to the sample plate. The matrix was allowed to dry for few minutes and later 1.0 μl of the purified fractions (from HPLC) were applied to the sample plate. The plate was finally dried for 30 min under vacuum and the samples were assayed on a MALDI operating in the reflectron mode.

ESI is a mass spectrometry technique similar to MALDI, except instead of using matrix to ionize the sample, a fine aerosol of sample is sprayed in to the ionization chamber under high vacuum. The ions are formed by extensive solvent evaporation and therefore typically the solvents used for ESI are prepared by mixing water with organic solvents (e.g. methanol, acetonitrile). For analysis of HPLC fractions using ESI, no further processing of the sample was necessary as the mobile phases contained both water and ACN. All the fractions corresponding to the peaks of interest were analyzed as described earlier using ESI or MALDI and the resulting pure peptide-amphiphile was dried, lyophilized, and stored for future use at -20°C.

Table 4.1 Solvent profile used for HPLC purification of peptide-amphiphile with the gradient method.

Time (min)	% Acetonitrile
0	30
5	30
32	46
53	95
60	95
68	30

4.3. Synthesis of aptamer-functionalized liposomes

Aptamer functionalized liposomes were synthesized using the post conjugation method of attaching amine modified ligands on preformed liposomes. The protocol described by Farokhzad and coworkers for the conjugation of aptamers to polymeric nanoparticles served as a starting point [12, 132, 133]. During the course of synthesis, several improvements and modifications were made in the protocol, to optimize it for the conjugation of aptamers to liposomes. Liposomes were prepared using the LUVET method as described in section 4.1, with a ratio of 60:35:5 of DSPC:Chol:DSPE-PEG2000-COOH, in an amine free 0.1 M MES buffer at pH 7.4 Figure 4.6 describes a schematic protocol for the conjugation of aptamers to the liposomes.

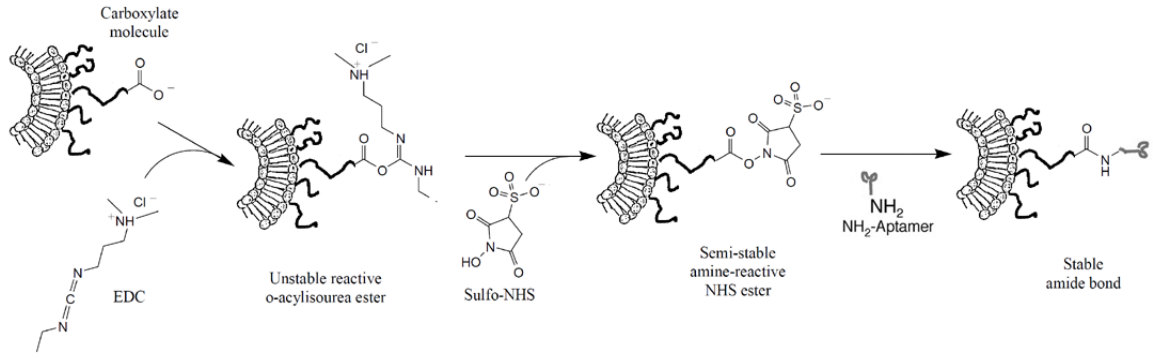

Figure 4.6 Schematic reaction diagram for conjugation of amine modified aptamer to liposomes bearing carboxyl groups.

To activate the COOH groups on the liposomes, EDC (1-ethyl-3-(3-dimethylaminopropyl) carbodiimide) at a concentration of 10 mM and NHSS (Sulfo-NHS, N-hydroxysulfosuccinimide) at a concentration of 25 mM were added to the liposome formulation. The activation reaction with EDC and NHSS is most efficient in MES buffer at pH 4.7-6.0 [134], therefore the pH of the mixture was decreased to 5.4 (by addition of small amounts of HCl) and the mixture was incubated at room temperature for 30 min under gentle shaking. This results in the formation of a semi-stable NHSS ester, which is then reacted with primary amines to form amide crosslink. Amine modified aptamers at a concentration of 10 mg/ml were added to the activated liposome mixture and the pH was raised back to 7.5 (by addition of small amounts of NaOH) because the reaction of NHSS-activated molecules with primary amines is most efficient between pH 7-8.

Typically 1 mg of aptamer was added to a 5 μmoles (total lipid) of liposome sample. Activated liposomes were allowed to react with amine modified aptamers for 2-3 hrs at room temperature. After conclusion of reaction, liposomes were purified over Sepharose CL-4B column to remove un-conjugated aptamers as described in section 4.1. Aptamer concentration was determined using the assay as described later.

4.4. Characterization of liposomes

The primary focus of this thesis has been towards the development of an optimal liposomal formulation which have targeting capabilities and show enhanced intracellular release when taken up by the cells. Therefore complete physicochemical characterization of liposomes is essential for complete understanding of the system. Liposomal formulations used in every single experiment were fully characterized in terms of their

chemical composition and physical properties. The experimental methods are discussed below with examples from the preparation of a typical liposome formulation. The compositions of liposomes listed are stochiometric concentrations at the lipid mixing stage.

4.4.1. Phosphate assay

In order to determine the concentration of lipids (including phospholipids, cholesterol and peptide-amphiphile) in liposomal formulation, total inorganic phosphorus concentration was assayed using a method developed by Chen et al. [135]. The organic phosphate in lipids (50 μl of liposomal sample) was first digested using an 8.9 N H_2SO_4 solution (450 μl) and heated at 210-220°C for 30 min to ash the sample. This was followed by addition of 30% hydrogen peroxide (150 μl) and further heating at 210-220°C for another 30 min. A clear sample should be obtained after the last step. The sample was cooled to room temperature and diluted with 3.9 ml of de-ionized water and the inorganic phosphate was complexed with 10% ascorbic acid (500 μl) and 2.5% ammonium molybdate solution (500 μl), which yields a color dependent on phosphorous concentration. To speed the color formation samples were covered and heated at 100°C for another 10 min and cooled to room temperature. Absorbance was measure at 820 nm on a SpectraMax Plus384 spectrophotometer using standard 1 cm polystyrene cuvettes.

A standard curve was generated for a 0.65 mM phosphorous standard solution. Figure 4.7 shows a phosphorous standard curve obtained from the colorimetric assay described above. Table 4.2 shows that the phosphorus content of liposome samples can be obtained from the standard curve and using the stochiometric composition of lipids, total lipid concentration of liposomes can be obtained.

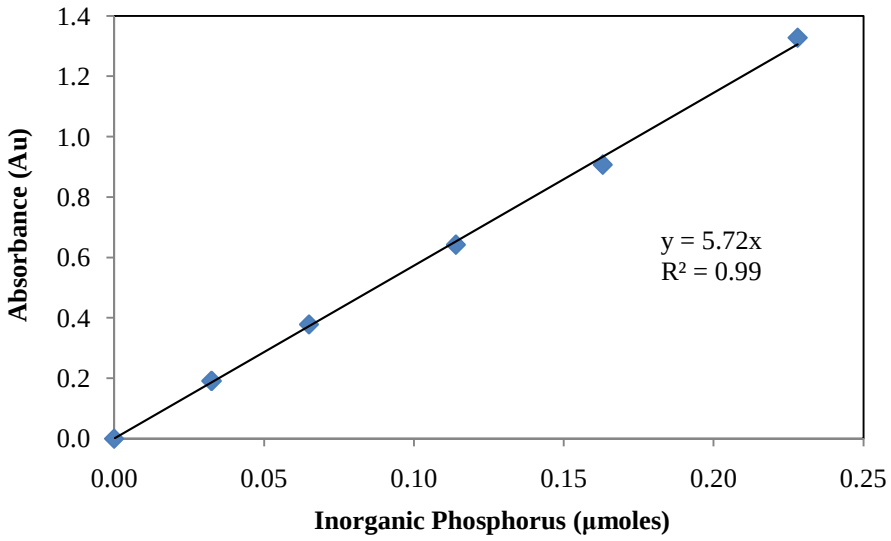

Figure 4.7 Phosphorus standard curve obtained from the phosphorus colorimetric assay.

Table 4.2 Lipid concentration of liposomes can be calculated from phosphorous assay since stochiometric amount of phospholipids in a liposomal formulation is known.

Liposome Sample (mol%)	Absorbance (820nm)	Amount of Phosphorus (µmoles in 50µl)	Concentration of Lipids (mM)
0% PR_b 2% PEG2000	0.568	0.0990	3.0463
2% PR_b 2% PEG2000	0.442	0.0769	2.4416
5% PR_b 2% PEG2000	0.536	0.0923	3.0777
2% RGD 2% PEG2000	0.544	0.0902	2.8627
5% RGD 2% PEG2000	0.549	0.0850	2.8321

4.4.2. Peptide assay

The amount of peptide that gets incorporated in the liposomes can vary from the stochiometric ratios added in the lipid mixtures. This is because of the presence of the peptide headgroup can affect the mixing behavior of lipids due to interactions like electrostatic, van der Walls etc. Moreover, due to the bilayer structure of the liposomes, some percentage of the peptide will also be present in the inner bilayer and will not contribute to the binding. Therefore it is critical to determine the percentage of peptide

present on the exterior surface of the liposomes. Peptide concentrations were determined using the bicinchoninic acid (BCA) protein assay [136]. BCA protein assay exploits the biuret reaction which is reduction of Cu^{2+} to Cu^{1+} by protein in an alkaline medium and is detected using a highly sensitive and selective colorimetric detection reagent containing bicinchoninic acid by measuring the absorbance at 562 nm.

A calibration curve (Figure 4.8) was first generated by dissolving known amounts of peptide in the buffer in which the liposomes were reconstituted in. To determine the peptide concentrations on the exterior of surface of liposomes, intact liposomes were used, while the total peptide incorporated in the liposomes was determined by lysing the liposomes with 4% SDS (sodium dodecyl sulfate) (w/v). Table 4.3 shows how the total amount of peptide in liposomes, calculated from the BCA assay and the phospholipid concentration described in the last section. Typically the ratio of 6:4 is observed, between the exterior and the interior peptide concentration for peptide functionalized liposomes.

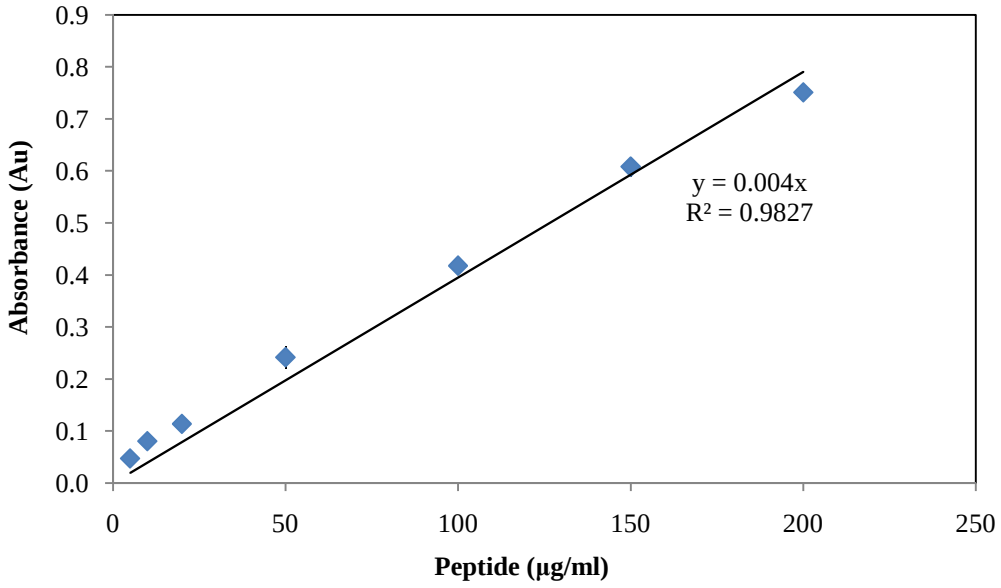

Figure 4.8 Peptide standard curve obtained from BCA protein assay.

Table 4.3 Peptide concentration of liposomes can be calculated from BCA protein assay. Peptide concentration of liposomes in mol% can be obtained from the lipid concentration of liposomes.

Liposome Sample (mol%)	Absorbance (562nm)	Concentration of PR_b (mg/ml)	Concentration of PR_b (mM)	Concentration of lipids (mM)	PR_b (mol%)
0% PR_b 5% PEG2000	0.0149	3.7250	1.3205	1673.70	0.1
5% PR_b 2% PEG2000	0.3540	88.5000	31.3719	1415.52	2.2

4.4.3. PEG assay

Determination of PEG concentration in liposomes is also an important factor for an optimal liposomal design. However PEG concentration in the liposomes could not be determined accurately due to experimental limitations. Following methods were explored for estimation of PEG but had limitations as described below:

a. *Complexation with Barium Chloride and Iodine* [137-141]: This method is a colorimetric assay based on a complex formation between barium-iodide and PEG which produces a band at 535 nm. However, this assay suffers because of the formation of precipitate in the liposomal samples during estimation. Sample wells cannot be directly measured over a plate reader because the precipitate formation hindered the light path during the absorbance measurement. Measuring the absorbance of supernatant after centrifuging the samples did not yield any conclusive results. One reason for the formation of precipitates could be the presence of lipids and peptides. Therefore an additional step for precipitating out the lipids and proteins using trichloroacetic acid was also explored. However when absorbance was measured, the readings for all samples were within the

standard deviation of each other and therefore the amount of PEG could not be estimated using this method.

b. *Ferrothiocyanate Method* [142, 143]: This method is also a colorimetric assay based on the partitioning of a chromophore present in the ammonium ferrothiocyanate from an aqueous to an organic phase in the presence of PEG. For estimation of PEG in stealth liposomes, enzymatic digestion of lipids is employed using phopholipase C to prevent interference from phospholipids. The organic phase is separated from the aqueous phase by centrifuging the mixture and then the absorbance of the organic phase is measured. The results from the absorbance measurements did not correlate with the sample. Experimental error was very high in this experiment as the chromophore could easily diffuse from the organic to the aqueous phase even on slight tapping of the sample. Since this method has been successfully used by other groups [142, 143] for estimation of PEG at higher concentrations, the problem with our present system could be that this method is not suitable for very low concentrations of PEG.

c. *Picric Acid Method* [144]: This method is another colorimetric assay based on the partitioning of a chromophore present in the sodium nitrate picrate solution, from an aqueous to an organic phase in the presence of PEG. This method requires significant amounts of sample which makes it difficult to work with based on the smaller amounts of sample we prepare for our experiments. Also standard deviations were very high due to the possibility of mixing when separating the aqueous and the organic layers.

d. *Bradford Assay* [145]: This assay is basically a protein assay which detects PEG using the peptide bond present on lipidated PEG molecules (one per molecule). Apparently this method also employs significant amounts of sample volume. Additionally, due to the presence of peptide in the liposomes the signal from PEG molecules is very weak. From the assay results we did not find any co-relation in absorbance measurements, either in the samples or the calibration curves which leads to that this method is not suitable at our working concentrations.

4.4.4. Drug concentration assay

5-Fluorouracil (5-FU) is a commonly used chemotherapy agent for the treatment of colon cancer. Free 5-FU has been used in clinical practice for more than 40 years but has serious side-effects such as gastrointestinal and bone marrow toxicity. Encapsulating 5-FU in liposomes can help its delivery to the target organs and reduce side effects [146, 147]. To study cytotoxicity of liposomes, different liposomal formulations encapsulating 5-FU were prepared and it was necessary to accurately estimate the concentration of 5-FU in liposomes. 5-FU strongly absorbs at 260 nm while other liposome components including lipids, peptides, and salts do not absorb in this range. Absorption spectra of all different components of liposomes were generated between 190 nm to 390 nm. The amount of 5-FU encapsulated in liposomes was determined by dissolving liposomes in 90% methanol (v/v) and measuring the absorbance at 260 nm.

A calibration curve was generated by dissolving known amounts of free 5-FU in 90% methanol and 10% liposomal buffer. Figure 4.9 shows calibration for 5-FU and Table 4.4 lists the 5-FU concentration in typical liposome formulations obtained from the absorbance data and calibrating it against the 5-FU standard curve.

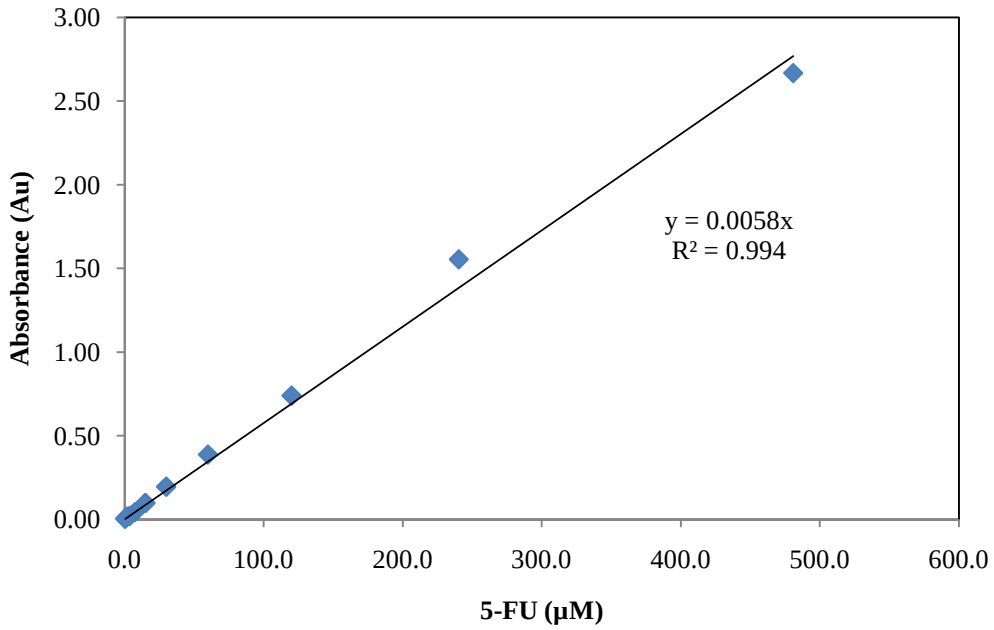

Figure 4.9 Standard curve for 5-FU obtained from absorbance measurement at 260 nm. The curve is linear within the concentration range of interest.

Table 4.4 Concentration of 5-FU in liposomes can be obtained by measuring absorbance of liposomes at 260 nm and calibrating against a standard curve for 5-FU.

Liposome Sample (mol%)	Absorbance (260nm)	Concentration of 5-FU (mM)
0% PR_b 2% PEG2000 Inert	0.0850	151.7857
5% PR_b 2% PEG2000 Inert	0.0871	155.5357
0% PR_b 2% PEG2000 pH-sensitive	0.0271	48.3929
5% PR_b 2% PEG2000 pH-sensitive	0.0289	51.6071

4.4.5. Aptamer assay

In order to optimize the liposomal formulation functionalized with aptamers it is necessary to estimate the amount of aptamer conjugated to liposomes. Traditional methods for determining oligonucleotide concentration involve measurement of absorbance at 260 nm. However, this method is not useful for the determination of

aptamer concentration in liposomes because of the relatively small amount of liposomal sample that is prepared, and the assay is not sensitive enough at lower concentrations. Therefore for the determination of aptamer concentration, the OliGreen® oligonucleotide reagent from Pierce Biotechnology Inc. (Rockford, IL) was used. OliGreen® is an ultra-sensitive fluorescent nucleic acid stain used for the quantification of oligonucleotides and single-stranded DNA in solution, and enables measurements at concentration as low as 100 pg/ml oligonucleotide, with a standard spectrofluorometer.

Figure 4.10 shows the calibration curve from the OliGreen® assay. To determine the aptamer concentration on the surface of the liposomes, 50 μl of liposome sample or aptamer standard were added to 96-well plates and 50 μl of 1.0% Triton X-100 was further added to break the liposomes. This step ensures that aptamer is in solution and reacts completely with the OliGreen® reagent. The sample plate was allowed to sit for 15 mins to ensure complete mixing of the content and then 100 μl of OliGreen® reagent was added. The well plate was further allowed to sit for 15 mins for reaction to complete and then the fluorescence was measured on a spectrofluorometer with ex/em wavelengths of 494/518 nm. Table 4.5 shows how the amount of aptamer is calculated for different liposome formulations based on the lipid concentration of the liposomes.

4.4.1. Particle size and zeta potential measurements

In addition to the chemical composition of liposomes, physical characterization of liposomes is equally important. The size of liposomes was measured using dynamic light scattering (DLS). DLS is a technique in which the time dependence of the light scattered from a very small region of colloidal solution is measured over a time range from tenths of a microsecond to milliseconds [148]. The diffusion of the particles due to the

Brownian motion from in and out of the region being studied, results in the intensity fluctuations of the scattered light which is dependent on the diffusion coefficients of the particles. From the diffusion coefficients, the hydrodynamic radius of the particles can be obtained using the Stokes-Einstein relationship, as viscosity of the water is known.

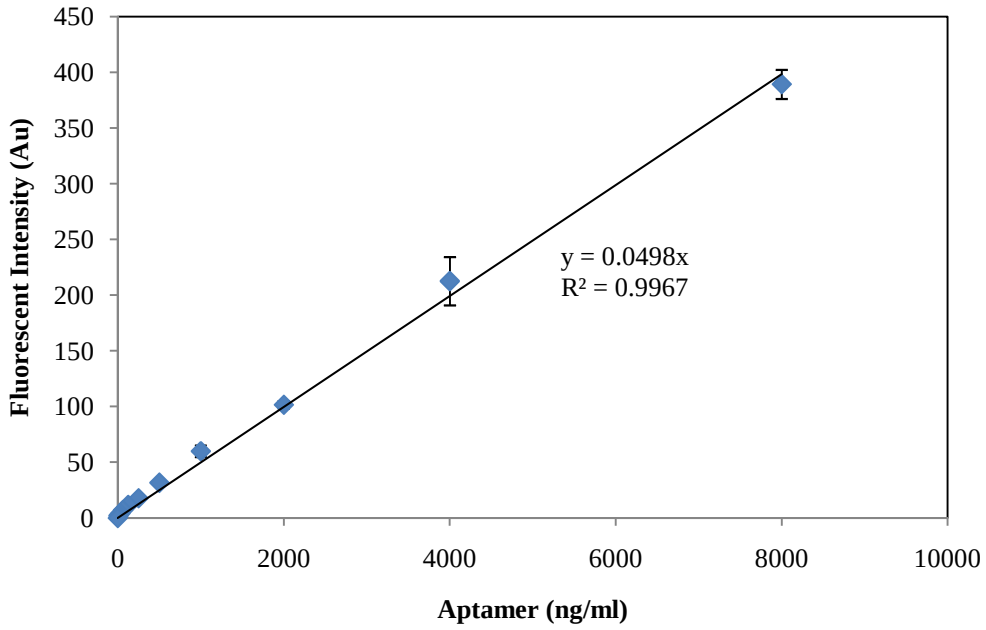

Figure 4.10 Aptamer standard curve obtained from OliGreen assay.

Table 4.5 Aptamer concentration of liposomes can be calculated from the OliGreen assay. Weight % of aptamers in liposomes was calculated based on the lipid concentration of liposomes.

Liposome Samples	Absorbance (Au)	Concentration of Aptamer (ng/ml)	Concentration of lipids (ng/ml)	Weight % of Aptamer
PEGCOOH Liposomes, Activated EDC/NHSS	4.36	88.92	535943.14	0.02
PEGCOOH Liposomes, Activated EDC/NHSS, Quenched with hydroxylamine, Aptamer	9.97	203.46	649854.40	0.03
PEGCOOH Liposomes, Activated EDC/NHSS, Aptamer	23.42	477.92	649854.40	0.07

To measure the size the liposomes, samples were diluted to a lipid concentration of 200 μM in de-ionized water and ran over a ZetaPALS instrument from Brookhaven Instruments. Figure 4.11 shows a particle size distribution histogram for a typical liposomal sample.

Zeta potential is the electrostatic potential that occurs at the surface of shear [104]. The surface of shear is the outermost layer where the relative velocity between the particle and surrounding medium is zero. The zeta potential is important to study in order to understand electrostatic interactions of particles, and more crucially, long term stability of colloidal suspensions. Zeta potential was measured by phase analysis light scattering (PALS) [149]. In PALS a laser beam is split in two components and the first component is scattered through a dilute suspension of particles moving in an oscillating electric field. The second component is later combined with the scattered light (first component) and analysis of the time dependency of the signal phase yields the electrophoretic mobility of the particles. Zeta potential can then be obtained from electrophoretic mobility using the Smoluchowski equation.

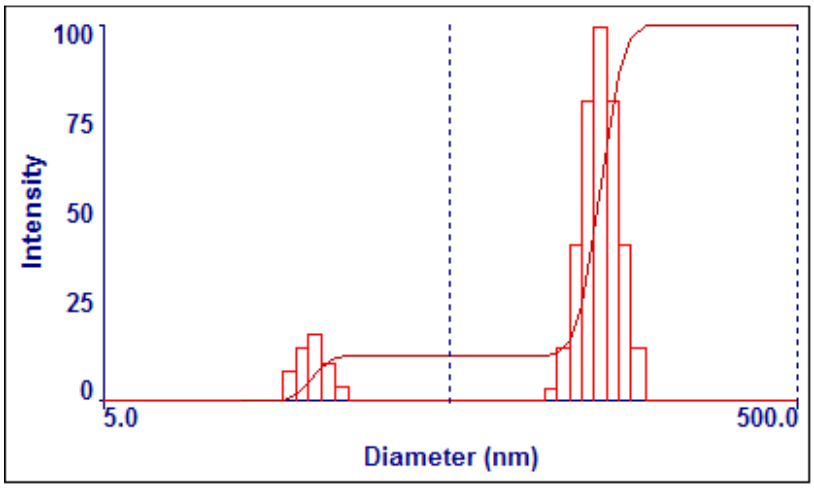

Figure 4.11 Particle size distribution of a typical liposomal sample. The histogram was obtained over a DLS at a scattering angle of 90°. The data is the average of 5 runs (each run is 4 min).

Table 4.6 Average diameter and zeta potential of liposome formulations obtained over a ZetaPALS instrument. The data is the average of 5 runs (each run is 4 min).

Liposome Sample (mol%)	Diameter (nm)	Zeta Potential (mV)
0% PR_b 2% PEG2000 pH-sensitive Liposomes	104.80 ± 0.40	-27.05 ± 2.23
5% PR_b 2% PEG2000 pH-sensitive Liposomes	97.70 ± 0.80	-51.08 ± 1.82
0% PR_b 2% PEG2000 Inert Liposomes	94.00 ± 0.40	-34.87 ± 2.93
5% PR_b 2% PEG2000 Inert Liposomes	94.00 ± 0.30	5.40 ± 3.90

To measure the zeta potential of liposomes, samples were diluted to a lipid concentration of 200 μM in de-ionized water and ran over a ZetaPALS instrument from Brookhaven Instruments. Table 4.6 lists the diameter and zeta potential measured for some typical liposomal samples.

5. Targeting colon cancer cells using PEGylated liposomes modified with a fibronectin-mimetic peptide

5.1. Introduction

Frequently, the use of novel therapeutics in medicine is hindered by the lack of efficiency in delivering these therapeutic agents to the target organs. As a result, research has been focused towards the development of targeted drug delivery systems for the treatment of diseases. Liposomes are phospholipid bilayer vesicles that have great potential as drug delivery carriers and have been extensively investigated in the past. The regulatory FDA (Food and Drug Administration) approval of stealth liposomes (liposomes sterically stabilized with poly(ethylene glycol) (PEG)) for diseases like breast cancer and ovarian cancer [103] has fueled research in the development of targeted stealth liposomal systems. Upon administration, stealth liposomes accumulate in tumor regions through a phenomenon known as the enhanced permeation and retention (EPR) effect [150], due to the presence of fenestrated endothelium in tumor blood vessels (passive targeting). By incorporating site-specific ligands on the surface of stealth liposomes, the vesicles upon accumulating in tumor regions, can specifically target the receptor of choice on the cell surface (active targeting).

Tumor growth and metastasis is critically dependent on the development of new blood vessels (angiogenesis) to supply nutrients, oxygen and growth factors [151, 152]. Angiogenesis itself is a highly complex process involving growth factors and interactions between integrin adhesion receptors and their ligand proteins from the extracellular matrix (ECM) [19, 26, 151, 153-156].

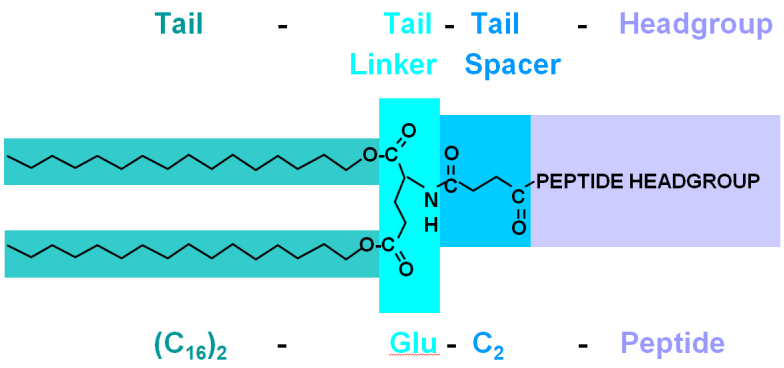

Figure 5.1 Structure of PR_b peptide-amphiphile.

Proliferating endothelial cells express several integrin molecules, which are not expressed on quiescent endothelial cells in normal tissue or blood vessels, like $\alpha_5\beta_1$, $\alpha_v\beta_3$, and $\alpha_4\beta_1$ [19-21]. In particular, integrin $\alpha_5\beta_1$ is minimally expressed in normal vasculature but is significantly up-regulated in tumor vasculature [20] and on tumor cells such as prostate, breast, colon and rectal cancer [20, 22-27]. Previous studies suggest that peptide and antibody antagonists of the integrin $\alpha_5\beta_1$ are potent inhibitors of tumor growth, tumor induced angiogenesis, and tumor metastasis [20, 22, 23, 28-33]. Additionally, ligands that bind to the integrin $\alpha_5\beta_1$ with high affinity are capable of mediating cellular internalization [34-39]. Therefore, $\alpha_5\beta_1$ is a strong candidate for targeting colon cancer, the third most common cancer type in this country.

Researchers have primarily employed RGD (the primary recognition site for $\alpha_5\beta_1$) peptide-based techniques to target the integrin $\alpha_5\beta_1$, but their success has been limited. RGD recognizes several integrins and therefore this makes specificity difficult to achieve. Also, the RGD design lacks the synergistic effect, which is provided by the PHSRN, the synergy site for $\alpha_5\beta_1$ (enhances the cell adhesion activity of the RGD sequence) [157]. Efforts in the past to construct a single peptide sequence incorporating both RGD and

PHSRN domains have also met with limited success [70-74]. We have previously developed a novel peptide-amphiphile sequence referred as PR_b in the text that closely mimics the cell adhesion domain of fibronectin. The design features C_{16} dialkyl ester tail, a glutamic acid (Glu) tail connector, a $–(CH_2)_2–$ tail spacer, and the peptide headgroup (Figure 5.1). The PR_b peptide headgroup consists of four building blocks: a spacer KSS, PHSRN (the synergy site for $\alpha_5\beta_1$), a linker $(SG)_5$, and RGDSP (the primary recognition site for $\alpha_5\beta_1$) [75]. The distance between the PHSRN and RGD domains on native fibronectin is approximately 30-40 Å [69] and the ratio of hydrophilic to hydrophobic residues between the two domains is close to one [77]. The linker has been designed to mimic these two important criteria; the length of the $(SG)_5$ linker is approximately 37 Å (10 amino acids × 3.7 Å per amino acid residue [78, 158]), and the ratio of the smallest "hydrophilic" amino acid serine (S) [159-161] to the smallest "hydrophobic" amino acid glycine (G) [162-164] is equal to one. The role of KSS spacer is to extend the bioactive region further away from the interface as the accessibility of the peptide can significantly affect the binding affinities to their target proteins [17, 77, 79, 165]. The performance of the PR_b peptide-amphiphile was evaluated with human umbilical vein endothelial cells in terms of cell adhesion, spreading, cytoskeletal organization, and extracellular fibronectin production. PR_b outperformed all other peptide sequences that were tested and performed comparably to fibronectin [75]. The specificity of the PR_b peptide for integrin $\alpha_5\beta_1$ was established with blocking antibodies [75].

In this study, we incorporated the PR_b peptide-amphiphile into stealth liposomes with the goal of targeting integrin $\alpha_5\beta_1$ that is expressed on colon cancer cells. Integrin $\alpha_5\beta_1$ is also expressed on the colon cancer endothelium but not on the endothelium of

normal colonic tissue [20, 26], and is expressed only on proliferating endothelial cells and not on quiescent endothelial cells found in normal tissue or blood vessels [19-21]. More importantly, highly invasive colon cancer cell lines express greater amount of integrin $\alpha_5\beta_1$, and its level of expression is usually positively correlated with their invasiveness [24].

In the present study, we demonstrate that functionalizing stealth liposomes with our novel PR_b peptide-amphiphile [75] is superior to conventional RGD targeting, allowing to achieve greater binding and larger uptake of liposomes on colon cancer cells. Also, we show that by varying the amount of PEG (PEG750 or PEG2000) and the amount of peptide-amphiphile incorporated in the liposomes we can achieve increased binding affinities. PR_b-targeted stealth liposomes are as affective as free 5-FU and more cytotoxic on CT26.WT cells compared to GRGDSP-targeted stealth liposomes and non-targeted stealth liposomes. Results are reported here mostly for the mouse colon carcinoma cell system (CT26.WT). We have repeated some experiments with other colon cancer cells such as the human colon cancer cell lines HCT116 and RKO, and have obtained similar results and trends.

5.2. Experimental methods

5.2.1. Materials

Lipids, 1,2-Dipalmitoyl-sn-Glycero-3-Phosphocholine (DPPC), cholesterol (CHOL), 1,2-Dipalmitoyl-sn-Glycero-3-Phosphoethanolamine-N-(Methoxy(Polyethylene glycol)-750)-Ammonium Salt) (PEG750) and 1,2-Dipalmitoyl-sn-Glycero-3-Phosphoethanolamine-N-(Methoxy(Polyethylene glycol)-2000)-(Ammonium Salt) (PEG-2000) were purchased from Avanti Polar Lipids Inc. (Alabaster, AL). The extruder and

the 100 nm polycarbonate membranes were obtained from Avestin Inc. (Ottawa, Canada). The peptide headgroups PR_b (KSSPHSRN$(SG)_5$RGDSP) and GRGDSP (KAbuGRGDSPAbuK) were purchased in crude form from the Microchemical Facility at the University of Minnesota. The PR_b peptide-amphiphile ($(C_{16})_2$-Glu-C_2-KSSPHSRN$(SG)_5$RGDSP), and GRGDSP peptide-amphiphile ($(C_{16})_2$-Glu-C_2-KAbuGRGDSPAbuK) were synthesized as described previously [75, 77, 130]. CT26.WT (mouse colon cancer cell line) and human colon cancer cell lines HCT116 and RKO were obtained from ATCC (Manassas, VA). Hoechst 33342 nucleic stain, Alexa Fluor® 594 wheat germ aggutin (WGA) cell membrane stain, and ProLong Gold antifade reagent were purchased from Invitrogen Corporation (Carlsbad, CA). Primary polyclonal antibody anti-integrin $\alpha_5\beta_1$ and secondary antibody donkey anti-Goat IgG FITC conjugated, were purchased from Chemicon International Inc. (Temecula, CA). Goat IgG isotype control was purchased from Sigma Aldrich Corporation (St. Louis, MO). Cell culture media was purchased from ATCC (Manassas, VA), fetal bovine serum (FBS) was purchased from Atlas Biologicals (Fort Collins, CO), and human fibronectin-coated round coverslips were purchased from BD Biosciences (San Jose, CA). The BCA (bicinchoninic acid) protein assay kit was purchased from Pierce (Rockford, IL). 5-Fluorouracil (5-FU) and all other reagents were purchased from Sigma Aldrich Corporation (St. Louis, MO) and were of biotechnology performance certified grade.

5.2.2. Cell culture

CT26.WT cell lines were grown in RGM (modified RPMI-1640 medium supplemented with 10% FBS, 2 mM L-Glutamine, 100 units/ml Penicillin, and 0.1 mg/ml Streptomycin). Cells were grown in T-75 flasks with a feeding cycle of 2 days. After

cells became 80% confluent (usually after 5 days) they were trypsinized (0.25% Trypsin + 0.1% EDTA) and were suspended in RGM. Cells were washed twice and finally were frozen under liquid nitrogen in RGM containing 10% DMSO (dimethyl sulfoxide) for future use. For subsequent passages cells were seeded in fresh T-75 flasks at a density 10,000 cells/cm^2 and were cultured in RGM with a feeding cycle of 2 days. HCT116 cell lines were grown in MGM (modified McCoy's 5A medium, supplemented with 10% FBS, 2 mM L-Glutamine, 100 units/ml Penicillin, and 0.1 mg/ml Streptomycin) and RKO cells were grown in EGM (modified Eagle's Minimum essential medium, supplemented with 10% FBS, 2 mM L-Glutamine, 100 units/ml Penicillin, and 0.1 mg/ml Streptomycin).

5.2.3. Liposome preparation and characterization

Liposomes were prepared as described elsewhere [166]. Briefly, lipids were dissolved in chloroform and peptide-amphiphiles were dissolved in methanol and water. Lipids and peptide-amphiphiles were combined at the ratios (65-x-y):35:x:y mol% of DPPC:CHOL:PEG:Peptide-Amphiphile, where x is the indicated mol% of PEG and y is the mol% of peptide-amphiphile. Solvents were removed by evaporating under a gentle stream of argon at 65°C, and lipids were dissolved again in chloroform to form a homogenous mixture. The lipid mixture was finally dried under a gentle stream of argon at 65°C until a uniform lipid film was formed, followed by drying under vacuum overnight. Fluorescently labeled liposomes were prepared by hydrating the lipid film with fluorescent HBSE buffer (10 mM Hepes, 150 mM NaCl, 0.1 mM EDTA, and 2 mM Calcein, pH 7.4) at 65°C and at a concentration of 10 mM total lipids. 5-FU encapsulated liposomes were prepared similarly by hydrating the lipid film with HBSE buffer

containing 10 mg/ml 5-FU (pH 7.4). Hydrated lipids were freeze-thawed five times, then extruded for 21 cycles through two stacks of 100 nm polycarbonate membranes using the hand-held extruder. Liposomes were filtered over a Sepharose CL-4B gel filtration column to remove unencapsulated fluorescent dye or 5-FU, which did not get incorporated in the liposomes. Liposome diameter was determined by dynamic light scattering and ranged from 80-150 nm. Phospholipid concentration was determined using the phosphorus colorimetric assay described elsewhere [135, 167]. Liposomes were stored at 4-8°C and were used within two weeks. Peptide concentration was determined using the BCA assay according to the manufacturer's protocol. We were not able to accurately determine the PEG concentration due to experimental limitations (see supplementary data); therefore, in the text we address PEG concentration either as low when 2 mol% PEG was included in starting lipid concentration or as high when 5 mol% PEG was used in the starting lipid concentration. The amount of 5-FU encapsulated in liposomes was determined by dissolving liposomes in methanol (10% liposome formulation and 90% methanol) and measuring their absorbance at 260 nm. A calibration curve was generated by dissolving known amounts of free 5-FU in 90% methanol and 10% HBSE buffer.

5.2.4. Flow cytometry

Confluent cell monolayers were trypsinized (0.25% Trypsin + 0.1% EDTA) and resuspended in ice-cold FB (fluorescent buffer: phosphate buffered saline (PBS) supplemented with 0.02% sodium azide and 2.5% fetal bovine serum) containing liposomes at a lipid concentration of 250 μM and a cell concentration of 1 million/ml in 15 ml centrifuge tubes. Tubes were incubated at 4°C or 37°C over a rotary shaker for the

specified duration of time. Cells were then pelleted and washed twice in FB. Flow cytometric analysis was carried out immediately. For peptide blocking experiments, the protocol specified above was used except cells were incubated with 200 μg/ml of free peptide-amphiphile in FB for one hour prior to incubating the cells with the liposomes. For integrin $\alpha_5\beta_1$ expression studies confluent cell monolayers were trypsinized (0.25% Trypsin + 0.1% EDTA) and resuspended in ice-cold FB at a cell concentration of 1 million/ml in 15 ml centrifuge tubes. Tubes were incubated at 4°C with primary antibody (anti-integrin $\alpha_5\beta_1$) or goat isotype control (goat IgG) over a rotary shaker for 35 min. Cells were then pelleted and washed twice in FB and then incubated again with the secondary antibody (anti-goat IgG FITC conjugated) for 35 min. Finally, cells were pelleted and washed again twice in FB. Flow cytometric analysis was carried out immediately. FACS Calibur located at the Flow Cytometry Core facility in the Cancer Research Center of the University of Minnesota was used. All flow cytometry experiments are representative of n=2, but results are presented from a single experiment.

5.2.5. Confocal microscopy

CT26.WT confluent cell monolayers grown on fibronectin coverslips were incubated with liposomes at a lipid concentration of 250 μM, in a 5% CO_2 incubator at 37°C or at 4°C for the specified duration in RGM. Cell monolayers were then washed with ice-cold FB twice. Cells were later fixed with a fixation buffer (4% paraformaldhyde in PBS, pH ~ 7.4) for 15 min at 37°C. Nuclear staining was carried out using a cell membrane permeable blue-fluorescent Hoechst 33342 dye at a concentration of 2.0 μmole/ml, and the cell membrane was stained with a cell impermeable red-fluorescent Alexa Fluor® 594 wheat germ aggutin (WGA) at 5.0 μg/ml in FB for 10 min. Cells were washed three

times with FB, and coverslips were mounted on glass slides over ProLong Gold antifade reagent. For every sample 40 z-scans (horizontal cross-section of a cell at a particular z height) were taken at 0.25 µm z-step height to cover the entire height of the cell. On the confocal images liposomes were labeled with green, cell membrane with red, and nucleus with a blue. Olympus Fluoview 1000 Confocal Laser Scanning Microscope at the Biomedical Image Processing Laboratory in the Department of Neuroscience at the University of Minnesota was used.

5.2.6. Cytotoxicity studies

Cytotoxicity of liposomes encapsulating 5-FU was determined by the sulforhodamine B colorimetric assay (SRB assay) [168]. CT26.WT confluent cell monolayers were trypsinized (0.25% Trypsin + 0.1% EDTA) and were suspended in RGM at a concentration of 100,000 cells/ml. 200 µl of cell suspension was transferred to each well on a 96-well tissue culture plate to give a final seeding density of 20,000 cells/well. Cells were allowed to attach to the plate overnight. The medium was then removed (t = 0 hrs), and 200 µl of medium containing two-fold serial dilutions of 5-FU ranging from 50 µM to 0.5 µM (concentration either encapsulated in liposomes or free drug) was added to the cells. A negative control (no liposome or free drug added) was included. The plates were incubated in 5% CO_2 incubator at 37°C for t = 6 hrs. Plates were later washed 4 times with PBS and incubated with fresh RGM at 37°C in 5% CO_2 incubator for a total of 72 hrs (t = 72 hrs). At t = 0 hrs, one plate was set aside for a no-growth control, to account for initial seeding density. On the no-growth control plate, the medium was replaced with 200 µl of cold RGM and cells were fixed by adding 100 µl of cold 10% (w/v) TCA (trichloro acetic acid) and the plate was incubated for 1 hrs at 4°C. Remaining plates were

fixed similarly at the conclusion of the experiment (t = 72 hrs). After fixation, plates were washed four times with de-ionized (DI) water and dried. Plates were stained with 100 µl 0.057% (w/v) SRB (sulforhodamine B solution in DI water) at room temperature for 1 hrs. Plates were washed again four times with 1% (v/v) acetic acid solution to remove the unbound SRB dye and dried. 200 µl of 10 mM Tris base solution (pH 10.5) was later added to dissolve the bound dye and plates were incubated at room temperature for another hour. Finally the OD (optical density) was measured on a plate reader at 510 nm. For IC_{50} (concentration of a drug that is required for 50% inhibition of cell growth) determination, a dose-response curve was generated by plotting the 5-FU concentration of the formulations versus the percent growth inhibition. IC_{50} values were obtained by fitting a sigmoidal curve and obtaining the 5-FU concentration at 50% growth inhibition. Percent growth inhibition was calculated using the following formulas below. Results are shown from three independent experiments (n=3). Each experiment was performed in quadruplet.

$$\%\ of\ control\ cell\ growth = \frac{mean\ OD_{sample} - mean\ OD_{no-growth\ control}}{mean\ OD_{neg\ control} - mean\ OD_{no-growth\ control}} \times 100$$

$$\%\ growth\ inhibition = 100 - \%\ of\ control\ cell\ growth$$

5.3. Results and discussion

5.3.1. Expression of integrin α5β1 on colon cancer cells

For a targeted drug delivery system to be effective the target should be upregulated on the cells of interest. Figure 5.2A shows the histogram for expression of $\alpha_5\beta_1$ on CT26.WT cells. 93.5% of the cell population tested positive for integrin $\alpha_5\beta_1$ expression. Isotype control binding was also characterized and was found to be minimal (shown on the same

histogram). This result confirms that integrin $\alpha_5\beta_1$ is upregulated on mouse colon carcinoma cells. Integrin $\alpha_5\beta_1$ expression was also found to be upregulated on human colon cancer cells HCT116 (Figure 5.2B) and RKO (Figure 5.2C).

5.3.2. Effect of PR_b on liposome targeting

To test the effect of PR_b on the binding of liposomes to colon cancer cells, liposome formulations were initially prepared without PEG and with increasing amounts of PR_b peptide-amphiphile. The minimum PR_b concentration that was investigated was 0.7 mol% and the maximum peptide concentration was arbitrarily chosen at five times the minimum (3.5 mol%). Liposomes were incubated with cells for 3 hrs at 4°C and 37°C. Cellular uptake of liposomes via endocytosis is inhibited at 4°C because the endocytotic pathways do not operate at lower temperatures [169, 170]. Therefore, conducting experiments at 4°C allows studying the effect of peptide concentration on surface binding of liposomes to cells with no contributions from endocytosis. Figure 3 shows the effect of peptide concentration on liposome binding at 4°C to the following $\alpha_5\beta_1$-expressing colon cancer cells: CT26.WT (Figure 5.3A), HCT116 (Figure 5.3B), and RKO (Figure 5.3C). Similar trends were observed at 37°C. For all three colon cancer cells, conventional liposomes (liposomes containing DPPC/Chol and no PR_b peptide-amphiphile) show no binding to cells since their fluorescent intensity overlaps with the auto-fluorescence of the cells. Even a small concentration of PR_b, 0.7 mol%, gives sufficient binding to the colon cancer cells (Figure 5.3). Increasing the peptide concentration improves further the binding of the liposomes to the cells with maximum binding observed at the highest concentrations of peptide studied, 2.2 and 3.5 mol%.

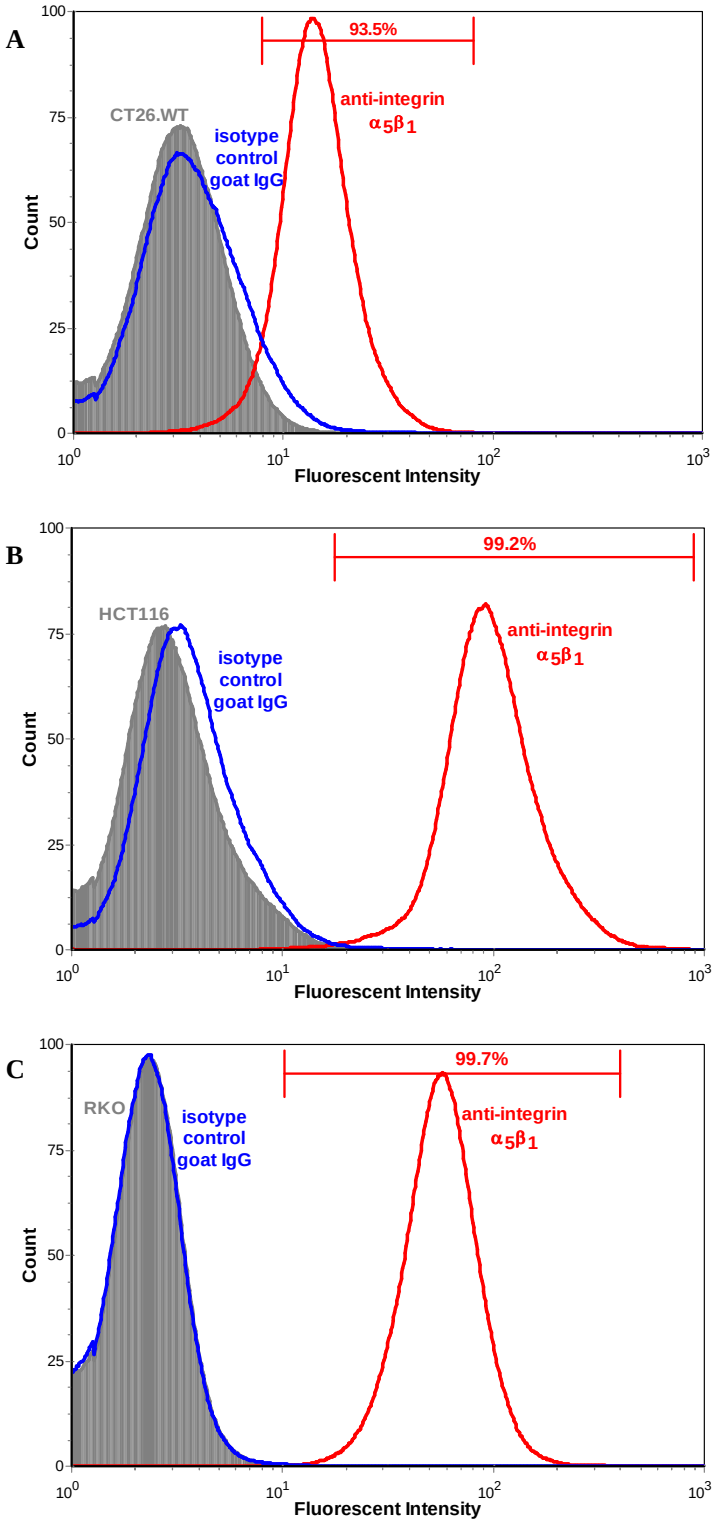

Figure 5.2 Expression of integrin $\alpha_5\beta_1$ on A) CT26.WT B) HCT116 and C) RKO. Cells were incubated with antibodies to integrin $\alpha_5\beta_1$. Appropriate isotype control is included. The number on the marker represents the percentage of cells tested positive for integrin $\alpha_5\beta_1$ expression. The results are representative for n=2 but are shown only from one single experiment.

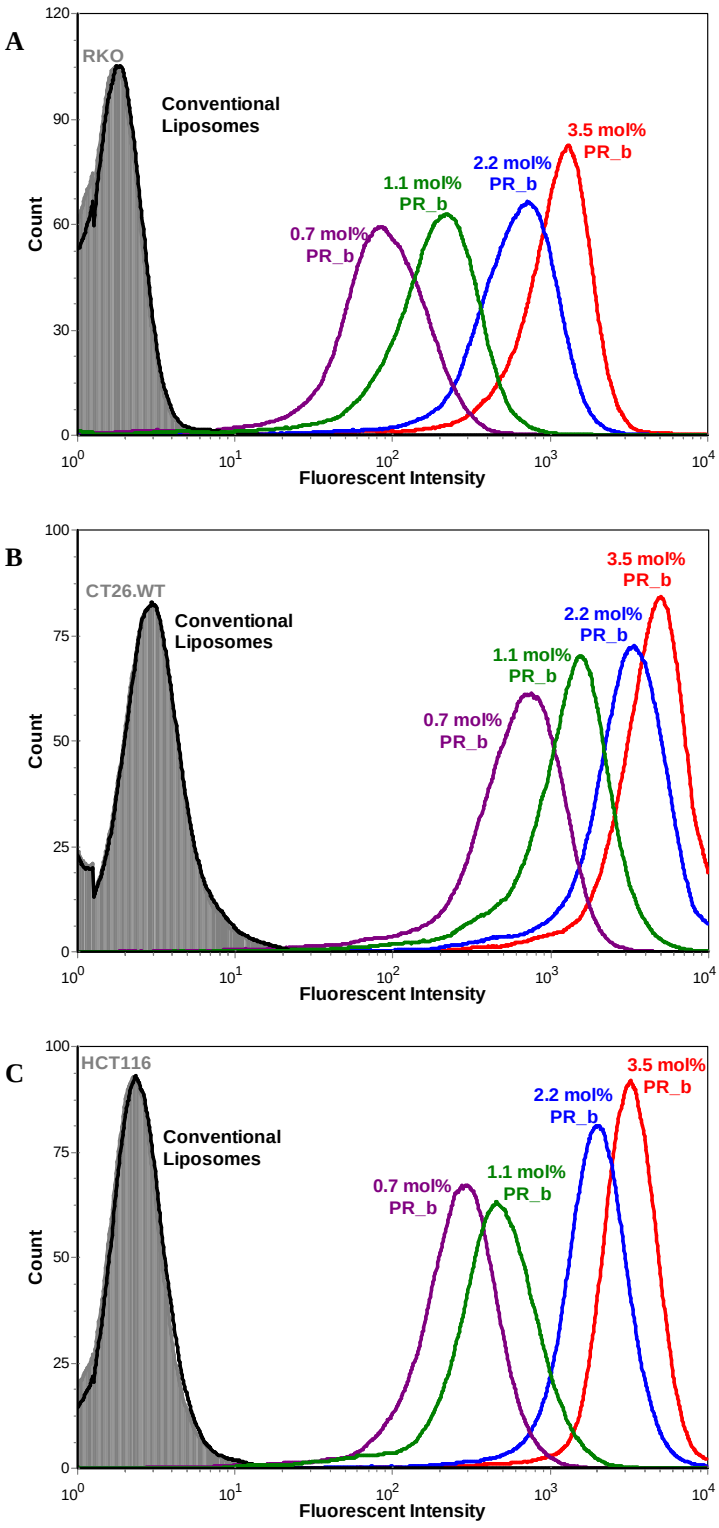

Figure 5.3 Effect of concentration of PR_b peptide-amphiphile on binding of liposomes to A) CT26.WT, B) HCT116, and C) RKO cells at 4°C for 3 hrs. Binding efficiency improves with increasing peptide concentration. Conventional liposomes show no binding to cells. The results are representative for n=2 but are shown only from one single experiment.

5.3.3. Effect of PR_b on stealth liposome targeting

Varying both the PEG layer thickness and concentration and the peptide concentration is critical for a liposome delivery system to be effective. Longer PEG molecules (e.g. PEG2000) provide a better steric barrier but may mask the peptide molecule at certain concentrations. Shorter PEG molecules (e.g. PEG750) may provide sufficient access for the peptide molecule to bind to the target receptor but may reduce the steric barrier. Therefore, two different lengths of PEG were studied, PEG750 and PEG2000. The goal of this study was to determine the amount of both the peptide and PEG concentration on the liposome formulation that will give binding to cancer cells, with the idea that the total concentration of PEG and PR_b should not exceed 8-10 mol%, as work in our lab showed that when higher molecular weight molecules like PEG2000 and PR_b peptide-amphiphiles are incorporated at a concentration of 8-10 mol%, it may result in the destabilization of the liposome membrane. PEG was studied at two different concentrations, low (2 mol% initial lipid concentration) and high (5 mol% initial lipid concentration). Therefore, to avoid functionalizing liposomes at concentrations higher than 8-10 mol% in the presence of high PEG, PR_b was included at a concentration of 2.2-2.6 mol%. Half of that peptide amount was also used for comparison (1.1-1.2 mol% PR_b). The reported peptide concentrations were determined by the BCA assay on the purified liposome formulations, and were usually lower than the ones initially mixed in solution. Previous work in our lab has shown that Langmuir-Blodgett bilayers of peptide-amphiphiles with lipidated PEG are mixed at peptide concentrations less than 10 mol% or higher than 35 mol%, whereas for peptide-amphiphile concentrations between 10-35 mol% the molecules are phase separated [75]. Therefore, we can speculate that for the

peptide-amphiphile concentrations investigated here the peptides are probably well mixed, although we have not verified this in the present study.

Flow cytometry results for PR_b functionalized PEGylated liposomes targeted to colon cancer cells for 3 hrs at 4°C are shown in Figure 5.4. Liposome binding to CT26.WT (Figure 5.4 A and B) and HCT116 (Figure 5.4 C and D) cells increased with increasing PR_b concentration and decreasing concentration of PEG750 (Figure 5.4 A and C) and PEG2000 (Figure 5.4 B and D).

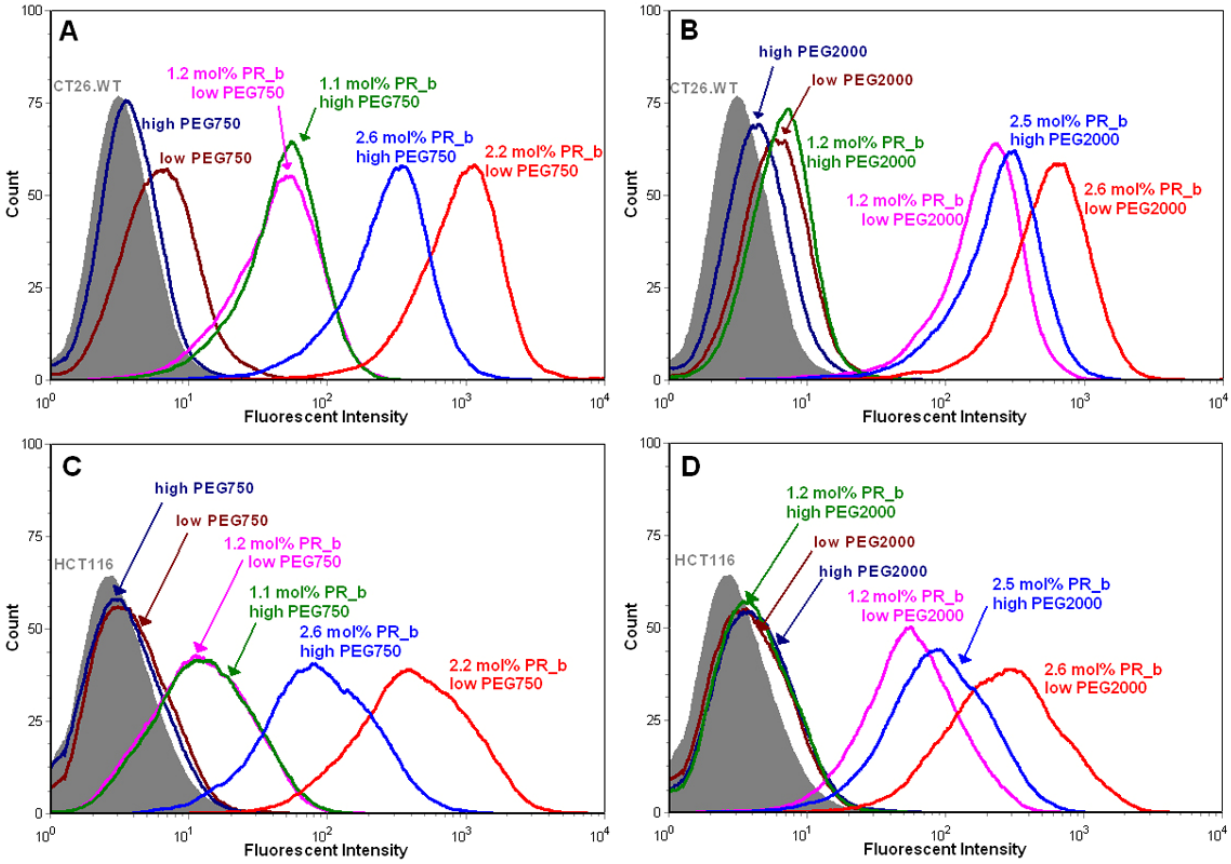

Figure 5.4 Binding of PR_b-targeted stealth liposomes to CT26.WT (A, B) and HCT116 (C, D) cells at 4°C for 3 hrs. The effect of PR_b concentration and PEG concentration were investigated. Low (2 mol% in the initial lipid mixture) and high (5 mol% in the initial lipid mixture) concentrations of PEG750 (A, C) and PEG2000 (B, D) were considered. Significant binding affinities were achieved for liposomes functionalized with PR_b and PEG molecules compared to PEGylated liposomes with no peptide. For both high and low concentrations of PEG750 and PEG2000, a concentration of 2.2-2.6 mol% PR_b peptide-amphiphile gave highest binding affinity to the CT26.WT cells. The results are representative of n=2 but are shown only from one single experiment.

Overall, comparison between the PEG750 and PEG2000 formulations with similar peptide concentrations shows that the PR_b functionalized liposomes show similar trends, with the PEG750 formulations giving slightly higher fluorescent intensities than the PEG2000. Conventional stealth liposome formulations (with no peptide) showed minimal binding. From the concentrations that were investigated, the maximum binding efficiency was achieved for a system containing 2.2-2.6 mol% PR_b and low PEG concentration for both PEG750 and PEG2000. Liposome formulations with peptide concentrations of about 2.5 mol% PR_b and high PEG750 or PEG2000 concentration were the next best option in terms of binding. Stealth liposomes of PEG750 or PEG2000 with smaller peptide concentrations of about 1.2 mol% showed reduced binding by approximately an order of magnitude, with the exception of 1.2 mol% PR_b and low PEG2000. A high PEG2000 concentration on a liposome system with a 1.2 mol% peptide concentration masked the peptide and reduced the binding to a minimum level.

5.3.4. PR_b versus GRGDSP targeting

PR_b functionalized stealth liposomes were compared to GRGDSP functionalized stealth liposomes in Figure 5.5. Figure 5.5A shows that when low concentrations of PEG750 are incorporated in the design, 3.3 mol% GRGDSP is less effective then 1.7 mol% PR_b, and 6.8 mol% GRGDSP shows similar or slightly better binding than 2.9 mol% PR_b. Addition of low concentration of PEG2000 to GRGDSP systems (Figure 5.5B) significantly decreases cell binding compared to PR_b formulations. A 2.5 mol% GRGDSP and low PEG2000 system shows minimal binding, while a 2.4 or 1.2 mol% concentration of PR_b and low PEG2000 shows significantly better performance with approximately two orders of magnitude increase of binding.

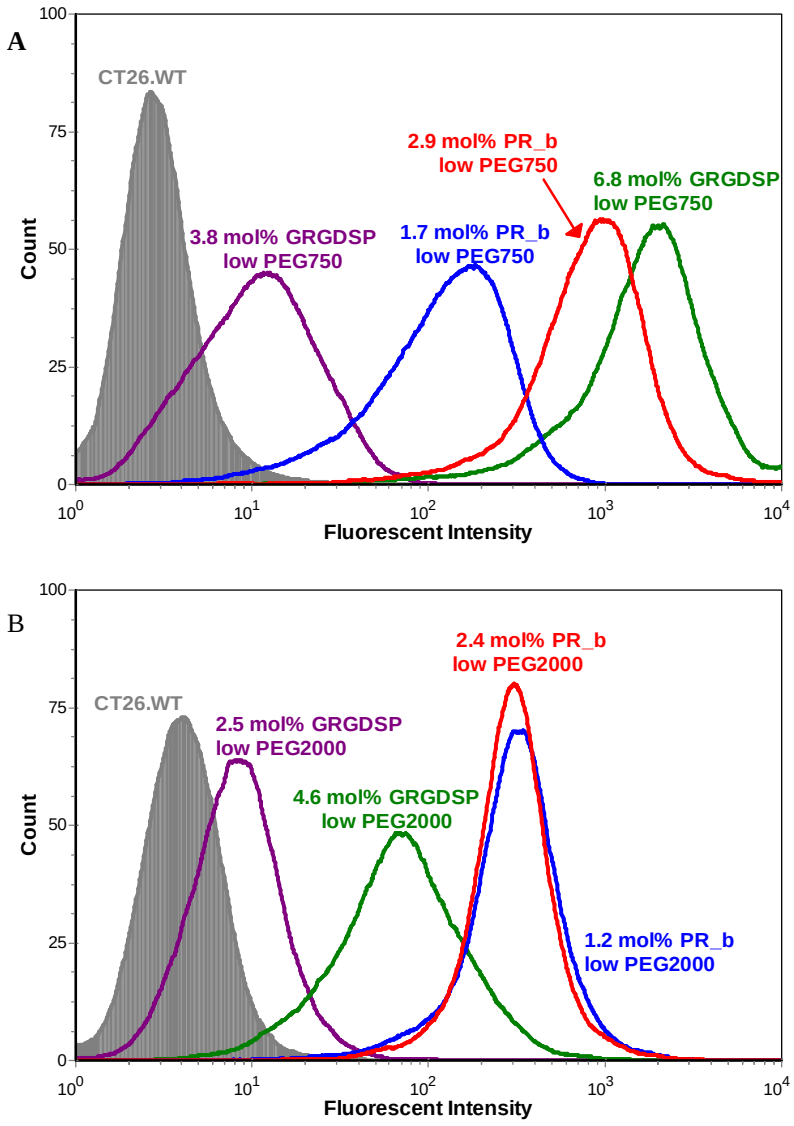

Figure 5.5 Comparison of binding affinities between PR_b-targeted liposomes and GRGDSP-targeted liposomes with A) PEG750 and B) PEG2000. CT26.WT colon cancer cells were incubated with different liposome formulations for 3 hrs at 4°C. The results demonstrate that PR_b targeting is superior to GRGDSP targeting. The results are representative for n=2 but are shown only from one single experiment.

A 4.6 mol% GRGDSP low PEG2000 system does show some increase in binding over a 2.5 mol% GRGDSP system but still is outperformed by both 1.2 and 2.4 mol% PR_b low PEG2000. These results demonstrate the superiority of our novel PR_b targeting over the GRGDSP-based targeting. Both the PR_b peptide amphiphile and PEG

molecules are incorporated in the liposome membrane and high binding efficiency can be achieved by varying the amounts of PEG and peptide in parallel.

These results demonstrate the limitation of non-targeted stealth liposome systems currently being used in clinical practice. Functionalization of PEGylated liposomes with the PR_b peptide, designed to specifically target the integrin $\alpha_5\beta_1$, can help achieve higher binding efficiencies. Both the PR_b peptide amphiphile and PEG molecules are incorporated in the liposome membrane and high binding efficiency can be achieved by varying the amounts of PEG and peptide in parallel.

5.3.5. Blocking experiments

We have previously reported that the PR_b peptide is a specific ligand for the integrin $\alpha_5\beta_1$ [75]. In order to establish that the peptide is mediating the binding of the peptide functionalized stealth liposomes to colon cancer cells, cells were incubated with an excess of free PR_b peptide-amphiphile for 1 hrs prior to incubating them with the liposomes for another 1 hrs at 4°C. Flow cytometry studies without any blocking with free peptide were also performed for the same formulations for 1 hrs at 4°C and results were similar to the ones shown in Figure 5.5B. Figure 5.6 shows flow cytometry results from blocking experiments for PR_b and GRGDSP functionalized stealth liposomes with low concentrations of PEG2000, using free PR_b peptide-amphiphile as the blocking agent at a concentration of 200 μg/ml. Comparison of Figure 5.5B and Figure 5.6 shows that addition of the free peptide completely blocks the binding of the functionalized stealth liposomes to CT26.WT cells. Therefore the peptides are mediating the binding of the peptide functionalized stealth liposomes to the cells.

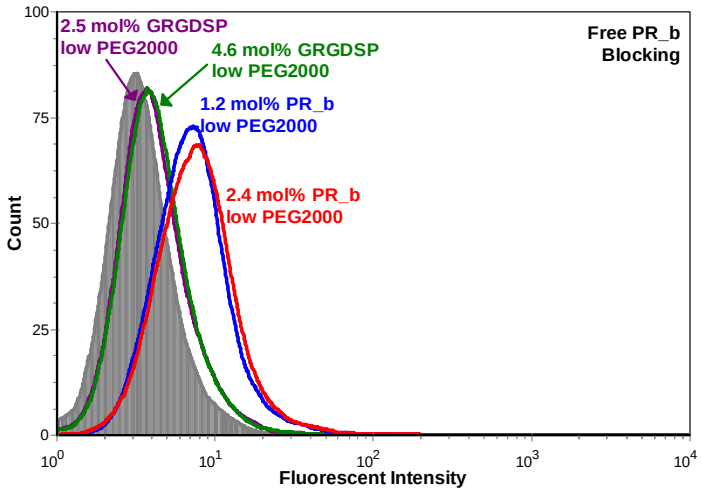

Figure 5.6 Binding of PR_b and GRGDSP targeted liposomes (with low concentrations of PEG2000) to CT26.WT cells was blocked by incubating the cells with PR_b at a concentration of 200 µg/ml for 1 hrs at 4°C before incubating the cells with liposomes for 1 hrs at 4°C. Cell adhesion was completely blocked in the presence of the free peptide.

5.3.6. Endocytosis of PR_b and RGD targeted stealth liposomes

Binding of targeted liposomes is only one aspect for the development of an effective drug delivery system. These liposomes also need to be uptaken by the target cells. In order to characterize endocytosis as the most probable mechanism of internalization for the PR_b and GRGDSP targeted stealth liposomes by CT26.WT cells, a confocal laser scanning microscope was used. Figure 5.7 shows confocal images for a horizontal cell section nearly 2-3 µm above the coverslip and 7-8 µm below the cell surface. Binding to the cell surface on these images can be identified by co-localization of red (cell membrane stain) and green (liposome stain) signal. Internalization is marked by localization of green fluorescent dots (liposomes) between the blue nuclear region and the red cell membrane. Figure 5.7 demonstrates that at all the times and temperatures examined binding and internalization of stealth liposomes with low concentration of PEG750 (Figure 5.7A) and PEG2000 (Figure 5.7B) is minimal.

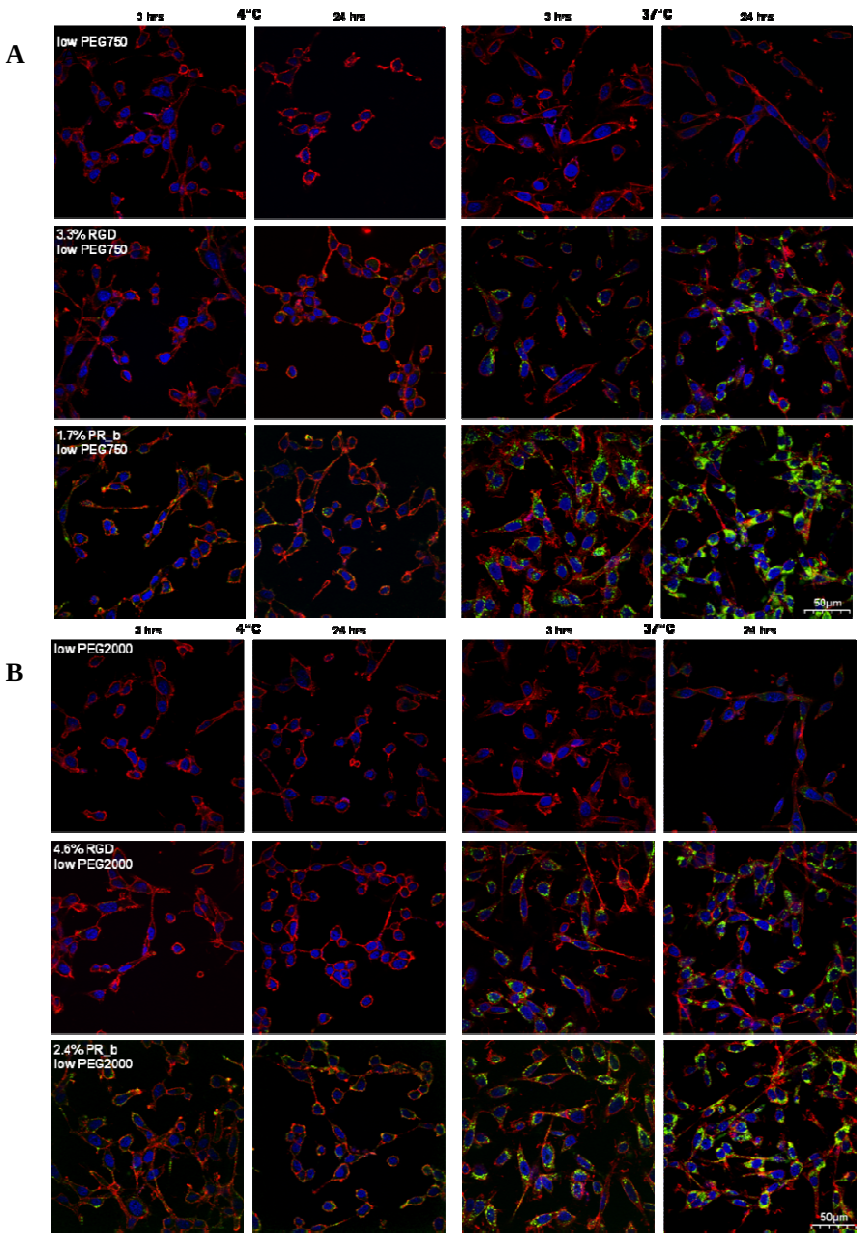

Figure 5.7 Intracellular uptake of various stealth liposomes to mouse CT26.WT colon carcinoma cells. A) Liposomes functionalized with low levels of PEG750. B) Liposomes functionalized with low levels of PEG2000. First row shows PEGylated formulations, second row shows PEGylated formulations functionalized with GRGDSP and third row shows PEGylated formulations functionalized with PR_b. Internalization of different stealth liposomal formulations loaded with calcein was determined with confocal microscopy. Liposomes (shown with green) were incubated with CT26.WT at 4ºC and 37ºC, for 3 and 24 hrs. 40 scans were taken (0.25μm step) across the body of the cells. Images shown are 2-3 μm above the coverslip, and 7-8 μm below the surface of the cells, and were merged with the nucleus (shown in blue) and cell membrane (shown in red). The scale bar is 50 μm for all images. Liposome binding to cell surface is represented by the orange colored cell membrane (co-localization of red cell membrane and green liposomes). Internalization can be identified by the green liposome signal in between the red cell membrane and blue nucleus. These images illustrate that PR_b-targeted stealth liposomes can be endocytosed by the colon cancer cells after binding to the integrin $\alpha_5\beta_1$. GRGDSP-targeted stealth liposomes show smaller levels of binding and uptake.

GRGDSP stealth liposomes with low levels of PEG750 (Figure 5.7A) or PEG2000 (Figure 5.7B) show surface binding at 4°C, and evidence of internalization at 37°C. Internalization is seen only at 37°C, since endocytosis mechanisms do not operate at 4°C, and is greater at 24 hrs compared to 3 hrs. One possible explanation for this is that 24 hrs of incubation allows more time for the recycling of integrins and thereby increasing the amount of endocytosed liposomes.

Similar trends are observed for PR_b-targeted stealth liposomes with low levels of PEG750 (Figure 5.7A) or PEG2000 (Figure 5.7B); except there is significantly higher level of internalization at 37°C and surface binding at 4°C compared to the GRGDSP formulations. Internalization studies at 37°C show that even at 3 hrs of incubation the amount of green fluorescence inside the red cell membrane is high, and at 24 hrs this effect is even more pronounced compared to GRGDSP stealth liposomes. With the PR_b formulations almost the entire cytoplasmic region is stained with the green internalized vesicles. These confocal images illustrate the internalization of PR_b-targeted stealth liposomes by the colon cancer cells, and show that when the PR_b peptide is used for targeting more stealth liposomes are internalized with only half the concentration of GRGDSP. These results support the surface binding studies from the flow cytometry experiments (Figure 5.5) and show that PR_b targeting can significantly improve the performance of stealth liposomes as compared to conventional RGD targeting techniques. Furthermore, qualitative comparisons between the lower right images on the third row, for PR_b-targeted stealth liposomes incubated with the colon cancer cells for 24 hrs at 37°C, show that the PR_b PEG750 functionalized liposomes (Figure 5.7A) show more internalization compared to the PR_b PEG2000 functionalized liposomes (Figure 5.7B)

consistent with the idea that shorter PEG molecules may show reduced steric barrier and thus allowing for more peptide functionalized stealth liposomes to bind and internalize.

5.3.7. Cytotoxicity of 5-FU encapsulated targeted stealth liposomes

In this study we examined the cytotoxicity of different formulations that encapsulated 5-FU. 5-FU was chosen as an anti-cancer agent since it is commonly used for the treatment of colon cancer. CT26.WT cells were initially incubated with either 5-FU containing liposomes or free 5-FU for 6 hrs, and allowed to grow for a total of 72 hrs. Using a negative control (no liposomes or free drug added) and a no-growth control that determined the initial seeding density, the amount of growth inhibition was examined.

Table 5.1 summarizes the IC_{50} values for free drug and different liposome formulations. At 6 hrs, PR_b-targeted stealth liposomes increased cytotoxicity from 11.14 ± 0.17 μM (IC_{50} for non targeted stealth liposomes) to 7.31 ± 0.14 μM, about 35% increase in 5-FU efficacy. When compared to GRGDSP-targeted stealth liposomes, PR_b-targeted stealth liposomes (with only half the concentration of peptide) show nearly 20% improvement in cytotoxicity. More importantly, PR_b-targeted stealth liposomes are as effective as free 5-FU.

Table 5.1 Cytotoxicity of 5-FU (IC_{50}) encapsulated stealth liposomes targeted to CT26.WT cells for 6 hrs. After washing cells were allowed to grow for a total of 72 hrs. All the values are representatives of mean ± SD from three independent experiments (n=3). Each experiment was performed in quadruplet.

Formulation	AVG	S.D.
5-Fluorouracil	7.50	0.17
low PEG2000	11.14	0.17
1.6-1.9% PR_b low PEG2000	7.31	0.14
2.9-3.8% GRGDSP low PEG2000	9.07	0.48

Recent studies reported that RGD-targeted stealth liposomes show increased cytotoxicity over non-targeted liposomes. For example, RGD-targeted liposomes containing the anti-cancer drug doxorubicin showed a 30-40% increase in efficacy over stealth liposomes delivered to murine B16 and human A375 melanoma cells after incubation for 8 hrs [35, 38]. The cytotoxicity studies in Table 5.1 support the binding and internalization data discussed in earlier sections, and indicate that using a PR_b peptide sequence, that has been shown to have higher affinity and specificity for the $\alpha_5\beta_1$ than GRGDSP [75], leads to significant improvement in both targeting capability and biological activity

5.4. Conclusion

In this study we have engineered a targeted delivery system that can deliver a therapeutic load to colon cancer cells using a peptide sequence (PR_b) that has been shown previously to specifically target the integrin $\alpha_5\beta_1$ with high affinity. We have optimized the delivery of the nano-vector by varying the amounts of both the peptide and PEG molecules on the liposome surface, and studying the effect of their concentration on binding to colon cancer cells. The PR_b-targeted stealth liposome system is capable of binding to the integrin $\alpha_5\beta_1$ expressing colon carcinoma cells, and undergoes cellular internalization via most likely an endocytosis mechanism. Our results are well correlated and the trends are logical based on our understanding of the effect of PEG and peptide-amphiphile on the liposome interface. Increasing the amount of PR_b peptide enhances the binding affinity of liposomes and increasing the amount of PEG reduces it. When PEG2000 is incorporated in the peptide functionalized liposomes, binding and internalization of the liposomes slightly decreases compared to systems with similar

concentrations of PEG750 and peptide. We have shown that by varying both the concentrations of peptide-amphiphile and PEG on the liposome interface, significant levels of binding can be achieved even when target functionality is implanted in parallel with PEG instead at the tip of the PEG chain. PR_b targeting is superior to GRGDSP targeting as shown by improved binding and internalization at lower concentrations of PR_b. For example, liposomes with 6.8 mol% GRGDSP and low levels of PEG750 are required to perform comparably to 2.9 mol% PR_b liposomes with low PEG750 concentrations, and similarly, liposomes with low concentrations of PEG2000 and 4.6 mol% GRGDSP are outperformed by low PEG 2000 formulations functionalized with 1.2 mol% PR_b. Furthermore, PR_b-targeted stealth liposomes can internalize in significantly higher amounts than the GRGDSP-targeted stealth liposomes. More importantly, PR_b has been shown in our previous work to be $\alpha_5\beta_1$ specific whereas many integrins bind to RGD peptides. PR_b-targeted stealth liposomes show significantly higher cytotoxicity than the GRGDSP-targeted stealth liposomes, and the non-targeted stealth liposomes, and are as effective as free 5-FU. Based on the above findings, we conclude that PR_b-targeted stealth liposomes can be potentially used *in-vivo*, to deliver a therapeutic load directly to cancer cells, and may help overcome the deleterious side effects present in non-targeted treatments.

5.5. Acknowledgements

We thank Anastasia Mardilovich for synthesizing the GRGDSP peptide-amphiphile. This work was supported in part by the University of Minnesota Nanobiotechnology Initiative, The American Cancer Society Institutional Research Grant (IRG-58-001-46-IRG45), the National Science Foundation (CBET-0553682), the MRSEC Program of the

National Science Foundation under Award Number DMR-0212302, the National Institute of Biomedical Imaging and Bioengineering (R03EB006125), and the National Cancer Institute (R01CA120383). We would like to acknowledge the assistance of the Flow Cytometry Core Facility at the University of Minnesota Cancer Center, a comprehensive cancer center designated by the National Cancer Institute, supported in part by P30 CA77598. The content is solely the responsibility of the authors and does not necessarily represent the official views of the National Institute of Biomedical Imaging and Bioengineering, the National Cancer Institute, or the National Institutes of Health.

6. Enhanced intracellular delivery using sterically stabilized pH-sensitive liposomes functionalized with a fibronectin-mimetic peptide and targeted to colon cancer cells

6.1. Introduction

There is strong need for the development of targeted delivery systems because of the nonspecific nature of conventional drug delivery [7]. This is particularly important for treating diseases like cancer where the detrimental side effects of chemotherapy deteriorate both the quality of life and longevity of the patient. Some of the advantages of targeted drug delivery include reduction of side effects associated with the non-specific delivery of drugs, protection of biologically active drug molecules, and the ability to use smaller doses. Several carriers have been used in designing targeted drug delivery vehicles, and these are broadly divided into three classes: the particle-type carriers (*e.g.* liposomes, polymeric nanoparticles), soluble carriers (*e.g.* plasma proteins, polysaccharides), and cellular carriers (*e.g.* viruses) [1]. Amongst delivery systems, particle-type carriers represent the most diverse class and have the greatest potential for achieving the goal of drug targeting [60, 171]. In addition, their ability to encapsulate the drug and the capability of controlled release improves the drug's stability and efficacy.

Liposomes have been extensively studied for targeted drug delivery and are an excellent choice for a delivery system, because of their inherent resemblance to cell membranes [60, 103, 172]. They are both biocompatible and biodegradable and can incorporate both hydrophobic and hydrophilic drugs. Stealth liposomes (liposomes sterically stabilized with PEG) have already been FDA approved, *e.g.* DOXIL®

(doxorubicin in stealth liposomes), and are currently being used for the treatment of AIDS-related Kaposi's sarcoma, breast cancer, ovarian cancer, and other solid tumors. The versatile nature of liposomes in terms of size and composition offers excellent opportunity for designing them for controlled release, as well as functionalizing them with site specific ligands providing targeting capability.

Conventional stealth liposomes (in this paper we will refer to them as inert liposomes) that are actively targeted to a particular cell surface receptor of interest using moieties like peptides or antibodies are taken up by cells via receptor-mediated endocytosis and have shown to release their load in lysosomes [110, 173-175]. This may not be an effective method for the delivery of drugs (*e.g.* peptide or nucleic acid based drugs) that are unstable in the harsh acidic environment present in lysosomes. pH-sensitive liposomes can provide a significant improvement to intracellular drug release as they undergo rapid destabilization under mildly acidic conditions present in endocytotic vesicles [176-178]. Therefore they are susceptible to releasing their load earlier in the endocytotic pathway (endosomes) under more favorable conditions for the encapsulated drug molecules and can also promote the transfer of encapsulated drug to the cytosol [179]. In addition, pH-sensitive stealth liposomes functionalized with an appropriate targeting moiety (peptide or antibody) and targeted to cell surface receptors such as folate, transferrin, and epidermal growth factor receptor have shown to increase the intracellular delivery of their liposomal content significantly, compared to the non-targeted pH-sensitive stealth liposomes and the inert stealth liposomes (both targeted or non-targeted) [180-182]. This implies that pH-sensitive stealth liposomes targeted to a

cell surface receptor of interest can significantly improve the overall efficacy of the drug when compared to its delivery via inert liposomes.

We have previously reported that the efficacy of inert stealth liposomes can be significantly improved by incorporating the targeting moiety, PR_b. PR_b-targeted stealth liposomes can specifically target cancer cells expressing the integrin $\alpha_5\beta_1$ with high affinity and specificity and internalize through receptor-mediated endocytosis [10, 183]. PR_b (KSSPHSRN$(SG)_5$RGDSP) is a novel peptide sequence designed in our lab that mimics the cell adhesion domain of fibronectin and is specific to integrin $\alpha_5\beta_1$ [75]. The PR_b peptide-amphiphile design employed a hydrophobic tail (C_{16} dialkyl ester tail with a glutamic acid (Glu) tail connector and a -$(CH_2)_2$- tail spacer, $(C_{16})_2$-Glu-C_2-) connected to the N-terminus of a peptide headgroup that was composed of a spacer (KSS), the synergy site sequence (PHSRN), a linker ($(SG)_5$) mimicking both the distance and hydrophobicity/hydrophilicity present in the native protein fibronectin (thus presenting an overall "neutral" linker), and finally the primary binding sequence (RGDSP) [75]. Our original hypothesis was that the degree of hydrophobicity/hydrophilicity between the two sequences (RGD and PHSRN) in fibronectin is an important parameter in designing a fibronectin-mimetic peptide [77]. Previous work in our lab demonstrated that PR_b is a promising sequence compared to fibronectin and other fibronectin-mimetic peptides, and for the first time in the literature a surface functionalized with a peptide (PR_b) was shown to outperform a fibronectin-functionalized surface [75, 184]. We established specificity of the PR_b peptide for the integrin $\alpha_5\beta_1$ by blocking cell adhesion, and eliminating liposomal binding to cancer cells, with antibodies and free peptides [10, 75]. Integrin $\alpha_5\beta_1$ is highly up-regulated in

tumor vasculature and on tumor cells of colon, prostate, and breast cancer and is minimally expressed on normal vasculature [20, 22-27]. This makes integrin $\alpha_5\beta_1$ a strong candidate for targeting cancer.

To improve the efficacy of the PR_b-targeted stealth liposomes, in this study we engineered PR_b-targeted pH-sensitive stealth liposomes, capable of targeting the integrin $\alpha_5\beta_1$ expressed on CT26.WT colon cancer cells, and releasing their load intracellularly in a fast and effective manner. We have optimized the release profile of the pH-sensitive stealth liposomes by varying the composition of the liposomes and verifying that the incorporation of PEG and the PR_b peptide does not affect the pH-sensitivity of the liposomes. PR_b-targeted pH-sensitive stealth liposomes bind to mouse CT26.WT colon carcinoma cells, undergo cellular internalization, and release their load intracellularly in a shorter period of time compared to other formulations. PR_b-targeted pH-sensitive stealth liposomes also show significantly higher cytotoxicity than the PR_b-targeted inert stealth liposomes, and the non-targeted stealth liposomes (both pH-sensitive and inert).

6.2. Experimental methods

6.2.1. Materials

Lipids, 1,2-dipalmitoyl-sn-glycero-3-phosphocholine (DPPC), cholesterol (CHOL), 1,2-dipalmitoyl-sn-glycero-3-phosphoethanolamine-N-(methoxy(polyethylene glycol)-2000) (DPPE-PEG2000), 1,2-dioleoyl-sn-glycero-3-phosphoethanolamine (DOPE), 1,2-distearoyl-sn-glycero-3-phosphoethanolamine-N-(methoxy(polyethylene glycol)-2000) (DSPE-PEG2000) were purchased from Avanti Polar Lipids Inc. (Alabaster, AL), and cholesteryl hemisuccinate (CHEMS) was purchased from Sigma Aldrich Corporation (St.

Louis, MO). The extruder and the 100 nm polycarbonate membranes were obtained from Avestin Inc. (Ottawa, Canada). The peptide headgroup PR_b (KSSPHSRN$(SG)_5$RGDSP) was purchased in crude form from the Microchemical Facility at the University of Minnesota. The PR_b peptide-amphiphile ($(C_{16})_2$-Glu-C_2-KSSPHSRN$(SG)_5$RGDSP referred as PR_b peptide-amphiphile) was synthesized as described previously [77, 185]. Hoechst 33342 nucleic stain, Alexa Fluor® 594 wheat germ agglutinin (WGA) cell membrane stain, ProLong Gold antifade reagent, and CyQUANT® cell lysis buffer were purchased from Invitrogen Corporation (Carlsbad, CA). CT26.WT (mouse colon cancer cell line) and RPMI-1640 culture media were obtained from ATCC (Manassas, VA). Fetal bovine serum (FBS) was purchased from Atlas Biologicals (Fort Collins, CO), and human fibronectin-coated round coverslips were purchased from BD Biosciences (San Jose, CA). The BCA (bicinchoninic acid) protein assay kit was obtained from Pierce (Rockford, IL). 5-Fluorouracil (5-FU), calcein, and all other reagents were purchased from Sigma Aldrich Corporation (St. Louis, MO) and were of biotechnology performance certified grade.

6.2.2. Cell culture

CT26.WT cell lines were grown in RGM (modified RPMI-1640 medium supplemented with 10% FBS, 2 mM L-glutamine, 100 units/ml penicillin, and 0.1 mg/ml streptomycin). Cells were grown in T-75 flasks with a feeding cycle of 2 days. After cells became 80% confluent (usually after 5 days) they were trypsinized (0.25% trypsin + 0.1% EDTA) and were suspended in RGM. Cells were washed twice and finally were frozen under liquid nitrogen in RGM containing 10% DMSO (dimethyl sulfoxide) for

future use. For subsequent passages cells were seeded in fresh T-75 flasks at a density 10,000 cells/cm^2 and were cultured in RGM with a feeding cycle of 2 days.

6.2.3. Liposome preparation and characterization

Liposomes were prepared as described elsewhere [166]. Briefly, lipids were dissolved in chloroform and PR_b peptide-amphiphile was dissolved in water. For pH-sensitive stealth liposomes, lipids and PR_b peptide-amphiphile were combined at a ratio of (100-x-y-z):x:y:z mol% of DOPE:CHEMS:DSPE-PEG2000:PR_b peptide-amphiphile, where x is the mol% of CHEMS, y is the mol% of DSPE-PEG2000, and z is the mol% of PR_b peptide-amphiphile. For inert stealth liposomes, lipids and PR_b peptide-amphiphile were combined at a ratio of (65-y-z):35:y:z mol% of DPPC:CHOL:DPPE-PEG2000: PR_b peptide-amphiphile, where y is the mol% of DPPE-PEG2000, and z is the mol% of PR_b peptide-amphiphile. To form a homogenous mixture couple of drops of methanol were added to the chloroform-water lipid mixture. Solvents were removed by evaporation at 65°C under a gentle stream of argon, and the lipid mixture was dissolved again in chloroform and dried at 65°C under a gentle stream of argon until a uniform lipid film was formed. This was followed by drying under vacuum overnight. Liposomes with self-quenching concentration of calcein were prepared by hydrating the lipid film with 80 mM calcein solution (in 10 mM TES, 1 mM EDTA, pH ~7.4, adjusted to 300 mOsm by adding NaCl) at 65°C and at a concentration of 10 mM total lipids. Liposomes encapsulating 5-FU were prepared similarly by hydrating the lipid film with TBS buffer (10 mM TES, 140 mM NaCl, and 0.1 mM EDTA, pH~7.4) containing 10 mg/ml 5-FU. Hydrated lipids were freeze-thawed five times, then extruded for 21 cycles through two stacks of 100 nm polycarbonate membranes using the hand-held extruder. Liposomes

were filtered over a Sepharose CL-4B gel filtration column to remove unencapsulated calcein or 5-FU using TBS buffer. Liposome diameter was determined by dynamic light scattering and ranged from 80-150 nm. Phospholipid concentration was determined using the phosphorus colorimetric assay described elsewhere [135, 167]. Peptide concentration was determined using the BCA assay according to the manufacturer's protocol. For all the liposome formulations studied, 2 mol% PEG2000 was included in starting lipid concentration and is referred as low PEG2000 in text. Liposomes were stored at 4-8°C and were used within two weeks. The amount of 5-FU encapsulated in liposomes was determined by dissolving liposomes in 90% methanol (v/v) and measuring their absorbance at 260 nm. A calibration curve was generated by dissolving known amounts of free 5-FU in 90% methanol and 10% TBS buffer.

6.2.4. pH-Sensitive liposome leakage assay

Calcein was encapsulated in liposomes at a self-quenching concentration of 80 mM [186]. 40 nmoles of self-quenching liposomes were incubated in 1.5 ml of MES buffer (140 mM NaCl, 10 mM MES) at pH 4.5, 5.5, 6.5, and 7.4, in quartz cuvettes for 1 hrs and 37°C. Fluorescence was measured at intervals of 1 min over a period of 60 min on a Varian Cary Eclipse fluorescence spectrophotometer (λ_{ex} = 490 nm and λ_{em} = 520 nm). After 60 min, the total fluorescence intensity of the liposomes was measured by lysing them with 0.1% Triton X-100 (v/v).

Calcein fluorescence intensity varies with pH and decays with repeated measurements over time. Therefore the fluorescence intensity obtained was corrected for the effect of pH and time using the following equation: $I_t^{pH} = r_{pH}\left[I_{t,m}^{pH} + d_{pH}\ln(t)\right]$; where I_t^{pH} is the corrected fluorescence intensity, r_{pH} is the correction factor for the effect of pH, $I_{t,m}^{pH}$ is

the measured fluorescence intensity at a particular pH and time t of interest, and d_{pH} is the decay constant of calcein fluorescence at the pH of interest. The percent leakage was calculated using the following equation: $\%\, Leakage = \left[\left(I_t^{pH} - I_0^{7.4}\right)/\left(I_{100}^{pH} - I_0^{7.4}\right)\right] \times 100$; where I_t^{pH} is the corrected fluorescence intensity, I_{100}^{pH} is the total fluorescence intensity of the liposomes (corrected for the effect of pH), and $I_0^{7.4}$ is the initial fluorescence intensity at $t = 0$ min and pH 7.4. To obtain the correction factor for the effect of pH (r_{pH}), calibration curves were generated for the fluorescence intensity of free calcein at pH 7.4, 6.5, 5.5, and 4.5, within the concentration range of interest. The calibration curves were then fitted to linear regression and the r_{pH} values were obtained from the ratio of slope at pH 7.4 to the slope at a particular pH. To calculate the calcein decay constants d_{pH}, the fluorescence intensity of free calcein was measured at intervals of 1 min over a period of 60 min at several different concentrations (within the concentration range of interest). For every pH value and concentration, the data was fitted to the following equation: $i_{pH}^t = -d_{pH} \ln(t) + i_{pH}^0$; where i_{pH}^t is the fluorescence intensity at time t, i_{pH}^0 is the fluorescence intensity at time $t = 0$, and d_{pH} is the decay constant obtained from curve fitting. For each pH value, d_{pH} was obtained from the mean of d_{pH} values at different concentrations (within the concentration range of interest).

6.2.5. Liposome uptake experiments

CT26.WT confluent cell monolayers were trypsinized (0.25% trypsin + 0.1% EDTA) and were suspended in RGM at a concentration of 5×10^5 cells/ml. 2 ml of cell suspension was transferred to each well on a 6-well tissue culture plate to give a final seeding density of 10^6 cells/well. Cells were allowed to attach to the plate overnight. The medium was

then removed and cells were incubated in 1 ml of RGM with liposomes (encapsulating calcein at self-quenching concentration of 80 mM) at lipid concentration of 100 μM. The plates were incubated in 5% CO_2 incubator at 37°C for 4 hrs and 16 hrs. Plates were later gently washed 3 times with PBS (phosphate buffered saline), air dried, and stored at -80ºC for 1 day. At the end, cells were lysed with 1 ml of CyQUANT® cell lysis buffer for 1 hrs at 37ºC. The cell lysate was then centrifuged at 16,000g for 5 min and the supernatant was collected. The fluorescence intensity of the supernatant was then measured at λ_{ex} = 490 nm and λ_{em} = 520 nm, using quartz cuvettes on Varian Cary Eclipse Fluorescence Spectrophotometer.

6.2.6. Confocal microscopy

CT26.WT confluent cell monolayers grown on fibronectin coverslips were incubated with liposomes (encapsulating calcein at self-quenching concentration of 80 mM) at a lipid concentration of 100 μM, in a 5% CO_2 incubator at 37°C for the specified duration in RGM. Cell monolayers were then washed 2 times with FB (fluorescent buffer: PBS supplemented with 0.02% sodium azide and 2% FBS). Cells were fixed with a fixation buffer (4% paraformaldhyde in PBS, pH ~ 7.4) for 15 min at 37°C. Nuclear staining was carried out using a cell membrane permeable blue-fluorescent Hoechst 33342 dye at a concentration of 2.0 μmole/ml, and the cell membrane was stained with a cell impermeable red-fluorescent Alexa Fluor® 594 wheat germ agglutinin (WGA) at 5.0 μg/ml in FB for 10 min. Cells were washed again 3 times with FB, and coverslips were mounted on glass slides over ProLong Gold antifade reagent. On the confocal images liposomes are labeled with green, cell membrane with red, and nucleus with blue. The

Olympus Fluoview 1000 Confocal Laser Scanning Microscope at the Biomedical Image Processing Laboratory at the University of Minnesota was used.

6.2.7. Cytotoxicity studies

The cytotoxicity of liposomes encapsulating 5-FU was determined by the sulforhodamine B colorimetric assay (SRB assay) as described previously [10, 168]. CT26.WT confluent cell monolayers were trypsinized (0.25% trypsin + 0.1% EDTA) and were suspended in RGM at a concentration of 10^5 cells/ml. 200 µl of cell suspension was transferred to each well on a 96-well tissue culture plate to give a final seeding density of 20,000 cells/well. Cells were allowed to attach to the plate overnight. The medium was then removed (t = 0 hrs), and 200 µl of medium containing two-fold serial dilutions of 5-FU ranging from 50 µM to 0.5 µM (concentration either encapsulated in liposomes or free drug) was added to the cells. A negative control (no liposome or free drug added) was included. The plates were incubated in 5% CO_2 incubator at 37°C for t = 4 hrs. Plates were later washed 3 times with PBS and incubated with fresh RGM at 37°C in 5% CO_2 incubator for a total of 72 hrs (t = 72 hrs). At t = 0 hrs, one plate was set aside for a no-growth control to account for initial seeding density. On the no-growth control plate the medium was replaced with 200 µl of cold RGM, and cells were fixed by adding 100 µl of cold 10% (w/v) TCA (trichloro acetic acid) ,and the plate was incubated for 1 hrs at 4°C. Remaining plates were fixed similarly at the conclusion of the experiment (t = 72 hrs). After fixation, plates were washed 4 times with de-ionized (DI) water and dried. Plates were stained with 100 µl 0.057% (w/v) SRB (sulforhodamine B solution in DI water) at room temperature for 1 hrs. Plates were washed again 4 times with 1% (v/v) acetic acid solution to remove the unbound SRB dye and dried. 200 µl of 10 mM Tris base solution

(pH 10.5) was later added to dissolve the bound dye and plates were incubated at room temperature for another hour. Finally the OD (optical density) was measured on a plate reader at 510 nm. For IC_{50} (concentration of a drug that is required for 50% inhibition of cell growth) determination, a dose-response curve was generated by plotting the 5-FU concentration of the formulations versus the percent growth inhibition. IC_{50} values were obtained by fitting a sigmoidal curve and obtaining the 5-FU concentration at 50% growth inhibition. Percent growth inhibition was calculated using the following formulas:

$$\%\ of\ control\ cell\ growth = \frac{mean\ OD_{sample} - mean\ OD_{no-growth\ control}}{mean\ OD_{neg\ control} - mean\ OD_{no-growth\ control}} \times 100$$

$$\%\ growth\ inhibition = 100 - \%\ of\ control\ cell\ growth$$

6.3. Results and discussion

6.3.1. Calcein dequenching assays

To design pH-sensitive liposomes with optimal release characteristics, it is necessary to accurately estimate the leakage rates as a function of pH. Liposomes encapsulating calcein at very high concentration (80 mM or higher) are self-quenching, *i.e.* non-fluorescent. When pH-sensitive liposomes with self-quenching calcein concentrations are exposed to an acidic environment (low pH), the calcein is released due to destabilization of liposomes and is diluted in the surrounding media, resulting in a fluorescence signal. The effect of pH on calcein fluorescence is well documented [181, 187-189]. In order to accurately estimate the leakage of calcein from liposomes at a variety of pH values it is necessary to quantify the effect of pH on calcein fluorescence. Figure 6.1A shows the calibration curves for free calcein at different pH values within the concentration range of

interest. The calibration curves were fitted with linear regression and the correction factors (r_{pH}) were determined from the ratio of slope at pH 7.4 to slope at particular pH.

While analyzing the data for leakage rates of pH-sensitive liposomes, we observed that in some cases the calcein fluorescence intensity began to decrease with time. Since the total concentration of the released calcein due to destabilization of the liposomes can only increase as time progresses, the decrease in the fluorescence signal was indicative of calcein photo-bleaching due to repeated measurements. This effect has not been accounted for previously in the literature when estimating leakage rates from liposomes, but is important to consider as it results in the underestimation of leakage rates. In order to quantify this effect, we measured the fluorescence intensity of free calcein at intervals of 1 min over a period of 60 min (within the concentration range of interest and at different pH values). Figure 6.1B shows a representative plot of calcein fluorescence decay (2 mM concentration) at pH 7.4, 6.5, 5.5, and 4.5. Similar plots were obtained for other calcein concentrations (within the concentration range of interest) and the mean decay rates obtained for each pH value were used for the analysis of data ($d_{7.4}$ = 0.43, $d_{6.5}$ = 0.53, $d_{5.5}$ = 0.63, $d_{4.5}$ = 0.73). In order to estimate the liposomal leakage rates accurately, all the data obtained from the pH-sensitive liposome leakage experiments was corrected for both pH and time effects as discussed in the materials and methods.

6.3.1. Effect of liposome composition on leakage rates

pH-sensitive liposomes composed of DOPE/CHEMS have been studied in the literature and show significant release in acidic environments [181, 187-189]. DOPE is a cone shaped molecule and exists in the inverted hexagonal phase at temperatures greater than 10°C [190]. Intercalation of DOPE molecules with CHEMS, which contains a proto-

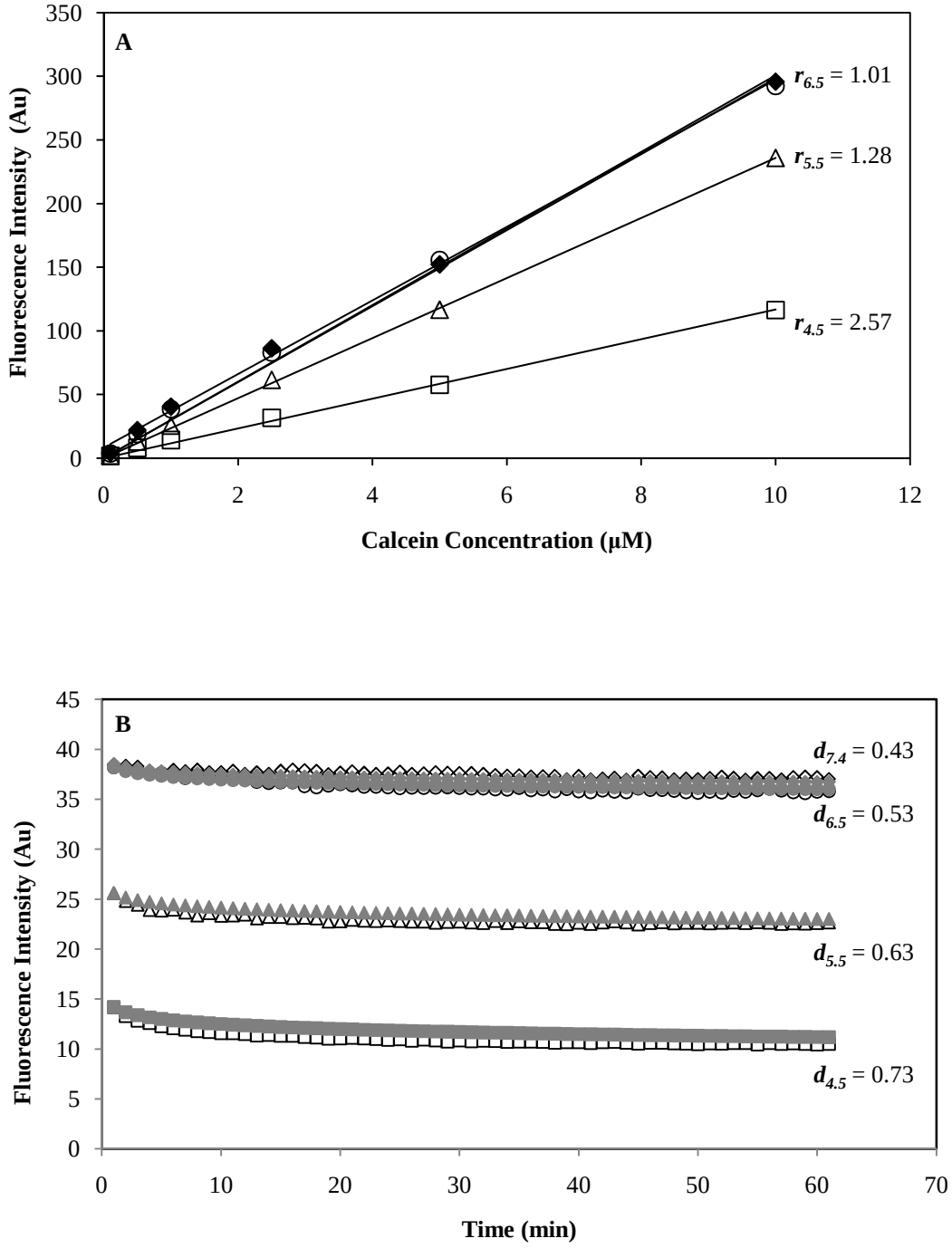

Figure 6.1 (A) Calcein calibration curves (within the concentration range of interest) at pH 7.4 (♦), 6.5 (○), 5.5 (Δ), and 4.5 (□). All curves were fitted with linear regression ($y = mx$, and have $R^2 > 0.99$). The correction factor (r_{pH}) was obtained from the ratio of slope at pH 7.4 to the slope at a particular pH. (B) Decay of 2 mM calcein fluorescence with time at pH 7.4 (♦), 6.5 (○), 5.5 (Δ), and 4.5 (□). The decay constant, d_{pH} is obtained by fitting the data to Eq. (3). Three independent experiments were done at several different concentrations (within the concentration range of interest) and mean d_{pH} values were obtained for each pH (shown in the graph).

-natable group and is negatively charged at physiological pH, stabilizes DOPE molecules in bilayers due to electrostatic repulsion at neutral pH [191-193]. At acidic pH, due to the excess protons, CHEMS is neutralized and DOPE molecules revert back to their inverted hexagonal structures. This leads to destabilization of the liposomal bilayer and leakage of the encapsulated contents. Since pH-sensitive liposomes composed of DOPE/CHEMS are easily recognized by opsonins and have a shorter circulation lifetime *in-vivo*, pH sensitive stealth liposomes (DOPE/CHEMS liposomes incorporating DSPE-PEG2000) were developed to provide longer circulation lifetimes. Inclusion of DSPE-PEG2000 in DOPE/CHEMS liposomes decreases their pH-sensitivity due to stabilization of the bilayer by PEG molecules [188, 189]. However, it has been shown that when these liposomes interact with cells, the intracellular release of calcein per liposome is not significantly affected and therefore incorporation of PEG does not decrease the efficacy of the pH-sensitive liposomes [188]. To further increase the efficacy of PR_b-targeted inert stealth liposomes pH-sensitivity was incorporated in the design so that upon endocytosis they can release their load more effectively. Since peptides can also stabilize the bilayer in a similar manner to PEG (and thus decrease the pH-sensitivity), it is necessary to test the effect of peptide and optimize the lipid composition of the liposomes in order to design targeted pH-sensitive stealth liposomes. The data here is presented for liposomes containing low concentration of PEG2000 because we have previously shown that these liposomes demonstrate the highest binding affinity to colon cancer cells [10]. Figure 6.2A shows the percent leakage of targeted and non-targeted pH-sensitive stealth liposomes, composed of different amounts of the stabilizing lipid, CHEMS, at pH 7.4, 6.5, 5.5, and 4.5, after 1 hrs incubation at 37°C.

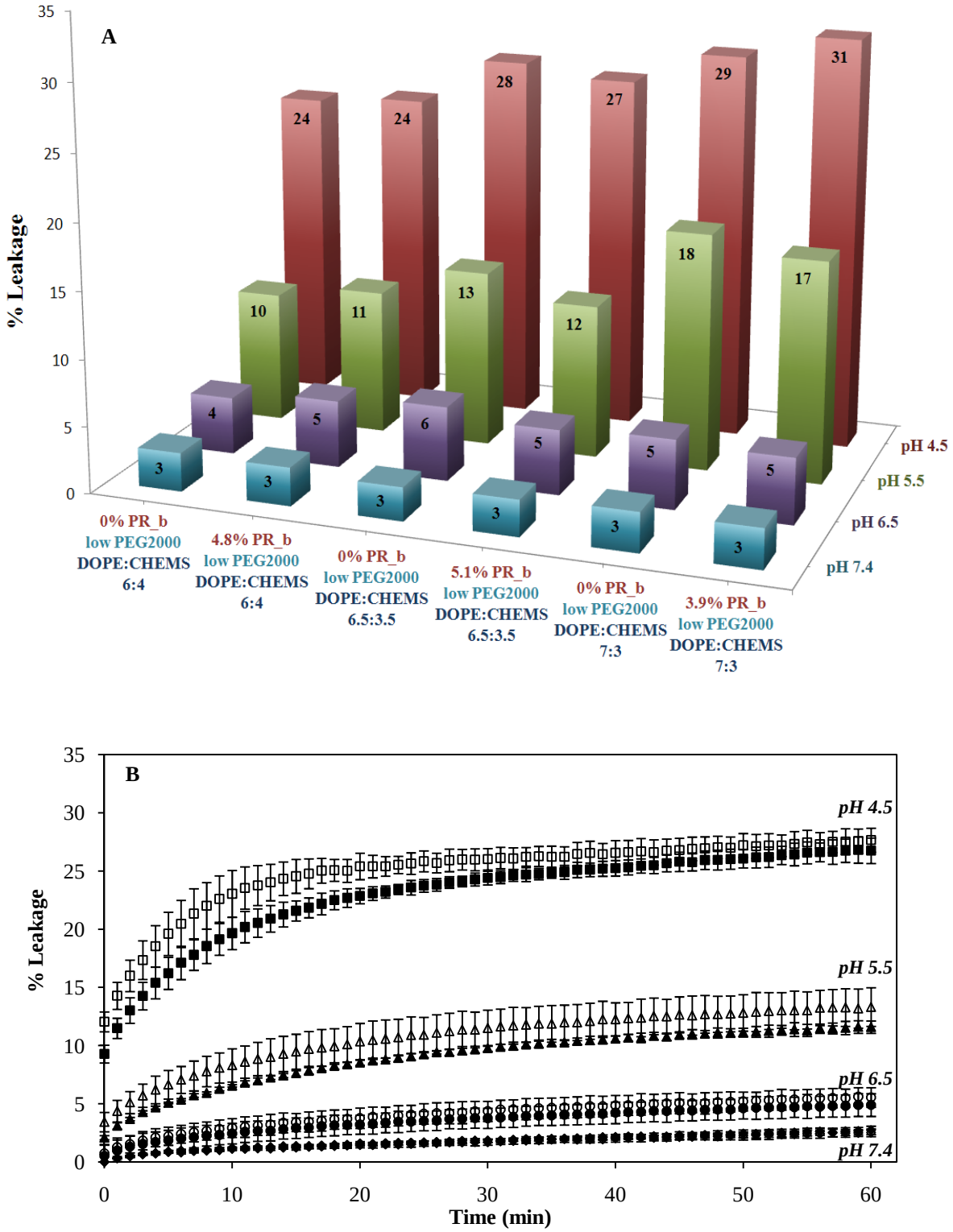

Figure 6.2 pH sensitivity of DOPE/CHEMS PEGylated liposomes. Data is shown as the mean ± SD of two independent experiments (n=2) and each experiment was performed in triplicate. (A) Percentage leakage of different liposome formulations at 60 min and various pH values (SD < 2% for all samples). (B) Release of calcein from pH-sensitive stealth liposomes containing 35% CHEMS, non-targeted (open symbols) and PR_b-targeted (solid symbols) at pH 7.4 (diamonds), 6.5 (circles), 5.5 (triangles), and 4.5 (squares).

The graph shows that for non-targeted pH-sensitive liposomes with DOPE:CHEMS ratio of 6:4 the percent leakage of contents increases from 3% to 24% as the pH is decreased from 7.4 to 4.5. Similar trends are observed for other formulations. Figure 6.2A also shows that decreasing the amount of the stabilizing lipid CHEMS increases the leakage rates from the liposome, as expected, and also illustrates that both the targeted and non-targeted pH-sensitive stealth liposomes show similar leakage rates at 60 min. Increasing the concentration of peptide in liposome formulation, decreases slightly the pH-sensitivity of liposomes but does not inhibit the pH-sensitive release. For example, at pH 4.5 targeted pH-sensitive liposome formulations, with DOPE:CHEMS ratio of 7:3, containing 5.4 mol% PR_b show leakage rate of 27%±0.9%, while formulations containing 3.9 mo% PR_b show leakage rate of 31%±0.6%. These results are from two independent experiments and difference between the leakage rates for the two formulations is statistically significant (student's t-test analysis $p < 0.01$).

To further investigate whether incorporation of the PR_b peptide affects the release characteristics of the pH-sensitive liposomes, the rate of calcein release from PR_b-targeted and non-targeted pH-sensitive stealth liposomes at 37°C and various pH values is plotted versus time (Figure 6.2B). Figure 6.2B shows that the pH-sensitive liposomes show an instantaneous release of calcein (~10-12% at pH 4.5, and ~2-4% at pH 5.5) at t = 0 immediately after exposure to an acidic pH, followed by a more prolonged slow release which was monitored for 60 min. Similar results were observed for the other formulations examined in Figure 6.2A (data not shown). The data presented in Figure 6.2B also shows that both the pH-sensitive stealth liposomes with (solid symbols) and without PR_b (open symbols) exhibit similar leakage profiles at the pH values studied, 7.4, 6.5, 5.5, and

4.5. Based on these results, we conclude that functionalizing the pH-sensitive stealth liposomes with PR_b does not significantly affect the pH-sensitivity of liposomes. Although liposomes with a DOPE/CHEMS ratio of 7:3 showed the highest leakage rate, they tend to be more unstable as observed by formation of aggregates (data not shown) when stored for longer than 1 week. Therefore for the experiments performed in the next sections, pH-sensitive liposomes with a DOPE/CHEMS ratio of 6.5:3.5 were studied, as they exhibit high pH-sensitivity and are also stable.

6.3.2. Binding and uptake of liposomes by colon cancer cells

We have previously demonstrated that PR_b-functionalized inert stealth liposomes can specifically target CT26.WT colon cancer cells, which overexpress the integrin $\alpha_5\beta_1$, through receptor-mediated endocytosis [10]. In order to test whether targeted pH-sensitive stealth liposomes are more effective than their non-targeted and inert counterparts, we compared the binding and uptake of pH-sensitive liposomes to that of inert liposomes to determine whether the pH-sensitive design offers any advantages. Liposomes encapsulating calcein were incubated with colon cancer cells, and total fluorescence signal from the liposomes bound to the cell surface or taken up by cells was measured by lysing the cells as described in the materials and methods section. Figure 6.3 shows the fluorescence intensity from the liposome binding and uptake by CT26.WT cells, at 4 hrs and 16 hrs. The graph illustrates that non-targeted pH-sensitive stealth liposomes show higher fluorescence intensity than non-targeted inert stealth liposomes at all times. This is in agreement with findings from other studies that show that pH-sensitive liposomes are more effectively taken up by cells compared to inert liposomes [181, 188, 189]. When comparing the targeted formulations to the non-targeted ones (pH-

sensitive and inert) it is observed that the PR_b-functionalized stealth formulations show higher fluorescence intensity at both 4 hrs and 16 hrs, and that the targeted pH-sensitive stealth liposomes show the highest fluorescence among all the formulations studied. When comparing data at 4 hrs and 16 hrs, the fluorescence increases with time for all the formulations. One possible explanation for this effect could be that the longer incubation period allows more time for recycling of integrins back to the cell surface where they can continue to aid in the binding and subsequent intracellular accumulation of liposomes. These results demonstrate that incorporation of the targeting peptide PR_b along with a pH-sensitive design can significantly increase the efficacy of the stealth liposomes by improving the binding and uptake of the liposomes.

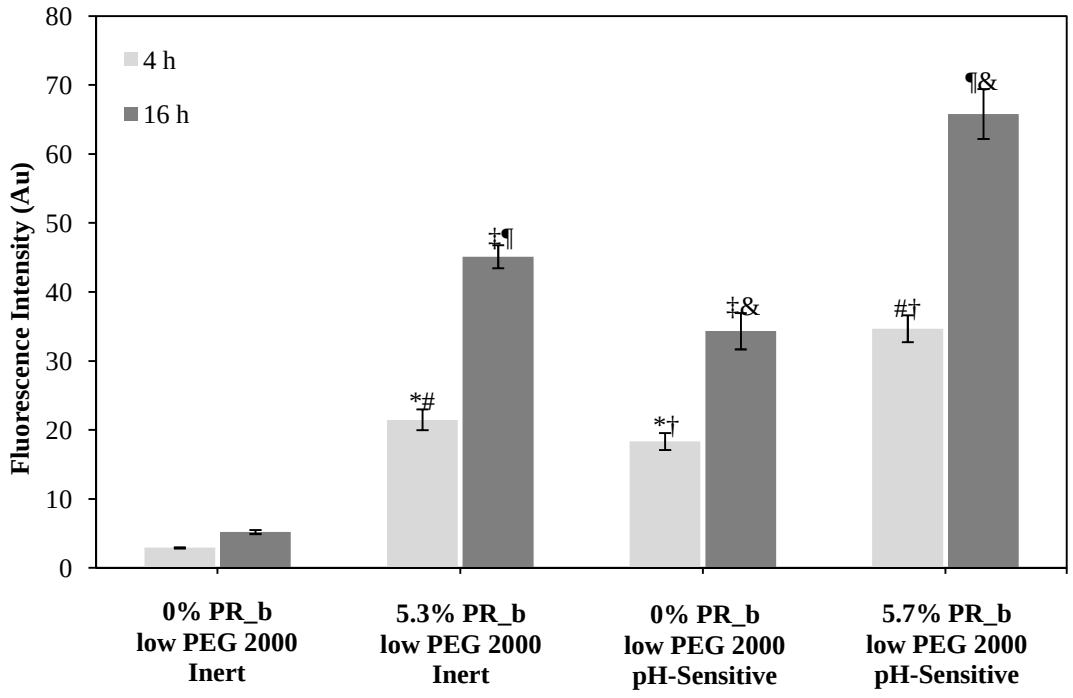

Figure 6.3 Binding and intracellular uptake of various stealth liposomal formulations with low concentrations of PEG2000 loaded with calcein at a self-quenching concentration of 80 mM. Liposomes were incubated with CT26.WT cells at 37ºC for 4 hrs and 16 hrs. At the conclusion of the experiment cells were washed and lysed, and the total fluorescence of samples was measured. Student's t-test analysis for # † ¶ &: $p < 0.001$, and for * ‡: $p < 0.01$, indicating significant statistical difference for all groups. Data is the mean ± SD of two independent experiments (n=2) and each experiment was performed in triplicate.

6.3.3. Intracellular release of liposomes

In the previous section we studied binding and uptake of the liposomes by CT26.WT cells by measuring the fluorescence of the cell lysates. However, this method cannot distinguish between the liposomes that are bound to the cell membrane and those that have internalized. To study whether liposomes release their load when endocytosed, pH-sensitive and inert stealth liposomes with or without PR_b, encapsulating calcein at self-quenching concentration, were incubated with CT26.WT cells for 1, 4, and 16 hrs at 37°C and confocal microscopy images were obtained (Figure 6.4). Binding of liposomes to the cell surface on these images cannot be identified by co-localization of red cell membrane stain and green liposome stain because intact liposomes containing calcein at self-quenching concentration are non-fluorescent. Therefore, the presence of green color between the red cell membrane and the blue nuclear region demonstrates the internalization of liposomes and release of calcein. If liposomes had been internalized without releasing their load, no green color would be observed. The release of the load is likely due to liposome destabilization under the mild acidic conditions present in endocytotic vesicles.

Figure 6.4 shows that at 1 hrs incubation (top row) no green fluorescent signal is observed for the liposome formulations except the PR_b-targeted pH-sensitive stealth liposomes. At 4 hrs, some evidence of internalization and release can be seen for PR_b-targeted inert stealth liposomes and non-targeted pH-sensitive liposomes. However, the PR_b-targeted pH-sensitive stealth liposomes show a very strong signal at 4 hrs that is higher compared to all other formulations studied, and at 16 hrs the effect is more pronounced. From the confocal images shown in Figure 6.4 it can be concluded that

PR_b-targeted pH-sensitive stealth liposomes can internalize and release their load at a shorter period of time compared to PR_b-targeted inert stealth liposomes. Non-targeted pH-sensitive liposomes also show uptake and release, but to a much lesser extent compared to their targeted counterparts. Non-targeted inert liposomes show minimal uptake at release even at 16 hrs, consistent with our previous experiments [10].

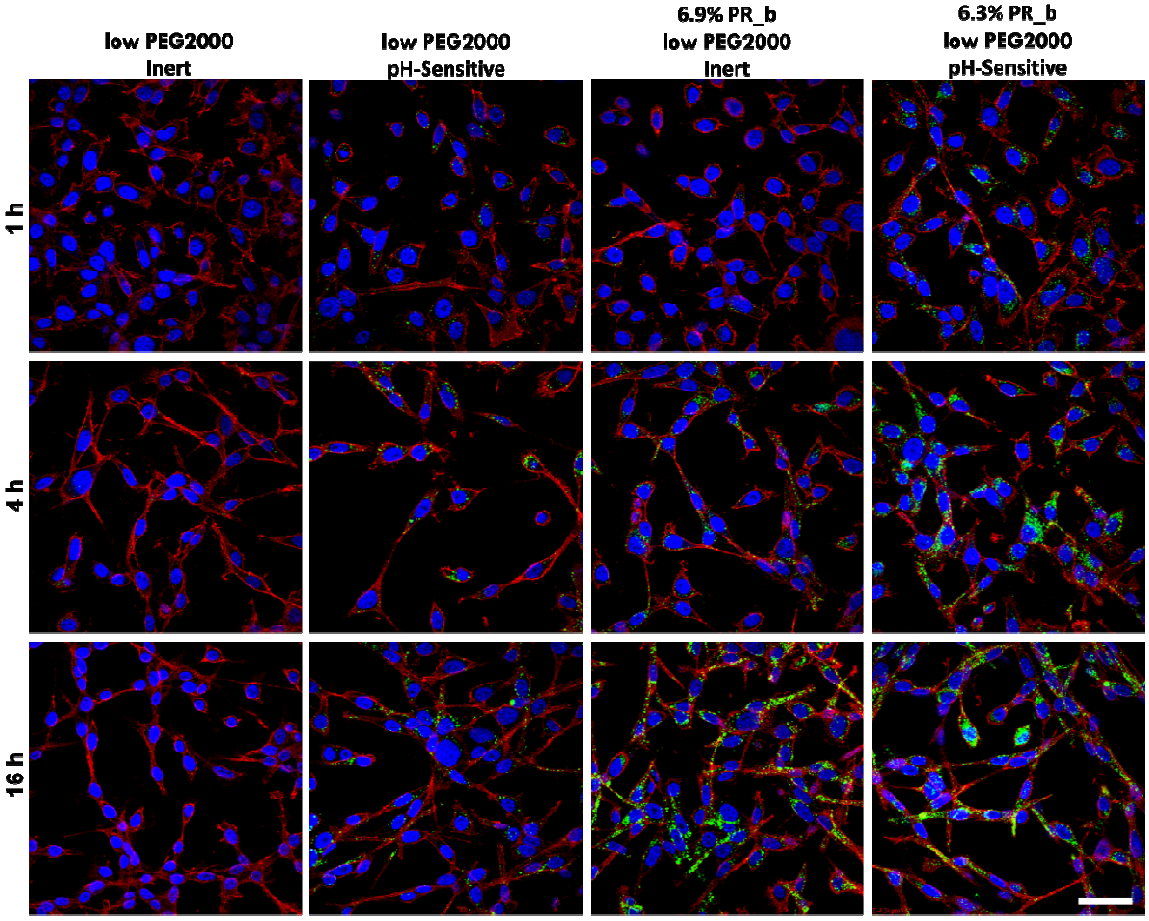

Figure 6.4 Confocal images depicting intracellular release of various stealth liposomal formulations encapsulating calcein at a self-quenching concentration of 80 mM. Liposomes (shown in green) were incubated with CT26.WT cells at 37ºC for 1, 4, and 16 hrs. The nucleus (shown in blue) was stained with Hoechst 33342 dye, and the cell membrane (shown in red) was stained with Alexa Fluor® 594 wheat germ agglutinin (WGA) as discussed in the materials and methods section. The scale bar is 50 μm for all images. Liposome binding to cell surface is not visible on these images because liposomes encapsulating calcein at self-quenching concentrations are non-fluorescent. Fluorescence can be detected only after intracellular release of calcein from the liposomes and can be identified by the green signal in between the red cell membrane and blue nucleus. These images illustrate that PR_b-targeted pH-sensitive stealth liposomes bind to colon carcinoma cells, undergo cellular internalization and release their load in a time period as short as 1 hrs compared to other formulations which can take up to 4 hrs.

The confocal images appear grainy which indicates that all studied liposome formulations release their load in endocytotic vesicles. However we have not verified using endocytotic markers, which endocytotic vesicles these liposome release their load. The observation of green fluorescent signal for targeted pH-sensitive liposomes at shorter incubation period of 1 hrs does indicate that pH-sensitive liposomes release their load earlier in endocytotic pathways when compared to inert targeted liposome formulation. The results obtained demonstrate that PR_b-functionalized pH-sensitive stealth liposomes can have significantly higher efficacy than all other formulations, as they can target integrin $\alpha_5\beta_1$-expressing colon cancer cells and release their contents intracellularly earlier than other formulations studied.

6.3.4. Cytotoxicity studies

5-Fluorouracil (5-FU) is a commonly used chemotherapy agent for the treatment of colon cancer. Free 5-FU has been used in clinical practice for more than 40 years but has serious side-effects such as gastrointestinal and bone marrow toxicity. Encapsulating 5-FU in liposomes can help its delivery to the target organs and reduce side effects [146, 147].

In this study, we prepared different liposomal formulations encapsulating 5-FU and examined their cytotoxicity to colon cancer cells. CT26.WT cells were incubated with either 5-FU containing liposomes or free 5-FU for 4 hrs, and allowed to grow for a total of 72 hrs. Using a negative control (no liposomes or free drug added) and a no-growth control that determined the initial seeding density, the amount of growth inhibition was examined as explained in the materials and methods section.

Table 6.1 Cytotoxicity of 5-FU encapsulated in stealth liposomes and targeted to CT26.WT cells for 4 hrs. All values are representatives of mean ± SD from two independent experiments (n=2) and each experiment was performed in quadruplet. Values reported are IC_{50} values in µM at t = 4 hrs.

Formulation	AVG	SD
Free 5-FU	12.82	0.98
0% PR_b low PEG2000 Inert	18.78	1.98
4.4% PR_b low PEG2000 Inert	14.71	1.41
0% PR_b low PEG2000 pH-Sensitive	16.65	0.59
5.6% PR_b low PEG2000 pH-Sensitive	12.04	1.11

Table 6.1 summarizes the IC_{50} values for the free drug and different liposomal formulations. At 4 hrs, PR_b-targeted pH-sensitive stealth liposomes show the highest cytotoxicity (12.04 ± 1.11 µM) compared to all the other liposome formulations and was comparable to that of free 5-FU. The IC_{50} values follow trends consistent with observations in the previous sections. When comparing the different liposomal formulations, the PR_b-targeted pH-sensitive stealth liposomes show the highest cytotoxicity (12.04 ± 1.11 µM), followed by PR_b-targeted inert stealth liposomes (14.71 ± 1.41 µM), non-targeted pH-sensitive stealth liposomes (16.65 ± 0.59 µM), and non-targeted inert stealth liposomes (18.78 ± 1.98 µM). The results obtained in this section are in agreement with those obtained in the previous sections and confirm that PR_b-functionalized pH-sensitive liposomes show higher efficacy than non-targeted pH-sensitive liposomes or inert liposomes, targeted or non-targeted, as they have the ability to target the integrin $\alpha_5\beta_1$ expressing colon cancer cells and are capable of releasing their load intracellularly in a fast and effective manner.

6.4. Conclusion

In this study, we have engineered a targeted drug delivery system capable of targeting colon cancer cells expressing the integrin $\alpha_5\beta_1$ and releasing their load intracellularly in a fast and effective manner. We have optimized the release of the encapsulated load from the pH-sensitive stealth liposomes by varying the composition of the liposomes (changing the ratio of DOPE/CHEMS) and verifying that incorporation of the targeting peptide PR_b does not affect the pH-sensitivity of the stealth liposomes. For the first time we present a detailed report on how to accurately measure the leakage rates at different pH values and time points of pH-sensitive liposomes encapsulating a dye such as calcein at a self-quenching concentration. Previously, similar studies have ignored the decay of fluorescence due to repeated measurements (photo-bleaching effect), which results in underestimation of leakage rates. PR_b-functionalized pH-sensitive stealth liposomes bind to colon carcinoma cells, undergo cellular internalization, possibly via $\alpha_5\beta_1$ integrin-mediated endocytosis, and can release a significant part of their load in a time period as short as 1 hrs. PR_b-targeted inert stealth liposomes can take up to 4 hrs before they start releasing some of their contents. This implies that *in-vivo* a pH-sensitive design may help improve the overall efficacy of the drug when compared to its delivery via inert liposomes. In addition, a faster release rate might be an indication of pH-sensitive liposomes releasing part of their load in endosomes (before they reach the lysosomes) in contrast with inert liposomes that release their load in lysosomes [110]. This could be particularly beneficial when delivering drugs that cannot withstand the harsh acidic environment present in lysosomes. Finally, PR_b-targeted pH-sensitive stealth liposomes show significantly higher cytotoxicity than the PR_b-targeted inert

stealth liposomes, as well as the non-targeted stealth liposomes (both pH-sensitive and inert), and are as effective as free 5-FU. Based on the above findings, we conclude that the pH-sensitive stealth liposome functionalized with PR_b can be potentially used *in-vivo* and may help reduce the deleterious side effects of alternative therapies by delivering a therapeutic load directly to colon cancer cells in a fast and effective manner.

6.5. Acknowledgements

This work was supported in part by the National Institute of Biomedical Imaging and Bioengineering (R03EB006125), the National Cancer Institute (R01CA120383), the Camille Dreyfus Teacher-Scholar Awards Program, and the MRSEC Program of the National Science Foundation under Award Number DMR-0212302. The content is solely the responsibility of the authors and does not necessarily represent the official views of the National Institute of Biomedical Imaging and Bioengineering, the National Cancer Institute, or the National Science Foundation.

7. Fractalkine targeted drug delivery

7.1. Introduction

Frequently the use of novel therapeutics in medicine is opposed by the lack of efficiency in delivery of these therapeutic agents to the target organs. After a therapeutical agent is administered to the body it undergoes even biodistribution throughout the body. In order to reach the site of action these agents have to cross several biological barriers in the body like organs, tissues, and cells, where these agents could be adsorbed, metabolized, or excreted out of the body. Therefore, to increase the effectiveness, the drug is usually administered in large quantities. In case of a potent drug, this results in deleterious effects on the healthy organs of the body, commonly referred to as *side effects*. Targeted drug delivery can address the above problems and can be defined as a strategy to efficiently transport the drug to its therapeutic site of action by the appropriate choice of carrier, route, and target [1].

Liposomes have long been used as carriers for drug delivery and have the inherent advantage of their resemblance to the cell membrane. Being composed of naturally occurring substances, liposomes are both biocompatible and biodegradable. In addition, they can encapsulate hydrophilic drugs in their interior aqueous space, and also are able to incorporate hydrophobic drugs in between their lipid bilayer. The flexibility of size and composition, aids in tailoring the liposomes as dictated by the needs of the drug and its target. Moreover because of the several methods available for preparing and formulating liposomes, high encapsulating efficiencies can be achieved for a variety of drugs, creating a tremendous potential for their use as pharmaceutical carriers [194]. The ability of liposomes to interact at the cellular level provides the opportunity for releasing the drug

both intracellularly and extracellularly [195]. Liposomes can also be functionalized with site-specific markers which provide an additional handle for site-directed targeting.

Vascular endothelium comprises of a cell monolayer, endothelial cells (ECs), forming the inner lining of the blood vessels, which are strategically positioned to control vascular physiology. The total surface area of vascular endothelium in the body is estimated close to 350 m^2, making it large and highly accessible from the systematic circulation [196]. ECs are strongly involved during inflammatory disorders, expressing several adhesion molecules on their surface, which makes them an attractive target for drug delivery. Fractalkine is a novel chemokine upregulated on vascular endothelium only during inflammation or infection and serves as an adhesion molecule in addition to its chemotactic properties [41]. This unique feature of fractalkine allows recruitment and arrest of a subset of leukocytes (monocytes, natural killer (NK), and T cells) from the systemic circulation in a selectin and integrin independent manner [42-47]. The role of fractalkine has been established in several inflammatory diseases like, rheumatoid arthritis, atherosclerosis, allograft rejection, AIDS, and very recently cancer [52-59]. These observations strongly suggest that fractalkine could play an important role in targeted drug delivery.

We have previously shown that a peptide sequence corresponding to residues 3-20 of the N-terminus of the fractalkine receptor (NTFR) binds specifically to the fractalkine molecule [17]. Figure 7.1 shows the design of the NTFR peptide-amphiphile (NTFR peptide-amphiphile) and a schematic of the fractalkine receptor (CX3CR1). The peptide-amphiphile structure consists of a 16-carbon dialkyl ester tail, a glutamic linker and a $(CH_2)_2$ spacer followed by the bioactive peptide sequence NTFR.

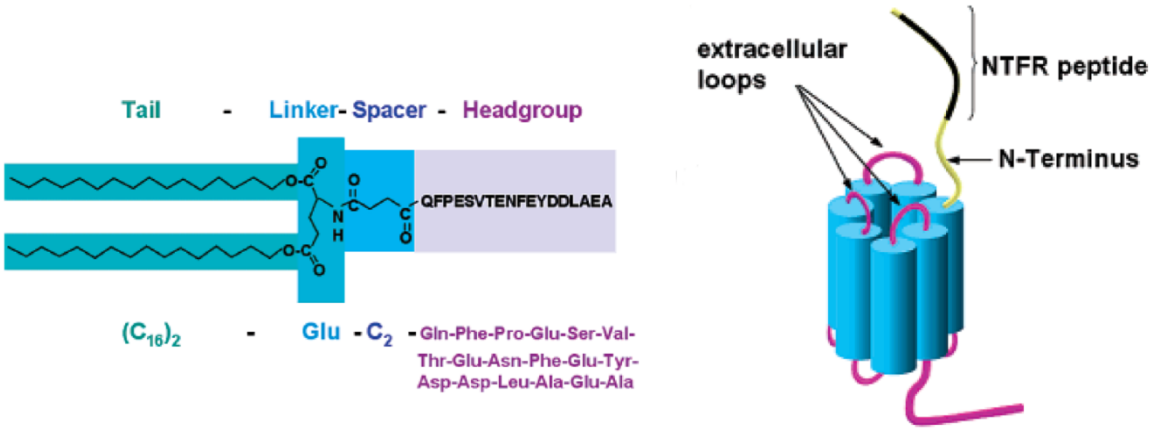

Figure 7.1 The design of the NTFR peptide-amphiphile based on the residues 3-20 of N-terminus of the fractalkine receptor (CX3CR1). Reprinted from [17], Copyright (2005) with permission from Elsevier.

In our previous work, bioartificial membranes (resembling liposome surfaces in two dimensions) comprising of NTFR peptide-amphiphile and DPPC phospholipids were constructed using the Langmuir-Blodgett (LB) technique. The binding of NTFR to fractalkine was determined using an atomic force microscopy (AFM). The results demonstrated that NTFR binds to fractalkine and the maximum adhesion was obtained for mixed surfaces with 75 mol% NTFR and 25 mol% DPPC concentration, as compared to pure NTFR peptide-amphiphile surfaces [17]. This was due to the presence of the shorter DPPC molecules that allowed more room for the NTFR peptide to bend and present the bioactive sequence at the interface for binding to fractalkine molecules. In order to examine the specificity of NTFR-fractalkine interaction, the adhesion receptor integrin $\alpha_5\beta_1$ and its ligand (peptide sequence GRGDSP) were used as controls, as integrins are adhesion receptors present on endothelial cells. Adhesion force measurement between the $\alpha_5\beta_1$ (immobilized on the AFM tip) and NTFR surfaces gave minimal adhesion as compared to fractalkine and NTFR. The NTFR-$\alpha_5\beta_1$ interaction was of comparable value to the $\alpha_5\beta_1$-GRGESP (inactive peptide) interaction and much smaller

than the $\alpha_5\beta_1$-GRGDSP adhesion [17]. The AFM adhesion data demonstrated that the NTFR binds preferentially to fractalkine with an affinity that is comparable to the $\alpha_5\beta_1$-GRGDSP specific interaction.

The focus of this work is to design and evaluate sterically stabilized liposomes (liposomes covered with poly(ethylene glycol), PEG) incorporating the NTFR peptide-amphiphile and targeted specifically to the fractalkine expressing cells. The majority of the work is done with inflamed endothelial cells (HUVEC) and some results are shown for colon cancer cells (DLD-1). The hypothesis is that the peptide-amphiphile on the surface of liposomes will recognize fractalkine expressing cells and bind in a specific manner, while the PEG molecules will provide a steric barrier minimizing any non-specific binding and allowing the liposomes to circulate for a long period of time. Thus our approach utilizes fractalkine molecule as the target, NTFR as the bullet, and liposome as the carrier.

7.2. Materials and methods

7.2.1. Materials

Lipids, 1,2-dipalmitoyl-sn-glycero-3-phosphocholine (DPPC), cholesterol (CHOL), and 1,2-dipalmitoyl-sn-glycero-3-phosphoethanolamine-N-(methoxy(polyethylene glycol)-2000) (DPPE-PEG2000) were purchased from Avanti Polar Lipids Inc. (Alabaster, AL). The extruder and the 100 nm polycarbonate membranes were obtained from Avestin Inc. (Ottawa, Canada). The peptide headgroup NTFR (Gln-Phe-Pro-Glu-Ser-Val-Thr-Glu-Asn-Phe-Glu-Tyr-Asp-Asp-Leu-Ala-Glu-Ala) corresponding to residues 3-20 of the N-terminus of CX_3CR1, as described by Kokkoli et al. [17], and the PR_b (KSSPHSRN$(SG)_5$RGDSP) peptide, were purchased in crude form from the

Oligonucleotide & Peptide Synthesis Facility at the University of Minnesota. The peptide-amphiphiles ($(C_{16})_2$-Glu-C_2-peptide) were synthesized as described previously [22, 23]. Human umbilical vein endothelial cells (HUVECs) were purchased from Lonza Inc. (Allendale, NJ) and MCDB-131 growth media was obtained from Sigma Aldrich Corporation (St. Louis, MO). DLD-1 human colon cancer cell line and RPMI-1640 culture media were obtained from ATCC (Manassas, VA). Fetal bovine serum (FBS) was purchased from Atlas Biologicals (Fort Collins, CO), and the BCA (bicinchoninic acid) protein assay kit was obtained from Pierce (Rockford, IL). All other reagents were purchased from Sigma Aldrich Corporation (St. Louis, MO) and were of biotechnology performance certified grade.

7.2.2. Preparation of liposomes

Conventional liposomes were prepared essentially as described elsewhere [166]. Briefly, lipids were dissolved in $CHCl_3$ and NTFR peptide-amphiphile or PR_b peptide-amphiphile were dissolved in $CHCl_3$:MeOH (few drops of methanol were added till solutions became clear). Lipids and peptide-amphiphile were combined at the ratios (65-x):35:x mol% of DPPC:Chol: peptide-amphiphile, where x is the indicated molar ratio of the peptide-amphiphile. Solvents were removed by evaporating under a gentle stream of argon at 65°C, followed by drying under vacuum for 2 hrs. The lipid film was hydrated with HBSE buffer (10 mM Hepes, 150 mM NaCl, and 0.1 mM EDTA) at 65°C at concentration of 10 mM total lipids. Hydrated lipids were freeze-thawed ten times, then extruded for 41 cycles through four stacks of 100 nm polycarbonate membranes using a hand-held extruder. Liposome diameter was determined by dynamic light scattering, and ranged from 80-150 nm. Phospholipid concentration was determined using the

phosphorus colorimetric assay described elsewhere [135, 167]. Peptide concentration was determined using the BCA assay according to the manufacturer's protocol. Liposomes were stored at 4-8°C and used within 10 days of preparation.

7.2.3. Cell culture

HUVEC cell cultures were carried out in growth media MGM (MCDB-131 basal media containing 20% fetal bovine serum (FBS), 50 μg/ml endothelial cell growth supplements, 50 μg/ml heparin, 2 mM glutamine, 2.5 μg/ml gentamicin, 2.5 μg/ml amphotericin B, 50 units/ml pencillin and 50 μg/ml streptomycin). Cells were grown in T-25 flasks with a feeding cycle of 2 days. After cells became 90% confluent (usually after 5-7 days), they were trypsinized using 0.25% trypsin/EDTA and were seeded in fresh T-25 flasks (7,500 cells/cm2) for the next passage.

DLD-1 were grown in RGM (modified RPMI-1640 medium supplemented with 10% FBS, 2 mM L-glutamine, 100 units/ml penicillin, and 0.1 mg/ml streptomycin). Cells were grown in T-75 flasks with a feeding cycle of 2 days. After cells became 80% confluent (usually after 5 days) they were trypsinized (0.25% trypsin + 0.1% EDTA) and were suspended in RGM. Cells were washed twice and finally were frozen under liquid nitrogen in RGM containing 10% DMSO (dimethyl sulfoxide) for future use. For subsequent passages cells were seeded in fresh T-75 flasks at a density 10,000 cells/cm^2 and were cultured in RGM with a feeding cycle of 2 days.

7.2.4. Cell inflammation

HUVEC monolayers between passages 2-4 were used for all the experiments. When cells became 80% confluent they were inflamed in MCDB-131 media containing 2% FBS with the specified concentration of the pro-inflammatory cytokines (TNF-α and

IFN-γ) for the specified period of time in 5% CO_2 incubator. DLD-1 monolayers were inflamed using a similar protocol in RPMI-1640 media containing 2% FBS.

7.2.5. Liposome binding assays

HUVEC monolayers between passages 2-4 were used for all the experiments. Cells were grown on standard T-25 tissue culture flask until they were confluent. Cells were inflamed in growth media containing pro-inflammatory cytokines (TNF-α and IFN-γ), at a concentration of 80 ng/ml for 12-16 hrs in 5% CO_2 incubator. Prior to experiment cells were trypsinized using 0.25% trypsin/EDTA, pelleted, and suspended in MCDB-131 media + 2% FBS, and seeded on tissue culture treated clear 96-well plates at a concentration of 100,000 cells per well and were allowed to attach for 4 hrs. At conclusion of 4 hrs, inflamed and healthy cells were incubated with fluorescently labeled liposomes at a 1 mM total lipid concentration, in MCDB-131 media + 0.1% BSA (bovine serum albumin) for 2 hrs at 37°C. Blank wells on 96-well plate were used as control to account for non-specific binding to well walls. At the conclusion of the experiment, cells washed three times with MCDB-131 media + 0.1% BSA and fluorescent intensity was measure with a microplate spectrofluorometer (SpectraMax, Molecular Devices). A standard curve was generated between fluorescent intensity of the liposomes and the lipid concentration. Fluorescent intensity data obtained from liposome binding experiment was calibrated against the standard curve to obtain lipid concentrations of liposomes bound to the cells.

7.2.6. Flow cytometry analysis

Confluent cell monolayers were trypsinized, pelleted and suspended in growth media. Cells were seeded on 6-well plate at a concentration of 1 million cells per well and

allowed to attach for 24 hrs. Inflammation was carried out prior to experiment by incubation the cells with pro-inflammatory cytokines (TNF-α and IFN-γ), at a concentration of 80 ng/ml for 12-16 hrs in 5% CO_2 incubator. Cells were washed two times with PBS and were incubated with either liposomes at a lipid concentration of 100 μM or 2.5 μg of anti-human fractalkine monoclonal antibody PE-conjugated (RnD Systems, Minneapolis) in MCDB-131 media + 2% FBS. Cells were incubated with liposomes for 3 hrs or with antibodies for 45 min, at 37 °C. At the conclusion of incubation, cell were washed twice with PBS, trypsinized, pelleted and re-suspended in 1 ml of PBS containing 1% BSA. Flow cytometry analysis was carried out immediately. FACS Calibur located at the Flow Cytometry Core facility in the Cancer Research Center of the University of Minnesota was used.

7.3. Results and discussion

7.3.1. Fractalkine expression on inflamed HUVECs or DLD-1 cells

The target molecule of interest should be constitutively overexpressed on the tissue of interest for successful targeting. Fractalkine expression on inflamed HUVECs (HUVECs incubated with pro-inflammatory cytokines TNF-α and IFN-γ) and on DLD-1 colon cancer cells under the influence of cytokines present in tumor conditions, was measured and optimized by variation of several different parameters. Figure 7.2 shows the light microscopy images for healthy and inflamed HUVECs. The images show that under the influence of pro-inflammatory condition cytokines, cells tend to be more elongated and less confluent when comparison to normal conditions, indicating a change in phenotype of the cell in response to cytokines.

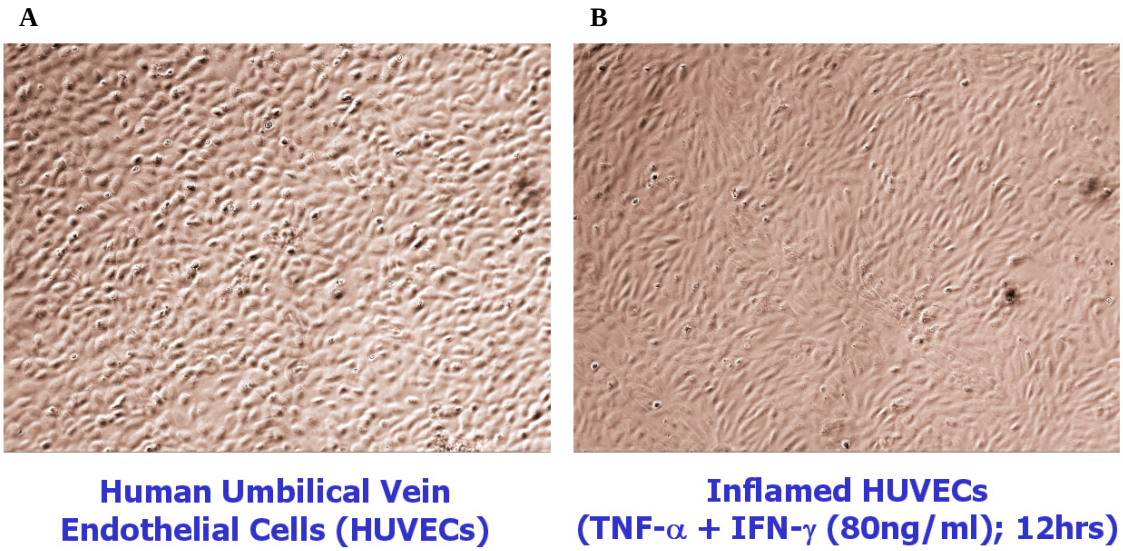

Figure 7.2 Light microscopy images at 10X for A) healthy and B) inflamed HUVECs.

Figure 7.3A shows results from a flow cytometry analysis of fractalkine expression on healthy and inflamed HUVECs under different concentrations of cytokines, TNF-α and IFN-γ. The results indicate that using a combination of cytokines significantly enhances the expression of fractalkine. Therefore a library was constructed with combinations of different concentrations of cytokines, TNF-α and IFN-γ and inflammation times. Flow cytometry histograms are presented in Figure 7.3B. Results show that fractalkine expression is very consistent for different concentration of cytokines and inflammation times. More than 50% of cells express fractalkine and the expression does not depend strongly on the concentration of cytokines, and duration of inflammation. Figure 7.4 presents similar data obtained for DLD-1 colon cancer cells.

The results presented demonstrate that the expression of fractalkine on inflamed HUVECs and DLD-1 cells, is consistent under the presence of pro-inflammatory cytokines TNF-α and IFN-γ and does not depend strongly on the concentration of cytokines and length of incubation.

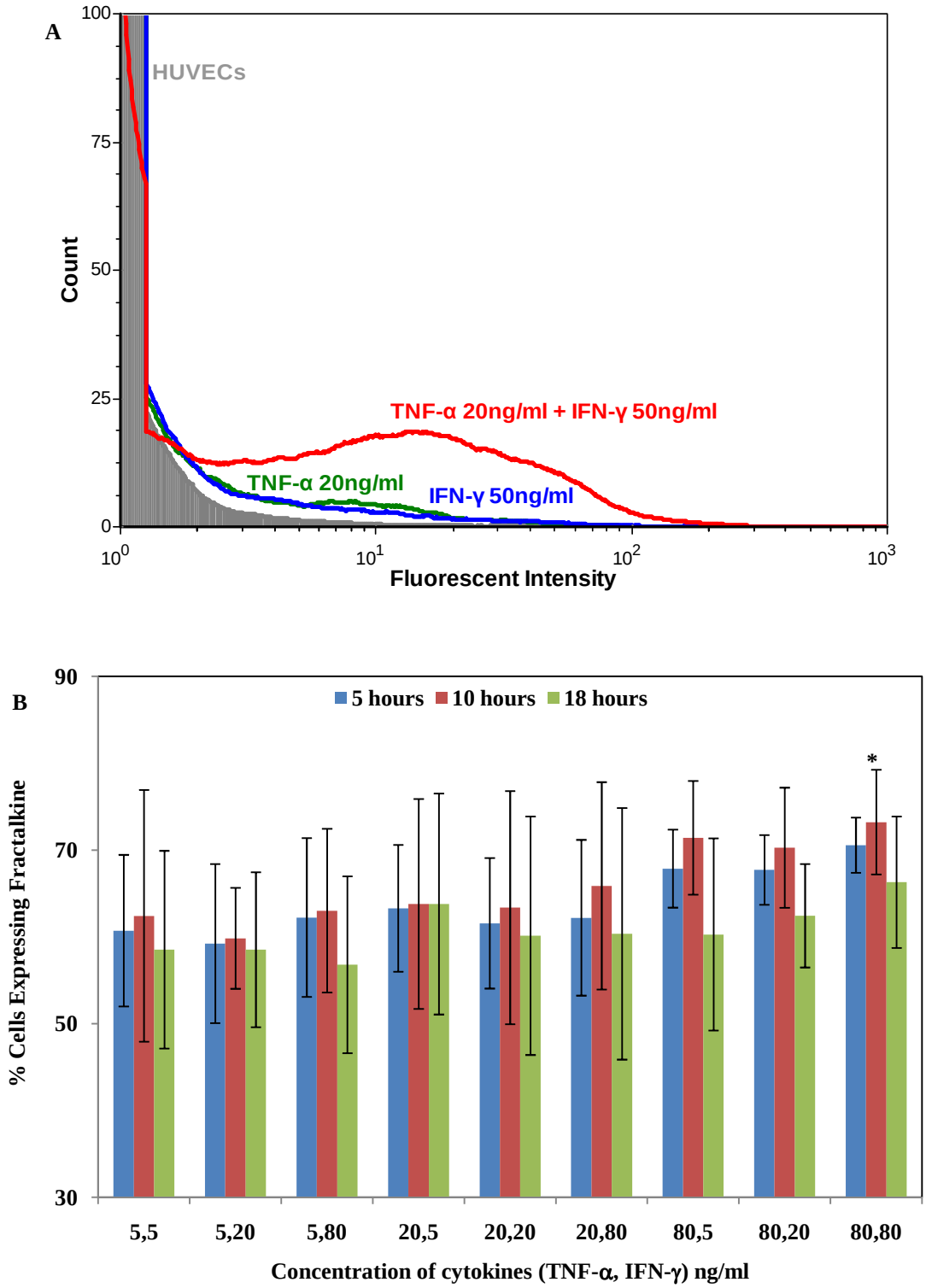

Figure 7.3 A) Flow cytometry data for inflammation of HUVECs with TNF-α and IFN-γ for 18 hrs. B) Flow cytometry analysis for inflammation of HUVECs with different concentrations and duration with TNF-α and IFN-γ. Y-axis represents percentage of cells expressing fractalkine. Concentrations of respective cytokines are on x-axis. Results are shown as mean ± SD from three measurements from a single experiment (n=1). * Represents the cocktail concentration and duration chosen for further experiments.

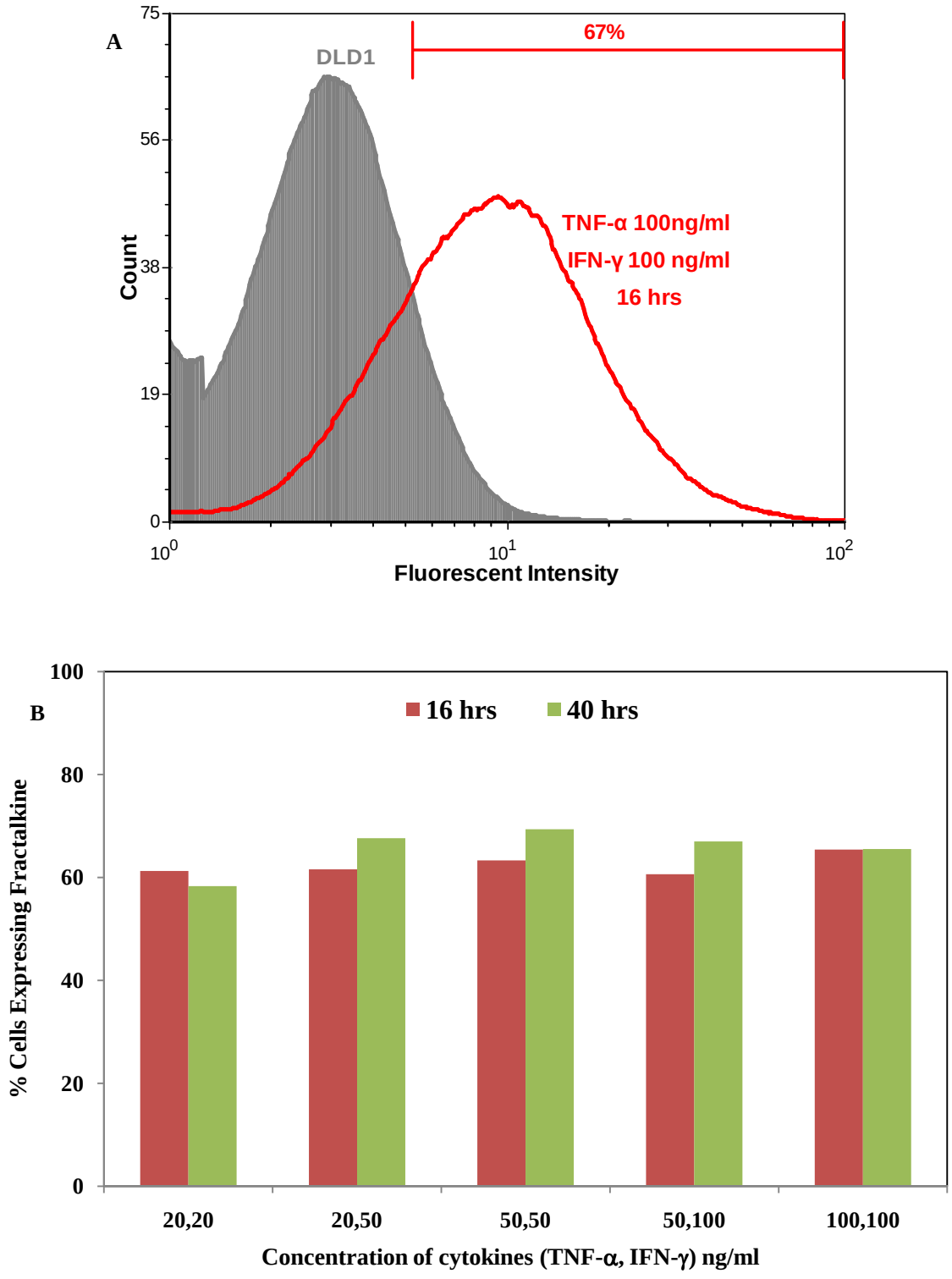

Figure 7.4 A) Fractalkine expression on DLD-1 colon cancer cells in presence of TNF-α and IFN-γ for 16 hrs. B) Flow cytometry analysis for DLD-1 under different concentrations and duration with TNF-α and IFN-γ. Y-axis represents percentage of cells expressing fractalkine. Concentrations of respective cytokines are on x-axis. The results are presented from one single experiment.

These experiments do not explore the minimum threshold concentration and length of incubation, needed for constitutive fractalkine expression, but are able to provide a range of concentrations and incubation periods to obtain a consistent expression for fractalkine (~60%). In order to keep variations from phenotype minimal within each set, every set of experiment was done at the same passage, and to account for the effect of phenotype, different sets of experiments were carried out at different passages.

7.3.2. Targeting and uptake of NTFR liposomes by inflamed HUVECs

HUVECs express fractalkine only in the presence of proinflammatory cytokines such as TNF-α and IFN-γ. Binding of NTFR liposomes was therefore tested on both inflamed and healthy HUVECs with 96-well plates and flow cytometery.

Figure 7.5 shows flow cytometry results for binding of liposomes to healthy and inflamed HUVECs. The results show that NTFR liposomes bind both to healthy and inflamed cells at similar levels. NTFR liposomes also do not show a significant shift in binding affinity when compared to conventional liposomes. PR_b functionalized liposomes are shown for comparison and they show an order of magnitude shift in binding affinity when compared to conventional liposomes. Mean fluorescent intensities obtained from the histograms in Figure 7.5 are presented in Table 7.1. The mean fluorescence intensity data clearly shows that NTFR liposomes do not show any selectivity towards fractalkine expressing inflamed HUVECs. PR_b targeted liposomes on the other hand show significantly higher binding to HUVECs when compared to conventional liposomes, and they seem to bind with higher affinity to healthy HUVECS than inflamed ones. The level of integrin $\alpha_5\beta_1$ expression on these cells was not examined.

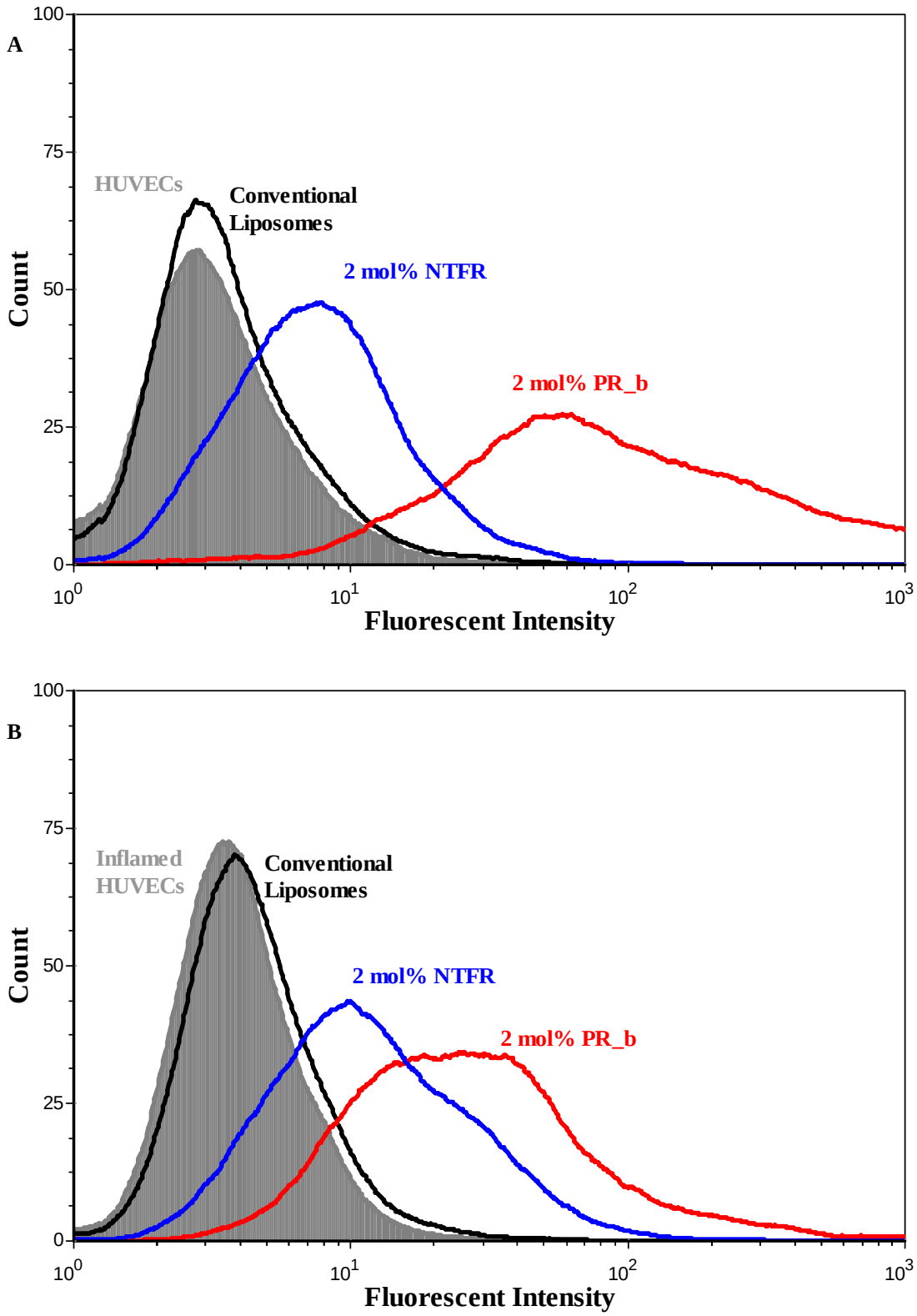

Figure 7.5 Flow cytometry results for binding of different liposomes to HUVECs A) Healthy HUVECs, no cytokines present; B) Inflamed HUVECs with cytokines TNF-α and IFN-γ at a concentration of 80 ng/ml each for 12 hrs.

Table 7.1 Mean fluorescence intensities obtained from Figure 7.5 for binding of liposomes to HUVECs.

	HUVECs	Inflamed HUVECs
Control (Cells)	4.07	4.63
Conventional Liposomes	4.89	5.32
2 mol% NTFR Liposomes	9.85	17.01
2 mol% PR_b Liposomes	290.02	60.51

Figure 7.6 shows result from the 96-well plate assay, and data demonstrates that NTFR liposomes show similar levels of binding and uptake to both inflamed and healthy HUVECs. Since PR_b functionalized liposomes show strong binding affinity towards HUVECs the PR_b peptide was incorporated in the NTFR liposomes to explore a dual targeting approach, where PR_b binds to the integrin $\alpha_5\beta_1$ and NTFR binds to fractalkine.

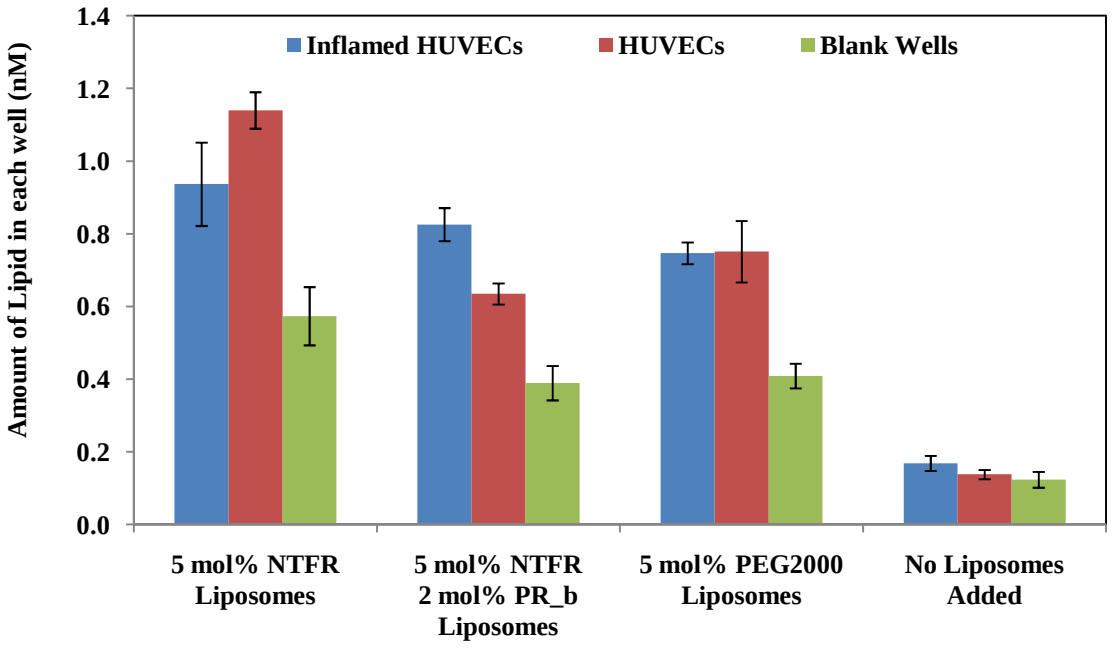

Figure 7.6 Binding of functionalized liposomes to HUVECs. The results show that NTFR liposomes show similar level of binding to both inflamed and healthy HUVECs.

The result from the dual targeted liposomes (5 mol% NTFR and 2 mol% PR_b) show higher binding and uptake of the liposomes by the inflamed HUVECs than the healthy HUVECs, but when compared to the data from the 5 mol% PEG2000 stealth liposomes (negative control) there is not a substantial increase. Therefore, results from Figure 7.5 and Figure 7.6 show that the NTFR liposomes lack affinity and specificity for fractalkine expressing cells (inflamed HUVECs).

7.4. Current work

NTFR functionalized liposomes do not show significant binding and selectivity towards fractalkine expressing HUVECs. The work with PR_b targeted stealth liposomes (discussed in chapters 5 and 6) has shown that peptide functionalized liposomes show high affinity and specificity towards their target cells. Therefore the reason for the poor performance of NTFR functionalized liposomes could be either the weak affinity of NTFR for fractalkine molecule, or the non-specific interactions with other cell surface receptors.

Current work in the Kokkoli group is focused towards the development of a better targeting vector for fractalkine. Aptamers are pursued as targeting ligands for fractalkine. Aptamers are single stranded oligonucleotides (DNA or RNA) selected from a randomly synthesized oligonucleotide library through the process of SELEX (systematic evolution of ligands by exponential enrichment) [197-199]. Aptamers have well defined three dimensional structures and are capable of recognizing target molecule of interest with high affinity and specificity [198]. Aptamers are usually 20 to 80 bases long and have affinities in the low nM to pM range, similar to antibodies. In comparison to antibodies aptamers are very stable. They can be heated to 80°C, stored in various solvents or harsh

environments, and return to their original conformation through the appropriate step of annealing. In addition, since aptamers are chemically synthesized they do not pose problems of an immunogenic response like antibodies [200].

Aptamer-functionalized liposomes have been successfully synthesized in the Kokkoli group and the protocol has been discussed in detail in section 4.3. Aptamer functionalized liposomes are currently being explored as targeted drug delivery systems.

7.5. Conclusions

In this study, we engineered and characterized functionalized liposomes targeted to fractalkine expressing cells, such as inflamed HUVECs and DLD1. We have shown that fractalkine is a promising target molecule for targeted drug delivery to inflamed endothelium (HUVECs) or cancer cells (DLD-1). Fractalkine is highly upregulated on endothelium during inflammation and is not present under normal conditions. Since pro-inflammatory cytokines are present in tumor conditions, fractalkine could be another potential target for cancer applications. Previous work has shown that NTFR peptide corresponding to residues 3-20 of N-terminus of the fractalkine receptor (NTFR) binds to pure fractalkine molecules. NTFR functionalized liposomes bind to fractalkine expressing HUVECs but fail to show high affinity and specificity. Currently the work is being focused towards development of aptamers and aptamer-functionalized liposomes.

8. Conclusions

Liposomes functionalized with moieties like antibodies, peptides, or aptamers, have a great potential for achieving the goal of drug targeting. Two important parameters in the development of targeted drug delivery carriers are: the delivery systems should show high selectivity towards their target and upon reaching the site of interest they are able to release their load effectively.

The work in this thesis has been primarily focused towards the development of optimized liposome formulations for targeted drug delivery applications. Liposomes functionalized with the PR_b peptide can specifically target integrin $\alpha_5\beta_1$ expressing colon cancer cells with high affinity, undergo cellular internalization via an endocytosis mechanism, and deliver a therapeutic load. Liposomes were optimized by varying the amounts of both the peptide and PEG molecules on the liposome surface and the effect of their concentration was studied. Increasing the amount of PR_b peptide enhances the binding affinity and intracellular uptake of liposomes, and increasing the amount of PEG reduces it. The size of PEG molecule also affects the binding affinity of liposomes. High molecular weight PEG2000 when incorporated in the peptide functionalized liposomes, shows reduced binding and internalization compared to formulations with similar concentrations of PEG750 and peptide. PR_b peptide shows superior targeting when compared to GRGDSP peptide targeting, as shown by improved binding and internalization at lower concentrations of PR_b. More importantly, PR_b is more specific towards integrin $\alpha_5\beta_1$ whereas many integrins bind to GRGDSP peptides. PR_b functionalized stealth liposomes show significantly higher cytotoxicity than the GRGDSP

functionalized stealth liposomes, and the non-targeted stealth liposomes, and are as effective as free 5-FU.

PR_b targeted liposomes were further optimized for controlled release of the encapsulated load by designing PR_b functionalized pH-sensitive stealth liposomes. These liposomes also bind to colon carcinoma cells, undergo cellular internalization, possibly via $\alpha_5\beta_1$ integrin-mediated endocytosis, and more importantly release a significant part of their load in a time period as short as 1 hrs. PR_b-targeted inert stealth liposomes take up to 4 hrs before they start releasing their contents. Therefore a pH-sensitive design will improve the overall efficacy of the drug when compared to its delivery via inert liposomes. Additionally, a faster release rate might indicate that pH-sensitive liposomes release part of their load in endosomes which will be beneficial in delivering drugs that cannot withstand the harsh acidic environment present in lysosomes. Finally, PR_b-targeted pH-sensitive stealth liposomes show significantly higher cytotoxicity than the PR_b-targeted inert stealth liposomes, as well as the non-targeted stealth liposomes (both pH-sensitive and inert), and are as effective as free 5-FU.

In summary, the work in this thesis demonstrates that using proper optimization techniques, targeted liposome formulations both inert and pH-sensitive can be designed which are capable of targeting tissue of interest with high affinity and specificity. These formulations can potentially be used *in-vivo* and may help in reducing the deleterious side effects associated with conventional drug delivery.

9. References

1. Garg, A. and E. Kokkoli, *Characterizing particulate drug-delivery carriers with atomic force microscopy*. IEEE Engineering in Medicine and Biology Magazine, 2005. **24**(1): p. 87-95.
2. Langer, R., *Drug delivery and targeting.* Nature, 1998. **392**(6679, Suppl.): p. 5-10.
3. Diederichs, J.E. and R.H. Muller, *Future strategies for drug delivery with particulate systems*. 1998, Boca Raton: CRC Press. ix, 194.
4. Molema, G. and D.K.F. Meijer, *Drug targeting : organ-specific strategies*. Methods and Principles in Medicinal Chemistry. Vol. 12. 2001, Weinheim New York: Wiley-VCH. xxxiv, 381.
5. Barratt, G., *Colloidal drug carriers: achievements and perspectives.* Cellular and Molecular Life Sciences, 2003. **60**(1): p. 21-37.
6. Dumitriu, S., *Polymeric biomaterials*. 2nd , rev. and expanded ed. 2002, New York: Marcel Dekker Inc. xiv, 1168.
7. Torchilin, V.P., *Drug targeting.* European Journal of Pharmaceutical Sciences, 2000. **11**: p. S81-S91.
8. Sinha, R., et al., *Nanotechnology in cancer therapeutics: bioconjugated nanoparticles for drug delivery.* Molecular Cancer Therapeutics, 2006. **5**(8): p. 1909-1917.
9. Bendas, G., et al., *Targetability of novel immunoliposomes prepared by a new antibody conjugation technique.* International Journal of Pharmaceutics, 1999. **181**(1): p. 79-93.
10. Garg, A., et al., *Targeting colon cancer cells using PEGylated liposomes modified with a fibronectin-mimetic peptide.* International Journal of Pharmaceutics, 2009. **366**(1-2): p. 201-210.
11. Lundberg, B., K. Hong, and D. Papahadjopoulos, *Conjugation of apolipoprotein B with liposomes and targeting to cells in culture.* Biochimica et Biophysica Acta, 1993. **1149**(2): p. 305-312.
12. Farokhzad, O.C., et al., *Cancer nanotechnology: drug encapsulated nanoparticle-aptamer bioconjugates for targeted delivery to prostate cancer cells.* Ejc Supplements, 2005. **3**(2): p. 229-230.
13. Heath, T.D., R.T. Fraley, and D. Papahadjopoulos, *Antibody Targeting of Liposomes - Cell Specificity Obtained by Conjugation of F(Ab')2 to Vesicle Surface.* Science, 1980. **210**(4469): p. 539-541.
14. Leserman, L.D., et al., *Targeting to Cells of Fluorescent Liposomes Covalently Coupled with Monoclonal Antibody or Protein-A.* Nature, 1980. **288**(5791): p. 602-604.
15. Farokhzad, O.C. and R. Langer, *Impact of Nanotechnology on Drug Delivery.* Acs Nano, 2009. **3**(1): p. 16-20.
16. Forssen, E. and M. Willis, *Ligand-targeted liposomes.* Advanced Drug Delivery Reviews, 1998. **29**(3): p. 249-271.
17. Kokkoli, E., et al., *Fractalkine targeting with a receptor-mimicking peptide-amphiphile.* Biomacromolecules, 2005. **6**(3): p. 1272-1279.

18. Tirrell, M., E. Kokkoli, and M. Biesalski, *The role of surface science in bioengineered materials.* Surface Science, 2002. **500**(1-3): p. 61-83.
19. Aiyer, A. and J.A. Varner, *Integrins in cancer progression and therapy.* Science and Medicine, 2005. **10**(2): p. 84-96.
20. Kim, S., et al., *Regulation of angiogenesis in vivo by ligation of integrin alpha(5)beta(1) with the central cell-binding domain of fibronectin.* American Journal of Pathology, 2000. **156**(4): p. 1345-1362.
21. Kim, S., M. Harris, and J.A. Varner, *Regulation of integrin alpha(v)beta(3)-mediated endothelial cell migration and angiogenesis by integrin alpha(5)beta(1) and protein kinase A.* Journal of Biological Chemistry, 2000. **275**(43): p. 33920-33928.
22. Livant, D.L., et al., *Anti-invasive, antitumorigenic, and antimetastatic activities of the PHSCN sequence in prostate carcinoma.* Cancer Research, 2000. **60**(2): p. 309-320.
23. Jia, Y., et al., *Integrin fibronectin receptors in matrix metalloproteinase-1-dependent invasion by breast cancer and mammary epithelial cells.* Cancer Research, 2004. **64**(23): p. 8674-8681.
24. Gong, J., et al., *Role of alpha(5)beta(1) integrin in determining malignant properties of colon carcinoma cells.* Cell Growth and Differentiation, 1997. **8**(1): p. 83-90.
25. Jayne, D.G., et al., *Extracellular matrix proteins and chemoradiotherapy: alpha(5)beta(1) integrin as a predictive marker in rectal cancer.* European Journal of Surgical Oncology, 2002. **28**(1): p. 30-36.
26. Ellis, L.M., *A targeted approach for antiangiogenic therapy of metastatic human colon cancer.* American Surgeon, 2003. **69**(1): p. 3-10.
27. Chen, J., et al., *Metastatic properties of prostate cancer cells are controlled by VEGF.* Cell Communication and Adhesion, 2004. **11**(1): p. 1-11.
28. White, E.S., et al., *Monocyte-fibronectin interactions, via alpha(5)beta(1) integrin, induce expression of CXC chemokine-dependent angiogenic activity.* Journal of Immunology, 2001. **167**(9): p. 5362-5366.
29. Stoeltzing, O., et al., *Reduction of colon cancer growth by a novel antiangiogenic agent that targets the integrin alpha(5)beta(1).* Clinical Cancer Research, 2001. **7**(11): p. 3656s-3656s.
30. Stoeltzing, O., et al., *Inhibition of integrin alpha(5)beta(1) function with a small peptide (ATN-161) plus continuous 5-FU infusion reduces colorectal liver metastases and improves survival in mice.* International Journal of Cancer, 2003. **104**(4): p. 496-503.
31. Meerovitch, K., et al., *A novel RGD antagonist that targets both alpha(v)beta(3) and alpha(5)beta(1) induces apoptosis of angiogenic endothelial cells on type I collagen.* Vascular Pharmacology, 2003. **40**(2): p. 77-89.
32. Yokoyama, Y. and S. Ramakrishnan, *Addition of integrin binding sequence to a mutant human endostatin improves inhibition of tumor growth.* International Journal of Cancer, 2004. **111**(6): p. 839-848.
33. Shannon, K.E., et al., *Anti-metastatic properties of RGD-peptidomimetic agents S137 and S247.* Clinical and Experimental Metastasis, 2004. **21**(2): p. 129-138.

34. Hart, S.L., et al., *Cell-Binding and Internalization by Filamentous Phage Displaying a Cyclic Arg-Gly-Asp-Containing Peptide.* Journal of Biological Chemistry, 1994. **269**(17): p. 12468-12474.
35. Xiong, X., et al., *Enhanced intracellular delivery and improved antitumor efficacy of doxorubicin by sterically stabilized liposomes modified with a synthetic RGD mimetic.* Journal of Controlled Release, 2005. **107**(2): p. 262-275.
36. Kintarak, S., et al., *Internalization of Staphylococcus aureus by human keratinocytes.* Infection and Immunity, 2004. **72**(10): p. 5668-5675.
37. Xiong, X., et al., *Enhanced intracellular uptake of sterically stabilized liposomal doxorubicin in vitro resulting in improved antitumor activity in vivo.* Pharmaceutical Research, 2005. **22**(6): p. 933-939.
38. Xiong, X., et al., *Intracellular delivery of doxorubicin with RGD-modified sterically stabilized liposomes for an improved antitumor efficacy: In vitro and in vivo.* Journal of Pharmaceutical Sciences, 2005. **94**(8): p. 1782-1793.
39. Uduehi, A., et al., *Enhancement of integrin-mediated transfection of haematopoietic cells with a synthetic vector system.* Biotechnology and Applied Biochemistry, 2003. **38**: p. 201-209.
40. Bazan, J.F., et al., *A new class of membrane-bound chemokine with a CX3C motif.* Nature, 1997. **385**(6617): p. 640-644.
41. Imai, T., et al., *Identification and molecular characterization of fractalkine receptor CX3CR1, which mediates both leukocyte migration and adhesion.* Cell, 1997. **91**(4): p. 521-530.
42. Umehara, H., et al., *Fractalkine in vascular biology.* Arteriosclerosis, Thrombosis, and Vascular Biology, 2004. **24**(1): p. 34-40.
43. Zujovic, V., J.K. Harrison, and T.I. Schall, *Fractalkine.* Cytokine Handbook, 2003. **2**: p. 1101-1116.
44. Goda, S., et al., *CX3C-chemokine, fractalkine-enhanced adhesion of THP-1 cells to endothelial cells through integrin-dependent and -independent mechanisms.* Journal of Immunology, 2000. **164**(8): p. 4313-4320.
45. Fong, A.M., et al., *Fractalkine and CX3CR1 mediate a novel mechanism of leukocyte capture, firm adhesion, and activation under physiologic flow*. Journal of Experimental Medicine, 1998. **188**(8): p. 1413-1419.
46. Haskell, C.A., M.D. Cleary, and I.F. Charo, *Molecular uncoupling of fractalkine-mediated cell adhesion and signal transduction. Rapid flow arrest of CX3CR1-expressing cells is independent of G-protein activation.* Journal of Biological Chemistry, 1999. **274**(15): p. 10053-10058.
47. Ancuta, P., et al., *Fractalkine preferentially mediates arrest and migration of CD16+ monocytes.* Journal of Experimental Medicine, 2003. **197**(12): p. 1701-1707.
48. Combadiere, C., et al., *Identification of CX3CR1*. Journal of Biological Chemistry, 1998. **273**(37): p. 23799-23804.
49. Fong, A.M., et al., *Ultrastructure and function of the fractalkine mucin domain in CX(3)C chemokine domain presentation.* Journal of Biological Chemistry, 2000. **275**(6): p. 3781-3786.

50. Haskell, C.A., M.D. Cleary, and I.F. Charo, *Unique role of the chemokine domain of fractalkine in cell capture.* Journal of Biological Chemistry, 2000. **275**(44): p. 34183-34189.
51. Fong, A.M., et al., *CX_3CR1 tyrosine sulfation enhances fractalkine-induced cell adhesion.* Journal of Biological Chemistry, 2002. **277**(22): p. 19418-19423.
52. McDermott, D.H., et al., *Association between polymorphism in the chemokine receptor CX3CR1 and coronary vascular endothelial dysfunction and atherosclerosis.* Circulation Research, 2001. **89**(5): p. 401-407.
53. Alexander, R.W., *Cytokine receptor CX3CR-1 and fractalkine. New factors in the atherosclerosis drama?* Circulation Research, 2001. **89**(5): p. 376-377.
54. Moatti, D., et al., *Polymorphism in the fractalkine receptor CX3CR1 as a genetic risk factor for coronary artery disease.* Blood, 2001. **97**(7): p. 1925-1928.
55. Ruth, J.H., et al., *Fractalkine, a novel chemokine in rheumatoid arthritis and in rat adjuvant-induced arthritis.* Arthritis & Rheumatism, 2001. **44**(7): p. 1568-1581.
56. Shulby, S.A., et al., *CX3CR1-fractalkine expression regulates cellular mechanisms involved in adhesion, migration, and survival of human prostate cancer cells.* Cancer Research, 2004. **64**(14): p. 4693-4698.
57. Tong, N., et al., *Neuronal fractalkine expression in HIV-1 encephalitis: roles for macrophage recruitment and neuroprotection in the central nervous system.* Journal of Immunology, 2000. **164**(3): p. 1333-1339.
58. Haskell, C.A., et al., *Targeted deletion of CX(3)CR1 reveals a role for fractalkine in cardiac allograft rejection.* Journal of Clinical Investigation, 2001. **108**(5): p. 679-688.
59. Faure, S., et al., *Rapid progress to AIDS in HIV+ individuals with a structural variant of the chemokine receptor CX3CR1.* Science, 2000. **287**(5461): p. 2274-2277.
60. Pangburn, T.O., et al., *Peptide- and aptamer-functionalized nanovectors for targeted delivery of therapeutics.* Journal of Biomechenical Engineering, 2009. **131**(7): p. 074005.
61. Allen, T.M., *Ligand-targeted therapeutics in anticancer therapy.* Nature Reviews Cancer, 2002. **2**(10): p. 750-63.
62. Vance, D., et al., *Polyvalency: A promising strategy for drug design.* Biotechnology and Bioengineering, 2008. **101**(3): p. 429-434.
63. Saul, J.M., A.V. Annapragada, and R.V. Bellamkonda, *A dual-ligand approach for enhancing targeting selectivity of therapeutic nanocarriers.* Journal of Controlled Release, 2006. **114**(3): p. 277-287.
64. Dubey, P.K., et al., *Liposomes modified with cyclic RGD peptide for tumor targeting.* Journal of Drug Targeting, 2004. **12**(5): p. 257-264.
65. Harvie, P., et al., *Targeting of Lipid-Protamine-DNA (LPD) lipopolyplexes using RGD motifs.* Journal of Liposome Research, 2003. **13**(3-4): p. 231-247.
66. Janssen, A.P.C.A., et al., *Peptide-targeted PEG-liposomes in anti-angiogenic therapy.* International Journal of Pharmaceutics, 2003. **254**(1): p. 55-58.
67. Takagi, J., *Structural basis for ligand recognition by RGD (Arg-Gly-Asp)-dependent integrins.* Biochemical Society Transactions, 2004. **32**: p. 403-406.

68. Ochsenhirt, S.E., et al., *Effect of RGD secondary structure and the synergy site PHSRN on cell adhesion, spreading and specific integrin engagement.* Biomaterials, 2006. **27**(20): p. 3863-3874.
69. Leahy, D.J., I. Aukhil, and H.P. Erickson, *2.0 angstrom crystal structure of a four-domain segment of human fibronectin encompassing the RGD loop and synergy region.* Cell, 1996. **84**(1): p. 155-164.
70. Aucoin, L., et al., *Interactions of corneal epithelial cells and surfaces modified with cell adhesion peptide combinations.* Journal of Biomaterials Science-Polymer Edition, 2002. **13**(4): p. 447-462.
71. Kao, W.J., *Evaluation of protein-modulated macrophage behavior on biomaterials: designing biomimetic materials for cellular engineering.* Biomaterials, 1999. **20**(23-24): p. 2213-2221.
72. Kim, T.I., et al., *Design and biological activity of synthetic oligopeptides with Pro-His-Ser-Arg-Asn (PHSRN) and Arg-Gly-Asp (RGD) motifs for human osteoblast-like cell (MG-63) adhesion.* Biotechnology Letters, 2002. **24**(24): p. 2029-2033.
73. Benoit, D.S.W. and K.S. Anseth, *The effect on osteoblast function of colocalized RGD and PHSRN epitopes on PEG surfaces.* Biomaterials, 2005. **26**(25): p. 5209-5220.
74. Susuki, Y., et al., *Preparation and biological activities of a bivalent poly (ethylene glycol) hybrid containing an active site and its synergistic site of fibronectin.* Chemical and Pharmaceutical Bulletin, 2002. **50**(9): p. 1229-1232.
75. Mardilovich, A., et al., *Design of a novel fibronectin-mimetic peptide-amphiphile for functionalized biomaterials.* Langmuir, 2006. **22**(7): p. 3259-3264.
76. Mardilovich, A., *Biomimetic peptide-amphiphiles for functional biomaterials*. 2006, Doctoral Thesis, University of Minnesota. p. 139.
77. Mardilovich, A. and E. Kokkoli, *Biomimetic peptide-amphiphiles for functional biomaterials: The role of GRGDSP and PHSRN*. Biomacromolecules, 2004. **5**(3): p. 950-957.
78. Idiris, A., M.T. Alam, and A. Ikai, *Spring mechanics of alpha-helical polypeptide*. Protein Engineering, 2000. **13**(11): p. 763-770.
79. Kokkoli, E., et al., *Self-assembly and applications of biomimetic and bioactive peptide-amphiphiles.* Soft Matter, 2006. **2**(12): p. 1015-1024.
80. Gayle, R., 3d, et al., *Importance of the amino terminus of the interleukin-8 receptor in ligand interactions.* Journal of Biological Chemistry, 1993. **268**(10): p. 7283-7289.
81. LaRosa, G., et al., *Amino terminus of the interleukin-8 receptor is a major determinant of receptor subtype specificity*. Journal of Biological Chemistry, 1992. **267**(35): p. 25402-25406.
82. Suzuki, H., et al., *The N terminus of interleukin-8 (IL-8) receptor confers high affinity binding to human IL-8.* Journal of Biological Chemistry, 1994. **269**(28): p. 18263-18266.
83. Ahuja, S.K., J.C. Lee, and P.M. Murphy, *CXC chemokines bind to unique sets of selectivity determinants that can function independently and are broadly distributed on multiple domains of human interleukin-8 receptor B.* Journal of Biological Chemistry, 1996. **271**(1): p. 225-232.

84. Wu, L., et al., *Discrete steps in binding and signaling of interleukin-8 with its receptor.* Journal of Biological Chemistry, 1996. **271**(49): p. 31202-31209.
85. Brelot, A., et al., *Identification of residues of CXCR4 critical for human immunodeficiency virus coreceptor and chemokine receptor.* Journal of Biological Chemistry, 2000. **275**(31): p. 23736-23744.
86. Pease, J.E., et al., *The N-terminal extracellular segments of the chemokine receptors CCR1 and CCR3 are determinants for MIP-1alpha and eotaxin binding, respectively, but a second domain is essential for efficient receptor activation.* Journal of Biological Chemistry, 1998. **273**(32): p. 19972-19976.
87. Monteclaro, F.S. and I.F. Charo, *The amino-terminal domain of CCR2 is both necessary and sufficient for high affinity binding of monocyte chemoattractant protein 1.* Journal of Biological Chemistry, 1997. **272**(37): p. 23186-23190.
88. Monteclaro, F.S. and I.F. Charo, *The amino-terminal extracellular domain of the MCP-1 receptor, but not the RANTES/MIP-1alpha receptor, confers chemokine selectivity.* Journal of Biological Chemistry, 1996. **271**(32): p. 19084-19092.
89. Hemmerich, S., et al., *Identification of residues in the monocyte chemotactic protein-1 that contact the MCP-1 receptor, CCR2.* Biochemistry, 1999. **38**(40): p. 13013-13025.
90. Mayer, M.R. and M.J. Stone, *Identification of receptor binding and activation determinants in the N-terminal and N-loop regions of the CC chemokine eotaxin.* Journal of Biological Chemistry, 2001. **276**(17): p. 13911-13916.
91. Blanpain, C., et al., *Multiple charged and aromatic residues in CCR5 amino-terminal domain are involved in high affinity binding of both chemokines and HIV-1 env protein.* Journal of Biological Chemistry, 1999. **274**(49): p. 34719-34727.
92. Lu, Z.H., et al., *The promiscuous chemokine binding profile of the Duffy antigen/receptor for chemokines is primarily localized to sequences in the amino-terminal domain.* Journal of Biological Chemistry, 1995. **270**(44): p. 26239-26245.
93. Mizoue, L.S., et al., *Solution structure and dynamics of the CX3C chemokine domain of fractalkine and its interaction with an N-terminal fragment of CX(3)CR1.* Biochemistry, 1999. **38**(5): p. 1402-1414.
94. Clubb, R.T., et al., *Mapping the binding surface of interleukin-8 complexed with an N-terminal fragment of the Type 1 human interleukin-8 receptor.* FEBS Letters, 1994. **338**(1): p. 93-97.
95. Gozansky, E.K., et al., *Mapping the binding of the N-terminal extracellular tail of the CXCR4 receptor to stromal cell-derived factor-1[alpha].* Journal of Molecular Biology, 2005. **345**(4): p. 651-658.
96. Mayer, K.L. and M.J. Stone, *NMR solution structure and receptor peptide binding of the CC chemokine eotaxin-2.* Biochemistry, 2000. **39**(29): p. 8382-8395.
97. Skelton, N.J., et al., *Structure of a CXC chemokine-receptor fragment in complex with interleukin-8.* Structure, 1999. **7**(2): p. 157-168.
98. Ye, J., L.L. Kohli, and M.J. Stone, *Characterization of binding between the chemokine eotaxin and peptides derived from the chemokine receptor CCR3.* Journal of Biological Chemistry, 2000. **275**(35): p. 27250-27257.

99. Fernandez, C., et al., *Regulation of the extracellular ligand binding activity of integrins.* Frontiers in Bioscience, 1998. **3**: p. d684-700.
100. Bangham, A.D., M.M. Standish, and J.C. Watkins, *Diffusion of univalent ions across the lamellae of swollen phospholipids.* Journal of Molecular Biology, 1965. **13**(1): p. 238-252.
101. Gregoriadis, G., *Engineering liposomes for drug delivery: progress and problems.* Trends in Biotechnology, 1995. **13**(12): p. 527-537.
102. Gregoriadis, G. and B.E. Ryman, *Liposomes as carriers of enzymes or drugs: a new approach to the treatment of storage diseases.* Biochemical Journal, 1971. **124**(5): p. 58.
103. Torchilin, V.P., *Recent advances with liposomes as pharmaceutical carriers.* Nature Reviews Drug Discovery, 2005. **4**(2): p. 145-160.
104. Hiemenz, P.C. and R. Rajagopalan, *Principles of colloid and surface chemistry*. 3rd , rev. and expanded / ed. Undergraduate chemistry ; 14. 1997, New York: Marcel Dekker. xix, 650.
105. Vemuri, S. and C.T. Rhodes, *Preparation and characterization of liposomes as therapeutic delivery systems: a review.* Pharmaceutica Acta Helvetiae, 1995. **70**(2): p. 95-111.
106. Sharma, A. and U.S. Sharma, *Liposomes in drug delivery: progress and limitations.* International Journal of Pharmaceutics, 1997. **154**(2): p. 123-140.
107. Lasic, D.D. and D. Papahadjopoulos, *Liposomes revisited.* Science, 1995. **267**(5202): p. 1275-1276.
108. Philippot, J.R. and F. Schuber, *Liposomes as tools in basic research and industry*. 1995, Boca Raton: CRC Press. 277.
109. Ranade, V.V., *Drug delivery systems. 1. site-specific drug delivery using liposomes as carriers.* Journal of Clinical Pharmacology, 1989. **29**(8): p. 685-694.
110. Straubinger, R.M., et al., *Endocytosis of liposomes and intracellular fate of encapsulated molecules - encounter with a low pH compartment after internalization in coated vesicles.* Cell, 1983. **32**(4): p. 1069-1079.
111. Gabizon, A. and D. Papahadjopoulos, *Liposome formulations with prolonged circulation time in blood and enhanced uptake by tumors.* Proceedings of the National Academy of Sciences of the United States of America, 1988. **85**(18): p. 6949-6953.
112. Sharma, A., N.L. Straubinger, and R.M. Straubinger, *Modulation of human ovarian tumor cell sensitivity to N-(phosphonacetyl)-L-aspartate (PALA) by liposome drug carriers.* Pharmaceutical Research, 1993. **10**(10): p. 1434-1441.
113. Felgner, J.H., et al., *Enhanced gene delivery and mechanism studies with a novel series of cationic lipid formulations.* Journal of Biological Chemistry, 1994. **269**(4): p. 2550-2561.
114. Duzgunes, N., et al., *Fusion of liposomes containing a novel cationic lipid, N-[2,3-(dioleyloxy)propyl]-N,N,N-trimethylammonium: induction by multivalent anions and asymmetric fusion with acidic phospholipid vesicles.* Biochemistry, 1989. **28**(23): p. 9179-9184.
115. Allen, T.M., J.L. Ryan, and D. Papahadjopoulos, *Gangliosides reduce leakage of aqueous-space markers from liposomes in the presence of human plasma.* Biochimica et Biophysica Acta, 1985. **818**(2): p. 205-210.

116. Klibanov, A.L., et al., *Amphipatic polyethyleneglycols effectively prolong the circulation time of liposomes.* FEBS Letters, 1990. **268**: p. 235-238.
117. Machy, P. and L.D. Leserman, *Small liposomes are better than large liposomes for specific drug delivery in vitro.* Biochimica et Biophysica Acta, 1983. **730**(2): p. 313-320.
118. Storm, G. and D.J.A. Crommelin, *Liposomes: quo vadis?* Pharmaceutical Science & Technology Today, 1998. **1**(1): p. 19-31.
119. Allen, T.M. and A. Chonn, *Large unilamellar liposomes with low uptake into the reticuloendothelial system.* FEBS Letters, 1987. **223**(1): p. 42-46.
120. Marjan, J.M.J. and T.M. Allen, *Long circulating liposomes: Past present and future.* Biotechnology Advances, 1996. **14**(2): p. 151-175.
121. Lasic, D.D., *Liposomes in gene delivery*. 1997, Boca Raton, FL: CRC Press. 295.
122. Deamer, D. and A.D. Bangham, *Large volume liposomes by an ether vaporization method.* Biochimica et Biophysica Acta, 1976. **443**(3): p. 629-634.
123. Szoka, F., Jr. and D. Papahadjopoulos, *Procedure for preparation of liposomes with large internal aqueous space and high capture by reverse-phase evaporation.* Proceedings of the National Academy of Sciences of the United States of America, 1978. **75**(9): p. 4194-4198.
124. MacDonald, R.C., et al., *Small-volume extrusion apparatus for preparation of large, unilamellar vesicles.* Biochimica et Biophysica Acta, 1991. **1061**(2): p. 297-303.
125. Hope, M.J., et al., *Production of large unilamellar vesicles by a rapid extrusion procedure. Characterization of size distribution, trapped volume and ability to maintain a membrane potential.* Biochimica et Biophysica Acta, 1985. **812**(1): p. 55-65.
126. Kirby, C.J. and G. Gregoriadis, *Dehydration–rehydration vesicles: a simple method for high yield drug encapsulation in liposomes.* Biotechnology, 1984. **2**: p. 979–984.
127. Brunner, J., P. Skrabal, and H. Hauser, *Single bilayer vesicles prepared without sonication. Physico-chemical properties.* Biochimica et Biophysica Acta, 1976. **455**(2): p. 322-331.
128. Kunitake, T., *Synthetic Bilayer-Membranes - Molecular Design, Self-Organization, and Application.* Angewandte Chemie-International Edition in English, 1992. **31**(6): p. 709-726.
129. Asakuma, S., H. Okada, and T. Kunitake, *Template Synthesis of 2-Dimensional Network of Cross-Linked Acrylate Polymer in a Cast Multibilayer Film.* Journal of the American Chemical Society, 1991. **113**(5): p. 1749-1755.
130. Berndt, P., G.B. Fields, and M. Tirrell, *Synthetic Lipidation of Peptides and Amino-Acids: Monolayer Structure and Properties.* Journal of the American Chemical Society, 1995. **117**(37): p. 9515-9522.
131. Kaiser, E., et al., *Color test for detection of free terminal amino groups in the solid-phase synthesis of peptides.* Anal Biochem, 1970. **34**(2): p. 595-8.
132. Dhar, S., et al., *Targeted delivery of cisplatin to prostate cancer cells by aptamer functionalized Pt(IV) prodrug-PLGA-PEG nanoparticles.* Proceedings of the National Academy of Sciences of the United States of America, 2008. **105**(45): p. 17356-17361.

133. Bagalkot, V., et al., *An aptamer-doxorubicin physical conjugate as a novel targeted drug-delivery platform.* Angewandte Chemie-International Edition, 2006. **45**(48): p. 8149-8152.
134. Pierce Biotechnology Inc.
135. Chen, P.S., Jr., T.Y. Toribara, and H. Warner, *Microdetermination of phosphorus.* Analytical Chemistry, 1956. **28**: p. 1756-1758.
136. Smith, P.K., et al., *Measurement of protein using bicinchoninic acid.* Analytical Biochemistry, 1985. **150**(1): p. 76-85.
137. Childs, C.E., *Determination of Polyethylene-Glycol in Gamma-Globulin Solutions.* Microchemical Journal, 1975. **20**(2): p. 190-192.
138. Gebicki, J., et al., *Peroxidation of proteins and lipids in suspensions of liposomes, in blood serum, and in mouse myeloma cells.* Acta Biochimica Polonica, 2000. **47**: p. 901-911.
139. Sims, G.E.C. and T.J. Snape, *A Method for the Estimation of Polyethylene-Glycol in Plasma-Protein Fractions.* Analytical Biochemistry, 1980. **107**(1): p. 60-63.
140. Skoog, B., *Determination of Polyethylene Glycol-4000 and Glycol-6000 in Plasma-Protein Preparations.* Vox Sanguinis, 1979. **37**(6): p. 345-349.
141. Selsiko, B., et al., *Analysis and purification of monomethoxy-polyethylene glycol by vesicle and gel permeation chromatography.* Journal of chromatography, 1993. **641**(1): p. 71-79.
142. Nag, A., G. Mitra, and P.C. Ghosh, *A colorimetric assay for estimation of polyethylene glycol and polyethylene glycolated protein using ammonium ferrothiocyanate.* Analytical Biochemistry, 1996. **237**(2): p. 224-231.
143. Nag, A., G. Mitra, and P.C. Ghosh, *A colorimetric estimation of polyethyleneglycol-conjugated phospholipid in stealth liposomes.* Analytical Biochemistry, 1997. **250**(1): p. 35-43.
144. Shimada, K., et al., *Determination of incorporated amounts of poly(ethylene glycol)-derivatized lipids in liposomes for the physicochemical characterization of stealth liposomes.* International Journal of Pharmaceutics, 2000. **203**(1-2): p. 255-263.
145. Allen, T.M., et al., *Liposomes Containing Synthetic Lipid Derivatives of Poly(Ethylene Glycol) Show Prolonged Circulation Half-Lives Invivo.* Biochimica Et Biophysica Acta, 1991. **1066**(1): p. 29-36.
146. Fresta, M., et al., *5-Fluorouracil - various kinds of loaded liposomes - encapsulation efficiency, storage stability and fusogenic properties.* International Journal of Pharmaceutics, 1993. **99**(2-3): p. 145-156.
147. Gupta, Y., et al., *Design and development of folate appended liposomes for enhanced delivery of 5-FU to tumor cells.* Journal of Drug Targeting, 2007. **15**(3): p. 231-240.
148. Pecora, R., *Dynamic light scattering : applications of photon correlation spectroscopy*. 1985, New York: Plenum Press. xiv, 420.
149. McNeil-Watson, F., W. Tscharnuter, and J. Miller, *A new instrument for the measurement of very small electrophoretic mobilities using phase analysis light scattering (PALS).* Colloids and Surfaces a-Physicochemical and Engineering Aspects, 1998. **140**(1-3): p. 53-57.

150. Maeda, H., T. Sawa, and T. Konno, *Mechanism of tumor-targeted delivery of macromolecular drugs, including the EPR effect in solid tumor and clinical overview of the prototype polymeric drug SMANCS.* Journal of Controlled Release, 2001. **74**(1-3): p. 47-61.
151. Folkman, J., *Angiogenesis in Cancer, Vascular, Rheumatoid and Other Disease.* Nature Medicine, 1995. **1**(1): p. 27-31.
152. Folkman, J., *What Is the evidence that tumors are angiogenesis dependent.* Journal of the National Cancer Institute, 1990. **82**(1): p. 4-6.
153. Risau, W., *Mechanisms of angiogenesis.* Nature, 1997. **386**(6626): p. 671-674.
154. Stromblad, S. and D.A. Cheresh, *Integrins, angiogenesis and vascular cell survival.* Chemistry and Biology, 1996. **3**(11): p. 881-885.
155. Goel, H.L. and L.R. Languino, *Integrin signaling in cancer.* Cancer Treatment and Research, 2004. **119**: p. 15-31.
156. Varner, J.A. and D.A. Cheresh, *Integrins and cancer.* Current Opinion in Cell Biology, 1996. **8**(5): p. 724-730.
157. Aota, S., M. Nomizu, and K.M. Yamada, *The Short Amino-Acid-Sequence Pro-His-Ser-Arg-Asn in Human Fibronectin Enhances Cell-Adhesive Function.* Journal of Biological Chemistry, 1994. **269**(40): p. 24756-24761.
158. Kokkoli, E., S.E. Ochsenhirt, and M. Tirrell, *Collective and single-molecule interactions of alpha(5)beta(1) integrins.* Langmuir, 2004. **20**(6): p. 2397-2404.
159. Fransson, B., U. Ragnarsson, and O. Zetterqvist, *Separation of Basic, Hydrophilic Peptides by Reversed-Phase Ion-Pair Chromatography.* Analytical Biochemistry, 1982. **126**(1): p. 174-178.
160. Litowski, J.R., et al., *Hydrophilic interaction/cation-exchange chromatography for the purification of synthetic peptides from closely related impurities: serine side-chain acetylated peptides.* Journal of Peptide Research, 1999. **54**(1): p. 1-11.
161. Trevino, S.R., J.M. Scholtz, and C.N. Pace, *Amino acid contribution to protein solubility: Asp, Glu, and Ser contribute more favorably than the other hydrophilic amino acids in RNase Sa.* Journal of Molecular Biology, 2007. **366**(2): p. 449-460.
162. Tzvetkov, G., M.G. Ramsey, and F.P. Netzer, *Glycine-ice nanolayers: Morphology and surface energetics.* Journal of Chemical Physics, 2005. **122**(11): p. 114712.
163. Berezovsky, I.N., et al., *Protein folding: Looping from hydrophobic nuclei.* Proteins-Structure Function and Genetics, 2001. **45**(4): p. 346-350.
164. Han, X., et al., *Interaction of mutant influenza virus hemagglutinin fusion peptides with lipid bilayers: Probing the role of hydrophobic residue size in the central region of the fusion peptide.* Biochemistry, 1999. **38**(45): p. 15052-15059.
165. Dori, Y., et al., *Ligand accessibility as means to control cell response to bioactive bilayer membranes.* Journal of Biomedical Materials Research, 2000. **50**(1): p. 75-81.
166. Fenske, D.B., N. Maurer, and P.R. Cullis, *Encapsulation of weakly-basic drugs, antisense oligonucleotides, and plasmid DNA within large unilamellar vesicles for drug delivery applications*. 2nd ed. Liposomes. 2003, New York: Oxford university press. 167-191.

167. Fiske, C.H. and Y. Subbarow, *The colorimetric determination of phosphorus.* Journal of Biological Chemistry, 1925. **66**(2): p. 375-400.
168. Vichai, V. and K. Kirtikara, *Sulforhodamine B colorimetric assay for cytotoxicity screening.* Nature Protocols, 2006. **1**(3): p. 1112-1116.
169. Lee, K.D., S. Nir, and D. Papahadjopoulos, *Quantitative analysis of liposome-cell interactions in vitro: rate constants of binding and endocytosis with suspension and adherent J774 cells and human monocytes.* Biochemistry, 1993. **32**(3): p. 889-899.
170. Kessner, S., et al., *Investigation of the cellular uptake of E-Selectin-targeted immunoliposomes by activated human endothelial cells.* Biochimica et Biophysica Acta, 2001. **1514**(2): p. 177-190.
171. Demirgöz, D., et al., *PR_b-targeted delivery of tumor necrosis factor-α by polymersomes for the treatment of prostate cancer.* Soft Matter, 2009. **5**(10): p. 2011–2019.
172. Sofou, S., *Surface-active liposomes for targeted cancer therapy.* Nanomed., 2007. **2**(5): p. 711-724.
173. Spragg, D.D., et al., *Immunotargeting of liposomes to activated vascular endothelial cells: a strategy for site-selective delivery in the cardiovascular system.* Proceedings of the National Academy of Sciences of the United States of America, 1997. **94**(16): p. 8795-8800.
174. Daleke, D.L., K.L. Hong, and D. Papahadjopoulos, *Endocytosis of liposomes by macrophages - binding, acidification and leakage of liposomes monitored by a new fluorescence assay.* Biochimica Et Biophysica Acta, 1990. **1024**(2): p. 352-366.
175. Straubinger, R.M., D. Papahadjopoulos, and K. Hong, *Endocytosis and intracellular fate of liposomes using pyranine as a probe.* Biochemistry, 1990. **29**(20): p. 4929-4939.
176. Connor, J., M.B. Yatvin, and L. Huang, *pH-sensitive liposomes - acid-induced liposome fusion.* Proceedings of the National Academy of Sciences of the United States of America, 1984. **81**(6): p. 1715-1718.
177. Alaouie, A.M. and S. Sofou, *Liposomes with triggered content release for cancer therapy.* Journal of Biomedical Nanotechnology., 2008. **4**(3): p. 234-244.
178. Kale, A.A. and V.P. Torchilin, *"Smart" drug carriers: PEGylated TATp-Modified pH-Sensitive Liposomes.* Journal of Liposome Research, 2007. **17**(3-4): p. 197-203.
179. Chu, C.J., et al., *Efficiency of cytoplasmic delivery by pH-sensitive liposomes to cells in culture.* Pharmaceutical Research, 1990. **7**(8): p. 824-834.
180. Kim, M.J., et al., *Preparation of pH-sensitive, long-circulating and EGFR-targeted immunoliposomes.* Arch. Pharm. Res., 2008. **31**(4): p. 539-546.
181. Shi, G.F., et al., *Efficient intracellular drug and gene delivery using folate receptor-targeted pH-sensitive liposomes composed of cationic/anionic lipid combinations.* Journal of Controlled Release, 2002. **80**(1-3): p. 309-319.
182. Fonseca, C., et al., *Targeting of sterically stabilised pH-sensitive liposomes to human T-leukaemia cells.* European Journal of Pharmaceutics and Biopharmaceutics, 2005. **59**(2): p. 359-366.

183. Demirgoz, D., A. Garg, and E. Kokkoli, *PR_b-targeted PEGylated liposomes for prostate cancer therapy.* Langmuir, 2008. **24**(23): p. 13518-13524.
184. Craig, J.A., et al., *Effect of linker and spacer on the design of a fibronectin mimetic peptide evaluated via cell studies and AFM adhesion forces.* Langmuir, 2008. **24**(18): p. 10282-10292.
185. Mardilovich, A. and E. Kokkoli, *Patterned biomimetic membranes: effect of concentration and pH.* Langmuir, 2005. **21**(16): p. 7468-7475.
186. Hamann, S., et al., *Measurement of cell volume changes by fluorescence self-quenching.* Journal of Fluorescence, 2002. **12**(2): p. 139-145.
187. Van Bambeke, F., et al., *Biophysical studies and intracellular destabilization of pH-sensitive liposomes.* Lipids, 2000. **35**(2): p. 213-223.
188. Slepushkin, V.A., et al., *Sterically stabilized pH-sensitive liposomes - intracellular delivery of aqueous contents and prolonged circulation in vivo.* Journal of Biological Chemistry, 1997. **272**(4): p. 2382-2388.
189. Simoes, S., et al., *On the mechanisms of internalization and intracellular delivery mediated by pH-sensitive liposomes.* Biochimica Et Biophysica Acta, 2001. **1515**(1): p. 23-37.
190. Cullis, P.R. and B. Dekruijff, *Polymorphic phase behavior of phosphatidylethanolamines of natural and synthetic origin - P-31 NMR-study.* Biochimica Et Biophysica Acta, 1978. **513**(1): p. 31-42.
191. Lai, M.Z., W.J. Vail, and F.C. Szoka, *Acid-induced and calcium-induced structural-changes in phosphatidylethanolamine membranes stabilized by cholesteryl hemisuccinate.* Biochemistry, 1985. **24**(7): p. 1654-1661.
192. Ellens, H., J. Bentz, and F.C. Szoka, *Destabilization of phosphatidylethanolamine liposomes at the hexagonal phase-transition temperature.* Biophysical Journal, 1985. **47**(2): p. A169-A169.
193. Ellens, H., J. Bentz, and F.C. Szoka, *pH-induced destabilization of phosphatidylethanolamine-containing liposomes - role of bilayer contact.* Biochemistry, 1984. **23**(7): p. 1532-1538.
194. Chrai, S.S., R. Murari, and I. Ahmad, *Liposomes (a review). part two: Drug delivery systems.* BioPharm International, 2002. **15**(1): p. 40,42-43,49.
195. Ranson, M., et al., *Liposomal drug delivery.* Cancer Treatment Reviews, 1996. **22**(5): p. 365-379.
196. Pries, A.R., T.W. Secomb, and P. Gaehtgens, *The endothelial surface layer.* Pflügers Archiv European Journal of Physiology, 2000. **440**(5): p. 653-666.
197. Tuerk, C. and L. Gold, *Systematic evolution of ligands by exponential enrichment: RNA ligands to bacteriophage T4 DNA polymerase.* Science, 1990. **249**(4968): p. 505-10.
198. Levy-Nissenbaum, E., et al., *Nanotechnology and aptamers: applications in drug delivery.* Trends in Biotechnology, 2008. **26**(8): p. 442-449.
199. Dausse, E., S. Da Rocha Gomes, and J.J. Toulme, *Aptamers: a new class of oligonucleotides in the drug discovery pipeline?* Curr Opin Pharmacol, 2009.
200. Ireson, C.R. and L.R. Kelland, *Discovery and development of anticancer aptamers.* Molecular Cancer Therapeutics, 2006. **5**(12): p. 2957-62.